Communauté
UNIVERSITÉ Grenoble Alpes

THÈSE

Pour obtenir le grade de

DOCTEUR DE L'UNIVERSITÉ DE GRENOBLE

Spécialité : **Mathématiques et Informatique**

Arrêté ministérial :

Présentée par

Santosh Arvind Adimoolam

Thèse dirigée par **Thao Dang**

préparée au sein **du laboratoire Verimag**
et de **Ecole Doctorale Mathématiques, Sciences et Technologies de l'Information, Informatique**

A Calculus of Complex Zonotopes for Invariance and Stability Verification of Hybrid Systems

Thèse soutenue publiquement le ,
devant le jury composé de :

Sylvie Putot
Professor of Computer Science
École Polytechnique, Rapporteur

Mahesh Viswanathan
Professor, Department of Computer Science
University of Illinois UrbanaChampaign, Rapporteur

Laurent Fribourg
Research Director
CNRS, ENS Cachan, Examinateur

Luc Jaulin
Professor
University Bretagne Occidentale, Examinateur

Thao Dang
Research Director
CNRS, Directeur de thèse

Abstract

Computing reachable sets is a de facto approach used in many formal verification methods for hybrid systems. But exact computation of the reachable set is an intractable problem for many kinds of hybrid systems, either due to undecidability or high computational complexity. Alternatively, quite a lot of research has been focused on using *set representations* that can be efficiently manipulated to compute sufficiently accurate over-approximation of the reachable set. Zonotopes are a useful set representation in reachability analysis because of their closure and low complexity for computing linear transformation and Minkowski sum operations. But for approximating the unbounded time reachable sets by *positive invariants*, zonotopes have the following drawback. The effectiveness of a set representation for computing a positive invariant depends on efficiently encoding the directions for convergence of the states to an equilibrium. In an affine hybrid system, some of the directions for convergence can be encoded by the complex valued eigenvectors of the transformation matrices. But the zonotope representation can not exploit the complex eigenstructure of the transformation matrices because it only has real valued generators.

Therefore, we extend real zonotopes to the complex valued domain in a way that can capture contraction along complex valued vectors. This yields a new set representation called *complex zonotope*. Geometrically, complex zonotopes represent a wider class of sets that include some non-polytopic sets as well as polytopic zonotopes. They retain the merit of real zonotopes that we can efficiently perform linear transformation and Minkowski sum operations and compute the support function. Additionally, we show that they can capture contraction along complex valued eigenvectors. Furthermore, we develop computationally tractable approximations for inclusion-checking and intersection with half-spaces. Using these set operations on complex zonotopes, we develop convex programs to verify *linear invariance properties* of discrete time affine hybrid systems and exponential stability of *linear impulsive systems*. Our experiments on some benchmark examples demonstrate the efficiency of the verification techniques based on complex zonotopes.

Résumé

Le calcul de l'ensemble atteignable est une approche utilisée dans de nombreuses méthodes de vérification formelles pour des systèmes hybrides. Mais le calcul exact de l'ensemble atteignable est un problème dûr pour plusieurs classes de systèmes hybrides, soit en raison de l'indécidabilité ou de la complexité de calcul élevée. Alternativement, beaucoup de recherches ont été centrées sur le dévéloppement des représentations d'ensembles qui peuvent être manipulées efficacement pour calculer une surapproximation suffisamment précise de l'ensemble atteignable. Les zonotopes sont une représentation d'ensemble utile pour l'analyse d'accessibilité en raison de leur fermeture et de leur faible complexité pour le calcul de la transformation linéaire et de la somme de Minkowski. Mais pour approximer l'ensemble atteignable pour une durée de temps non bornée par des invariants positifs, les zonotopes présentent l'inconvénient suivant. L'efficacité d'une représentation d'ensemble pour calculer un invariant positif dépend de l'encodage efficace des directions de convergence des états vers un point d'équilibre. Dans un systéme hybride affine, certaines des directions de convergence peuvent être dérivées à partir des vecteurs propres des matrices de dynamiques continues. Mais la représentation zonotopique usuelle ne peut pas exploiter la structure des vecteurs propres complexe de ces matrices de transformation car la représentation zonotopique usuelle ne se définit avec des générateurs á valeurs réelles.

Par conséquent, nous étendons les zonotopes réels au domaine complexe afin de capturer la contraction le long des vecteurs propres complexes, ce qui amène à une nouvelle représentation d'ensemble appelée *zonotope complexe*. Géométriquement parlant, les zonotopes complexes représentent une classe d'ensembles plus large qui comprennent des ensembles non-polytopiques ainsi que des zonotopes polytopiques. Ils conservent les avantages des zonotopes réels permettant d'effectuer efficacement la transformation linéaire et les opérations de somme de Minkowski et calculer la fonction de support. De plus, nous développons des algorithmes approximatifs pour le test d'inclusion et le calcul d'intersection avec des demi-espaces. En utilisant ces opérations sur des zonotopes complexes, nous développons ensuite des programmes convexes pour vérifier les propriétés d'invariance linéaire des systémes hybrides affines á temps discret et la stabilité exponentielle des

systémes impulsifs linéaires. Nos résultats expérimentaux sur certains exemples de benchmarks démontrent l'efficacité nos techniques de vérification basées sur des zonotopes complexes.

Acknowledgements

I have learned a lot through discussions with my adviser Dr. Thao Dang. She has inspired me by explaining many interesting research problems. I had the flexibility to work on any topic, which provided me a wide exposure. Her constant enthusiasm for research has been a motivating factor. She has also been a very friendly and light-hearted person. I remain grateful to her for providing me the opportunity to work under her supervision and thank her for the valuable time she has invested in guiding me.

I had the valuable opportunity to exchange ideas with the members of MALTHY project. Especially, I would like to thank Dr. Tristan Le Gall for inviting me to CEA Saclay at the beginning of my research. Some of the essential ideas in my research have been developed during the visit. I also thank him for showing me around Paris and making the time enjoyable.

My interaction with the research team at Toyota in North America has given me very useful exposure to the problems relevant to industry. I am thankful to Jim Kapinski, Xiaoqing Jin and Jyotirmoy Deshmukh for inviting to visit Toyota and collaborating with me in research. I would like to thank Alexandre Donzé for the ideas that we have discussed, his research collaboration and help with the Breach toolbox.

I would like to thank Prof. Sylvie Putot, Prof. Mahesh Viswanathan, Dr. Laurent Fribourg and Prof. Luc Jaulin for serving on my thesis committee and providing valuable feedback.

My interaction with the researchers and colleagues at VERIMAG has been very fruitful. I am thankful to Marcelo Forets for giving time to together ponder over research problems and his keen interest in my ideas. I am thankful to Dr. Oded Maler for organizing the group meetings through which I could get to know about new research directions. I would like to thank my friends Dogan, Alexandre, Nikolaos, Irini and Alexey, the researchers, colleagues and staff at VERIMAG for creating a lively work atmosphere. I also thank my friend Deepankar for the fun times and his support.

I am thankful to my parents for their love and always encouraging me.

Publications

The work done during my Doctoral studies is published in the following peer reviewed conferences.

1. Arvind Adimoolam and Thao Dang. Augmented complex zonotopes for computing invariants of affine hybrid systems. In *International Conference on Formal Modeling and Analysis of Timed Systems*, pages 97–115. Springer, 2017.

2. Arvind Adimoolam, Thao Dang, Alexandre Donzé, James Kapinski, and Xiaoqing Jin. Classification and coverage-based falsification for embedded control systems. In *International Conference on Computer Aided Verification*, pages 483–503. Springer, 2017.

3. Arvind Adimoolam and Thao Dang. Template complex zonotopes for stability and invariant computation. In *American Control Conference (ACC), 2017*. IEEE, 2017.

4. Arvind S Adimoolam and Thao Dang. Using complex zonotopes for stability verification. In *American Control Conference (ACC), 2016*, pages 4269–4274. IEEE, 2016.

Contents

List of Figures

List of Tables

Notation

- $\mathbb{R}$: Real numbers, $\mathbb{C}$: Complex numbers, $\mathbb{Z}$: Integers.
- $\overline{\mathbb{R}} = \mathbb{R} \bigcup \{\infty, -\infty\}$.
- If $a, b \in \mathbb{R} \bigcap -\infty, \infty$, then $(a, b) = \left\{x \in \overline{\mathbb{R}} : \ a < x < b\right\}$, $[a, b) = \left\{x \in \overline{\mathbb{R}} : \ a \leq x < b\right\}$, $(a, b] = \left\{x \in \overline{\mathbb{R}} : \ a < x \leq b\right\}$ and $[a, b] = \left\{x \in \overline{\mathbb{R}} : \ a \leq x \leq b\right\}$
- $\mathbb{M}_{n \times m}(S)$: Set of $n \times m$ matrices over the set S.
- If $X \in \mathbb{M}_{n \times m}(S)$, then X_i is the i^{th} row of X. X_{ij} is the i^{th} row j^{th} column entry of X.
- Let $a \in \mathbb{R}$, $n \in \mathbb{Z}$, $S \subseteq \mathbb{R}$ and $\bowtie \in \{\geq, \leq, >, <\}$. Then $S_{\bowtie a} = \{x \in S : x \bowtie a\}$ and $S^n = \mathbb{M}_{n \times 1}(S)$.
- If $\bowtie \in \{\geq, \leq, <, >\}$, and $x, y \in \mathbb{R}^n$, then $x \bowtie y$ iff $x_i \bowtie y_i$ for all $i \in \{1, \ldots, n\}$.
- For any $x, y \in \mathbb{R}^n$, their join is denoted $x \bigvee y$ and meet is denoted $x \bigwedge y$, which are defined as follows. For any $i \in \{1, \ldots, n\}$,

$$\left(x \bigvee y\right)_i = \sup\{x_i, y_i\}, \quad \left(x \bigwedge y\right)_i = \inf\{x_i, y_i\}.$$

- For any $c = a + \imath b \in \mathbb{C}$, $\operatorname{Re} c = a$, $\operatorname{Im} c = b$ and $|c| = \sqrt{a^2 + b^2}$.
- If $y \in \mathbb{C}^n$, then $\|y\|_2 = \sqrt{\sum_{i=1}^n |y|^2}$ and $\|y\|_\infty = \sup_{i=1}^n |y|$.
- If $A \in \mathbb{M}_{n \times m}(\mathbb{C})$, then $\|A\|_2 = \sup\{\|Ax\|_2 : \|x\|_2 = 1\}$ and $\|A\|_\infty = \sup\{\|Ax\|_\infty : \|x\|_\infty = 1\}$.
- If S is a finite set, then $|S|$ is the number of elements in S. On the other hand, if S is an infinite set, then $|S| = \infty$.
- If $S \subseteq \mathbb{C}^n$ and is a finite set, i.e., $|S| < \infty$, then the convex hull of S is

$$\boldsymbol{Conv}(S) = \left\{ \sum_{i=1}^{|S|} a_i x_i : \ x_i \in S, \ a \in \mathbb{R}_{\geq 0}^{|S|}, \ \sum_{i=1}^{|S|} a_i = 1 \right\}.$$

– For an infinite subset $S \subseteq \mathbb{C}^n$, its convex hull is defined in terms of the convex hulls of finte subsets as follows.

$$\boldsymbol{Conv}\left(S\right) = \bigcup_{\{V \subseteq S:\ |V| < \infty\}} \boldsymbol{Conv}\left(V\right)$$

– The set of all real valued polynomials of multiple variables $\{x_1, \ldots, x_n\}$ is $\mathbb{R}\left[x_1, \ldots, x_n\right]$.

– A point $p \in \mathbb{C}^n$ is called an interior point of a set $S \subseteq \mathbb{C}^n$ if there exists $b \in \mathbb{R}_{\geq 0}$ such that $\{x : \left\|p - x\right\|_\infty \leq b\} \subseteq S$. The set S is called an open set if all of its elements are interior points.

– A set is closed if it is the complement of an open set.

– A set $S \subseteq \mathbb{C}^n$ is bounded if $\sup_{x \in S} \left\|x\right\|_2 < \infty$. The set S is compact if it is closed and bounded.

– The null-space of a matrix $A \in \mathbb{M}_{m \times n}\left(\mathbb{C}\right)$ is

$$\mathrm{null}\left(A\right) = \left\{x \in \mathbb{C}^n :\ Ax = 0\right\}.$$

CHAPTER 1

Introduction

Physical systems controlled by digital logic exhibit a mix of continuous dynamics, described by differential or difference equations, and discrete dynamics described by switching of discrete valued variables. Mathematical models describing the behavior of such systems are called *hybrid systems*. Formal verification of hybrid systems generally requires computing the set of reachable states of the system. But exactly computing the reachable states of a hybrid system is either undecidable or computationally expensive. For hybrid systems that have differential equations, exact computation of the reachable set is undecidable [ACH+95], except in particular cases [LPY98]. Even in a simpler case like a discrete time affine hybrid system, the exact reachable set at any time is a union of sets whose number is exponential in the number of time steps. An alternative is find a sufficiently accurate over-approximation of the infinite set of reachable states. To do so, we need to represent an infinite set of states symbolically by a *set representation*, which can be efficiently manipulated for the computation of the desired over-approximation.

Verification of some properties of hybrid systems requires over-approximating the unbounded time reachable set of a system. The unbounded time reachable set can be approximated by a *positive invariant*, which is a set of states whose set of successor states is contained within itself. The efficiency, in terms of accuracy and computational speed, for computing positive invariants using a set representation is related to the following characteristics of the set representation.

1. Closure under set operations used in reachability analysis and computational complexity of performing them. Some of these operations are linear transformation, Minkowski sum, intersection, computation of support function and inclusion-checking.

2. Efficient encoding of positive invariants in the set representation.

Well-known set representations have some of the above characteristics, but not all. For example, polytopes have the advantage that they are closed under linear transformation, Minkowski sum and intersection. However, for a half-space representation of a polytope, the Minkowski sum operation is computationally expensive in higher dimensions. Moreover, to our knowledge, there is no upper bound on the representation size of a polytopic positive invariant having non-empty interior for a stable linear system. Ellipsoids have the advantage that they are closed under linear transformation and also efficiently encode the positive invariant of a stable linear system. But ellipsoids are not closed under Minkowski sum and intersection with half-spaces. Although there has been work on over-approximation of the Minkowski sum and intersection with half-spaces for ellipsoids [AGG+17, KV06], still there can be a significant approximation error. Zonotope [Gir05a] is yet another set representation, which is a type of polytope specified as a linear combination of real vectors whose combining coefficients are bounded inside intervals. Geometrically, they are Minkowski sums of line segments.

Zonotopes have the advantage that they are closed under linear transformation and Minkowski sum operations, which can also be computed efficiently. Therefore, they have been successfully applied to the computation of bounded time reachable sets of uncertain continuous linear systems [Gir05a] and affine hybrid systems with simple switching [MK14, GLG08]. But for over-approximation of the *unbounded time reachable set by a positive invariant*, a drawback of real zonotopes can be explained as follows. The accuracy of over-approximation by a positive invariant is closely related to the capturing the directions for convergence of the states to an equilibrium. In affine hybrid systems, some of these directions can be encoded by the complex eigenvectors of a linear transformation. In case of real zonotopes, we shall show that when the eigenvectors of a stable linear transformation are real valued, then collecting the eigenvectors of the matrix among the generators of the zonotope gives a positively invariant real zonotope. However, this result does not hold when the eigenvectors have complex values, i.e., have non-zero imaginary and real parts. In other words, real zonotopes can not exploit the complex valued eigenstructure of the transformation matrices for efficient computation of a positive invariant, because they have real valued generators.

To capture contraction along complex valued vectors, we extend real zonotopes to the complex valued domain to yield a set representation called *complex zonotope*. A complex zonotope is a linear combination of complex valued vectors with absolute valued bounds on the combining coefficients. It can capture contraction along the complex eigenvectors of a linear system, due to which they

Set representation	Linear transformation	Minkowski sum	Intersection with half-space	Positive Invariant (non-empty interior) stable invertible linear transformation
Convex polytope H-representation	Efficient only for invertible matrix	More than exponential complexity	Efficient	Maximum complexity of encoding not bounded
Zonotope	Efficient	Efficient	Not closed	May not exist
Ellipsoid	Efficient	Not closed	Not closed	Efficient encoding
Polynomial sub-level set	More than exponential complexity	More than exponential complexity	Efficient	Efficient encoding
Complex Zonotope	Efficient	Efficient	Not closed	Efficient encoding

Table 1.1: Comparison of set representations

can efficiently encode positive invariants of a linear system. It is also geometrically more expressive than real zonotope because its real projection can represent Minkowski sums of some ellipsoids in addition to line segments. They are also different from other extensions of complex zonotopes, like quadratic zonotopes [AGW15], which we shall explain later in a separate section. Still, complex zonotopes retain the merit of real zonotopes that they are closed under linear transformation and Minkowski sum, which can also be computed efficiently. In Table 1.1, we draw comparison of complex zonotopes with four other categories of set representations comprising convex polytopes, zonotopes, ellipsoids and polynomial sub-level sets. A review of the other set representations and related work on computing positive invariants will be presented in a separate section.

We apply complex zonotopes to two problems in the domain of hybrid systems that require computing accurate positive invariants. One problem is verifying *linear invariance properties* of discrete time affine hybrid systems. A linear invariance property is a linear constraint on the state of the system that is satisfied by all the reachable states. We derive a convex program based for computing positively invariant complex zonotopes that verify a linear invariance property. We demonstrate the efficiency of our method by experiments on some benchmark examples. The other problem is verifying stability of linear impulsive systems with sampling uncertainty. We develop an algorithm that finds a contractive complex zonotope using the eigenstructure of the system. Our experiments on two benchmark examples show either better or comparable performance compared to other approaches.

1.1 Review of set representations and related work

We shall briefly review some of the set representations that are mainly used in the reachability analysis of hybrid systems, particularly focusing on affine hybrid systems. Along the way, we also discuss the related work and draw comparison with our complex zonotopes. We categorize the set representations into four classes and discuss them in separate sections: polytopes, zonotopes, ellipsoids and polynomial sub-level sets. Reachability analysis techniques using non-convex polytopes generally extend techniques used for convex polytopes. Therefore, we review convex polytopes instead of polytopes. Although zonotopes are a subclass of polytopes, we discuss them in a separate section. We particularly focus our review on real zonotopes since our work extends them to complex zonotopes.

1.1.1 Convex polytopes

Polytopes are sets that satisfy Boolean combinations of linear inequalities. Polytopes have been used in many tools for verification [KGBM04, SRKC00, ADM02, BHZ08, Fre08]. A convex polytope is a special case where a polytope is convex. Generally, a half-space representation of a convex polytope, also called a H-representation, is used in the verification algorithms for hybrid systems, which is defined as follows.

Definition 1.1.1 (H-representation)**.** Let us consider a matrix $T \in \mathbb{M}_{r\times n}(\mathbb{R})$ and a vector $d \in \mathbb{R}^r$. The H-representation of a convex polytope is a tuple (T, d) that is assigned to the set

$$[\![T, d]\!] = \{x \in \mathbb{R}^n : Tx \leq d\}.$$

The row vectors of T are sometimes called *support vectors* [FLGD+11]. An invertible linear transformation of a H-representation can be computed by the following formula. Let A be an invertible matrix. Then

$$A\,[\![T, d]\!] = [\![TA^{-1}, d]\!].$$

But when the matrix A is not invertible, the computation of the transformed polytope can be expensive.

Computing the Minkowski sum of two H-representations in an n-dimensional space can require elimination of at least n-variables in a system of more than $2n$ linear inequalities, which is discussed in [Kva05]. The complexity of variable elimination by known algorithms is more than exponential. Therefore, computation of Minkowski sum of two H-representations can be costly in higher dimensions.

The intersection of two H-representations having the same set of supporting hyperplanes is easy to compute, as follows.

$$[\![T, d]\!] \bigcap [\![T, e]\!] = \left[\!\!\left[T, d \bigwedge e\right]\!\!\right]. \tag{1.1}$$

The above operation also generalizes to the intersection with half-spaces by including the support vectors of the half-spaces among the support vectors of a H-representation. Therefore, a H-representation is efficient while computing intersections with linear guards of hybrid systems.

In [RGK+04], a method for computing the maximal polytopic positive invariant set for a piecewise affine hybrid system is implemented using the MPT toolbox[1]. However, the method involves partitioning of the state space, which can be computationally expensive in higher dimensions. Some sub-classes of convex polytopes that have been used for computing positive invariants include template polyhedra [DG11, SDI08a], hypercube [CC76, Tiw08], parallelotopes [AS12], octagons [Min06] and support vectors [FLGD+11]. In these set representations, generally mathematical optimization is used for performing the operations required for computing a positive invariant (for example [DG11, DM98]). In simpler abstract domains [Min06, CC76, AS12], algebraic methods can be used to compute positive invariants. In [DG11], the normals to the bounding hyperplanes are fixed and the algorithm tries to find the tightest possible bounds of a positive invariant. Our template based approach to compute complex zonotopic positive invariants is in a similar spirit. We fix a set directions for the generators and optimize their magnitudes. However, in our approach we can choose complex valued templates that can capture contraction along the complex eigenvectors of the transformation matrices. But such complex valued templates can not be selected for polytopes.

It is known that for any stable linear system, there exists a positively invariant polytope with non-empty interior given by a polyhedral Lyapunov function [BM08]. However, to our knowledge, there is no known upper bound on the smallest possible representation size of a polyhedral lyapunov function for a stable linear systems. In contrast, for a stable and invertible linear transformation, a complex zonotopic positive invariant containing the origin in its interior can be computed by just having the n-eigenvectors as its generators.

Real zonotopes are also a sub-class of polytopes, which we discuss in a separate section.

[1] http://people.ee.ethz.ch/~mpt/3/

1.1.2 Zonotopes and their generalizations

Simple zonotopes are linear projections of higher dimensional hypercubes onto lower dimensional spaces, therefore a sub-class of polytopes. A simple zonotope is represented by a linear combination of real valued vectors plus a center, such that the real valued combining coefficients are contained in a hypercube symmetric around the origin. Geometrically speaking, a simple zonotope is a Minkowski sum of line segments.

Definition 1.1.2 (Simple zonotope)**.** Let us consider $\mathcal{V} \in \mathbb{R}^m$, whose column vectors are called *generators*, and $c \in \mathbb{R}^n$ called the *center*. The following is the representation of a real zonotope.

$$\mathcal{Z}(\mathcal{V}, c) := \{c + \mathcal{V}\zeta : \zeta \in [-1, 1]^m\}.$$

For the rest of this chapter, we use the notation $\mathcal{V} \in \mathbb{R}^m$ and $c \in \mathbb{R}^n$, unless otherwise specified.

A main advantage of the zonotope set representation is that besides being closed under linear transformation and Minkowski sum, these operations can be computed efficiently. The computation of linear transformation of a zonotope is given below.

Lemma 1.1.3 (Linear transformation)**.** *Let $A \in \mathbb{M}_{n\times n}(\mathbb{R})$. Then*

$$A\mathcal{Z}(\mathcal{V}, c) = \mathcal{Z}(A\mathcal{V}, Ac).$$

Proof. We derive the following.

$$\begin{aligned} &A\mathcal{Z}(\mathcal{V}, c) = A\{c + \mathcal{V}\zeta : \zeta \in [-1, 1]^m\} \\ &= \{Ac + A\mathcal{V}\zeta : \zeta \in [-1, 1]^m\} = \mathcal{Z}(A\mathcal{V}, Ac). \end{aligned}$$ □

The Minkowski sum of two zonotopes can be computed as follows.

Lemma 1.1.4 (Minkowski sum)**.** *Let us consider two matrices $\mathcal{V} \in \mathbb{M}_{n\times m}(\mathbb{R})$ and $\mathcal{V}' \in \mathbb{M}_{n\times r}(\mathbb{R})$. Then the following is true.*

$$\mathcal{Z}(\mathcal{V}, c) \oplus \mathcal{Z}(\mathcal{V}', c') = \mathcal{Z}\left(\begin{bmatrix}\mathcal{V} & \mathcal{V}'\end{bmatrix}, c + c'\right).$$

Proof. We derive the following.

$$\begin{aligned} &\mathcal{Z}(\mathcal{V}, c) \oplus \mathcal{Z}(\mathcal{V}', c') \\ &= \{c + \mathcal{V}\zeta : \zeta \in [-1, 1]^m\} \oplus \{c' + \mathcal{V}'\zeta' : \zeta' \in [-1, 1]^r\} \\ &= \{(c + c') + \mathcal{V}\zeta + \mathcal{V}\zeta' : \zeta \in [-1, 1]^m,\ \zeta' \in [-1, 1]^r\} \\ &= \left\{(c + c') + \begin{bmatrix}\mathcal{V} & \mathcal{V}'\end{bmatrix}\begin{bmatrix}\zeta \\ \zeta'\end{bmatrix} : \begin{bmatrix}\zeta \\ \zeta'\end{bmatrix} \in [-1, 1]^{m+r}\right\} \\ &= \mathcal{Z}\left(\begin{bmatrix}\mathcal{V} & \mathcal{V}'\end{bmatrix}, c + c'\right). \end{aligned}$$ □

We have earlier discussed that for a H-representation of a polytope, the complexity of Minkowski sum can be more than exponential. On the other hand, the complexity of both Minkowski sum and linear transformation operations for a zonotope is only linear. This is an advantage of the zonotope representation compared to the H-representation of a polytope. Therefore, simple zonotopes have been successfully applied for reachability analysis of uncertain linear systems and some affine hybrid systems with simple switching conditions [MK14, Gir05b, GLG08, BGP+09]. Still, zonotopes have the following drawback while computing positive invariants of affine hybrid systems. Even for the simple case of a stable linear system having complex valued eigenvectors, we do not know if a positively invariant non-zero zonotope exists. When a stable linear system has real eigenvectors, the computation of a non-zero positively invariant zonotope is guaranteed by the following proposition.

Proposition 1.1.5. *Let us consider $\mathcal{V} \in \mathbb{M}_{n\times n}(\mathbb{R})$ consists of the real eigenvectors of a matrix $A \in \mathbb{M}_{n\times n}(\mathbb{R})$ as its column vectors, where $\mu \in [-1,1]^n$ is the vector of real eigenvalues, i.e., $A\mathcal{V} = \mathcal{V}\,\mathrm{diag}(\mu)$. Then, $A(\mathcal{Z}(\mathcal{V},0)) \subseteq \mathcal{Z}(\mathcal{V},0)$.*

Proof. We derive

$$\begin{aligned} &A(\mathcal{Z}(\mathcal{V},0)) = A\{\mathcal{V}\zeta :\ \zeta \in [-1,1]^n\} \\ &= \{A\mathcal{V}\zeta :\ \zeta \in [-1,1]^n\} = \{V\,\mathrm{diag}(\mu)\,\zeta :\ \zeta \in [-1,1]^n\}. \end{aligned} \tag{1.2}$$

Let y be a point in $\mathcal{Z}(\mathcal{V},0)$. By Equation 1.2, we get

$$\exists \delta \in [-1,1]^n :\ y = \mathcal{V}\,\mathrm{diag}(\mu)\,\delta.$$

Let $\zeta = \mathrm{diag}(\mu)\,\delta$. Since $\mu \in [-1,1]^n$ and $\delta \in [-1,1]^n$, we get $\zeta = \mathrm{diag}(\mu)\,\delta \in [-1,1]^n$. So,

$$\begin{aligned} &y = \mathcal{V}\zeta \quad \text{where } \zeta \in [-1,1]^n \\ &\therefore\ y \in \mathcal{Z}(\mathcal{V},0). \end{aligned}$$

As the above is true for any $y \in A\mathcal{Z}(\mathcal{V},0)$, we get $A(\mathcal{Z}(\mathcal{V},0)) \subseteq \mathcal{Z}(\mathcal{V},0)$ when $\mu \in [-1,1]^n$. □

However, the eigenvalues of a linear matrix can have non-zero imaginary part, in addition to the real part. Whereas, simple zonotopes are defined on real numbers. So, when the eigenvalues are complex valued, we can not rely on the above proposition to find a positive invariant. Therefore, in the next chapter we introduce complex zonotopes that can capture contraction along complex vectors.

To approximate non-linear transformations of zonotopes, they have been extended to quadratic zonotopes [AGW15], and more generally, polynomial zonotopes [Alt13]. Although a polynomial zonotope and the complex zonotope that we introduce are both non-polytopic sets, these representations are geometrically different. While a polynomial zonotope is described by a polynomial function of real valued intervals, a complex zonotope shall be described as a complex valued linear function of circles in the complex plane.

Definition 1.1.6. [Alt13] Let $f \in \mathbb{R}[x_1, \ldots, x_n]$. Then $\{f(x) : x \in [-1, 1]^n\}$ is a polynomial zonotope.

Another drawback of simple zonotopes is that they not closed under intersection with half-spaces. The computation of intersection with half-spaces and hyperplanes is required in reachability analysis of hybrid systems having linear guards (pre-conditions) for switching. To compute the intersection, we can try to convert a zonotope to a polytope, compute the intersection with the polytope and over-approximate the intersection by another zonotope. However, a zonotope with m generators in an n dimensional space can have as many as $2\binom{m}{n-1}$ faces [Zas75], which is exponential in n. It means that the conversion of a zonotope to a polytope can be intractable in higher dimensions. To address this problem, an algorithm for the tight over-approximation of the intersection between a zonotope and a hyperplane is proposed in [GLG08], that is based on the projection of the zonotope onto 2-dimensional hyperplanes. Alternatively, there are approaches to extend the zonotope to a more general set representation in which the intersection with a half-space is a closed operation and can be computed efficiently. Constrained zonotopes [SRMB16], constrained affine sets [GGP10] and zonotopic bundles [AK11b] are examples of such extensions.

In a constrained zonotope, there are linear equality constraints in addition to interval constraints on the combining coefficients. Therefore, the intersection of a hyperplane and a constrained zonotope can be represented by another constrained zonotope. Moreover, they retain the closure property under linear transformation and Minkowski sum, which can also be computed efficiently.

Definition 1.1.7 (Constrained zonotope)**.** [SRMB16] A constrained zonotope is represented by a tuple $(\mathcal{V}, c, A, b)$, where $\mathcal{V} \in \mathbb{M}_{n\times m}(\mathbb{R})$, $A \in \mathbb{M}_{k\times m}(\mathbb{R})$, $c \in \mathbb{R}^n$ and $b \in \mathbb{R}^m$, and the tuple is assigned to the set

$$\{c + \mathcal{V}\zeta : \zeta \in [-1, 1]^m, A\zeta = b\}.$$

An even more general representation is a constrained affine set [GGP10], where the combining coefficients can range in some abstract domain. To represent

the intersection of a constrained affine set with half-spaces, the abstract domain constraining the combining coefficients can be chosen such that it has linear relations. Another generalization is a zonotopic bundle set representation [AK11b], which is closed under mutual intersection.

1.1.3 Ellipsoids

Ellipsoids are sub-level sets of positive semi-definite quadratic forms. In control theory, they are implicitly found while computing quadratic Lyapunov functions for proving stability or stabilizability of systems [BM08]. An ellipsoid is represented by a pair of a positive semi-definite symmetric matrix $Q \in \mathbb{M}_{n\times n}(\mathbb{R})$ and a center $c \in \mathbb{R}^n$, which is assigned to the following set.

$$[\![Q, c]\!] := c \oplus \left\{x \in \mathbb{R}^n : \; x^T Q x \leq 1\right\}.$$

The existence of ellipsoidal positive invariants is guaranteed for specific classes of affine hybrid systems [SNM03]. Many techniques for computing ellipsoidal approximations of reachable set for affine hybrid system use mathematical optimization [BM08, KV06, RJGF12]. An alternative approach for computing positively invariant ellipsoids was presented in [AaNSGP16], which uses fixed point iteration based on Löwner order. In this work, each iteration involves only algebraic computations, which possibly resulted in better computational efficiency than semi-definite programming on the tested examples.

Ellipsoids are closed under invertible linear transformations. But they are not closed under Minkowski sum and intersection with half-spaces. The ellipsoidal toolbox [KV06] and a recent approach based on Löwner order [AGG+17] have addressed the problem of over-approximating the Minkowski sum of ellipsoids and their intersection with half-spaces. For Minkowski sum, the ellipsoidal toolbox can compute an approximation that is tight along a specified direction. But a single ellipsoid can not provide a tight approximation of a Minkowski sum along all the directions. Whereas, zonotopes and complex zonotopes have the advantage that they are closed under Minkowski sum, which can also be computed efficiently.

1.1.4 Polynomial sub-level sets

A polynomial sub-level set encodes a set of points that satisfy a collection of multi-variate polynomials. It is a natural extension of the H-representation of the polytope to non-polytopic sets for better approximation. Mathematically, a polynomial sub-level set is defined as follows.

Definition 1.1.8. A polynomial sub-level set is represented by a tuple (f, d), where $f \in (\mathbb{R}[x_1, \ldots, x_n])^r$ and $d \in \mathbb{R}^r$, which is assigned to the following set.

$$[\![f, d]\!] = \{x \in \mathbb{R}^n : \forall i \in \{1, \ldots, r\}, \ f_i(x) \leq d_i\}$$

In [DT13], it was shown that the safety verification problem for linear systems is decidable when the initial set is a sub-level set of eigen-functions, which can be quadratic polynomials. Our extension of real zonotopes to complex zonotopes is inspired by their work, which analyzes the eigenstructure of linear systems. In [SSM04], positive invariants represented by polynomial equalities are computed for a general class of hybrid systems, where the polynomial is a linear combination of pre-chosen templates that have to be guessed. On the other hand, the method of [RCT05] computes polynomial equality invariants for affine hybrid systems without having to guess a template polynomial. But [SSM04, RCT05] can not handle an additive disturbance input set having a non-empty interior, because polynomial equalities represent hyper-surfaces which have an empty interior.

On the other hand, polynomial sub-level sets specified by polynomial inequalities can over-approximate sets having a non-empty interior. A sub-level set of a single multi-variate polynomial is implicitly found while computing barrier certificates by sum of squares programming [PJ04]. For certain classes of hybrid systems [PR05], the existence of a barrier certificate is both necessary and sufficient for safety. However, the accuracy of over-approximation provided by a single multi-variate polynomial naturally depends on the degree of the polynomial. But representing polynomials of higher degree in high dimensional spaces can be computationally expensive. Alternatively, we can use multiple number of easily encodable multi-variate polynomials for better accuracy. But computing tight approximations of reachable sets by intersection of polynomial sub-level sets requires non-convex optimization, which is expensive. To alleviate complexity of non-convex optimization problem in the case of multiple polynomials, an approach using semi-definite relaxation coupled with policy iterations has been developed in [AGG10]. However, this approach uses a recursion of convex optimization steps. So, the convergence of the recursion can be slower than polyhedral abstract domains, which generally use linear programming in the recursion. In contrast, the algorithm that we develop based on complex zonotopes for computing positive invariants of affine hybrid systems has only a single step of convex optimization.

1.2 Organization

This dissertation contains five main chapters and a conclusive chapter. In the first chapter, we have briefly discussed the desirable characteristics of a good set rep-

resentation for computing accurate positive invariants of hybrid systems. In the light of these characteristics, we provided a short review of some set representations and discuss their advantages and drawbacks. We have discussed simple zonotopes, which are defined over real numbers, and the linear transformation and Minkowski sum operations on them. We explained the shortcoming of real zonotopes that they can not capture contraction along complex valued eigenvectors, which is closely related to computing positive invariants. We also reviewed some of the previously known extensions of real zonotopes.

In Chapter 2, we introduce the complex zonotope set representation and discuss set operations on them required for reachability analysis. We first define the basic representation of a complex zonotope. We derive a result that a complex zonotope can efficiently represent a non-zero positive invariant for a stable linear transformation based on the eigenstructure. Next we introduce the template based representation of a complex zonotope, called *template complex zonotope*. It allows adding more generators to a template for increasing the quality of approximation of a given set. Later we discuss set operations on template complex zonotopes and derive a second order conic program for checking inclusion between two template complex zonotopes.

In Chapter 3, we generalize complex zonotope to an *augmented complex zonotope* representation for computing over-approximation of the intersection with a class of sub-level sets of linear inequalities called *sub-parallelotopes*. We first introduce a representation called *interval zonotope*, which is a different but geometrically equivalent representation of a simple zonotope. An interval zonotope has variable interval bounds on the combining coefficients. We show that the intersection between an interval zonotope and a suitably aligned sub-parallelotope is another interval zonotope which can be computed algebraically. Motivated by this result, we define an augmented complex zonotope as a Minkowski sum of a complex zonotope and a real zonotope. By this representation, we can efficiently compute the over-approximation of its intersection with a sub-parallelotope, where the approximation error can be regulated by adjusting the scaling factors. Latter we discuss other set operations on augmented complex zonotopes. We extend the inclusion-checking relation between template complex zonotopes to augmented complex zonotopes.

In Chapter 4, we describe a discrete time affine hybrid system, its positive invariants and the problem of verifying a *linear invariance property*. We develop a convex program to verify a linear invariance property based on computing a positively invariant augmented complex zonotope. We implement the method on some benchmark examples to demonstrate its efficiency.

In Chapter 5, we develop an algorithm for exponential stability verification of linear impulsive systems with sampling uncertainty using template complex zonotopes. The algorithm uses the eigenstructure of reachability operators to compute

a contractive set. We implement the algorithm for stability verification of two benchmark examples and compare the results with the state-of-the-art methods.

The concluding remarks are given in Chapter 6.

CHAPTER 2

Complex Zonotopes

In the previous chapter, we have explained the advantage of simple zonotopes that they are closed under linear transformation and Minkowski sum operations and these can be computed efficiently. Regarding computation of a positive invariant real zonotope for a linear system, we showed in Proposition 1.1.5 that it can be done efficiently when the eigenvectors are real valued. However, when the eigenvectors of a stable linear system are complex valued, we can not guarantee the existence of a non-zero real zonotopic positive invariant. Overcoming this drawback of real zonotopes, we extend them to a new class of sets called *complex zonotopes* by which we can easily specify positive invariants of a stable linear system using the eigenstructure. Henceforth, we believe that even for affine hybrid systems, a complex zonotope can capture contraction along the complex eigenvectors of some of the transformation matrices. Complex zonotopes are also geometrically more expressive, since their real projections can describe some non-polytopic sets as well as polytopic zonotopes. Apart from computing simple operations on complex zonotopes like linear transformation and Minkowski sum, we shall derive a convex program for checking inclusion between two complex zonotopes. The inclusion relation is a key ingredient for efficient invariant computation, which we shall discuss in latter chapters.

This chapter is organized into three main sections. In Section 2.1, we shall introduce the basic representation of a complex zonotope that naturally extends the Definition 1.1.2 of real zonotopes. Further on, we shall introduce a more general but geometrically equivalent representation, called *template complex zonotope*, which allows efficient modification of complex zonotopic sets for increasing accuracy of abstraction of sets. In Section 2.2, we shall discuss basic operations on a

template complex zonotope like linear transformation, Minkowski sum and computation of support function. In Section 2.3, we shall derive a convex program for checking the inclusion between two template complex zonotopes.

2.1 Representation of a complex zonotope

The basic representation of a complex zonotope is a linear combination of complex valued vectors with complex combining coefficients whose absolute value is bounded by unity. This is a generalization of the representation of a simple zonotope given in Definition 1.1.2 of previous chapter to the space of complex numbers. However, the real projection of a complex zonotope is expressive because it can represent some non-polyhedral sets in addition to the polyhedral zonotopes, which we shall discuss later.

Definition 2.1.1 (Complex zonotope)**.** Let $\mathcal{V} \in \mathbb{M}_{m\times n}(\mathbb{C})$ be a complex valued matrix whose columns are called *generators* and $c \in \mathbb{R}^n$ be a real vector called the *center*. The following is the representation of a complex zonotope.

$$\mathcal{C}(\mathcal{V}, c) := \{\mathcal{V}\zeta + c : \ \zeta \in \mathbb{C}^m, \ \ \|\zeta\|_\infty \leq 1\}. \tag{2.1}$$

Geometry of a complex zonotope : The real projection of the set of points represented by each generator can either be an ellipse in a higher dimensional space or a line segment. So, complex zonotopes can represent a Minkowski sum of a higher dimensional ellipses and line segments. Whereas, simple zonotopes represent only Minkowski sum of line segments. Therefore, complex zonotopes are geometrically more expressive than real zonotopes. For example, the real projection of the the following complex vector is the following ellipse.

$$\mathcal{C}\left(\begin{bmatrix}-0.1335+0.1769\imath\\ 0.2713+0.3991\imath\\ -0.8473\end{bmatrix}, 0\right) := \left\{\begin{bmatrix}-0.1335 & -0.1769\\ 0.2713 & -0.3991i\\ -0.8473 & 0\end{bmatrix}\begin{bmatrix}a\\ b\end{bmatrix} : \ a^2+b^2 \leq 1\right\}.$$

On the other hand, the real projection of the following real vector, which is a complex vector having zero imaginary part, is a line segment.

$$\mathcal{C}\left(\begin{bmatrix}-0.4544\\ 0.7379\\ 0.4991\end{bmatrix}, 0\right) := \left\{\begin{bmatrix}-0.4544\\ 0.7379\\ 0.4991\end{bmatrix} a : \ -1 \leq a \leq 1\right\}.$$

As the real projection of the generator of a complex zonotope can either be an ellipse or a line segment, a complex zonotope can represent a Minkowski sum of line segments as well as some ellipses. The non-polyhedral real projections along the three axis oriented hyperplanes of the following 3-D complex zonotope is shown in Figure 2.1

$$\mathcal{C}\left(\begin{bmatrix} -0.2226 & -0.1335+0.1769\imath & -0.1335-0.1769\imath \\ 0.3615 & 0.2713+0.3991\imath & 0.2713-0.3991\imath \\ 0.2446 & -0.8473 & -0.8473 \end{bmatrix}, 0\right)$$

Contraction along eigenvectors: A motivation for extending simple zonotopes to complex zonotopes is that a complex zonotope with its generators as the complex eigenvectors of a discrete time linear system is positively invariant if the complex eigenvalues corresponding to the generators are bounded within unity in their absolute values. This is because the generators of the resultant complex zonotope after transformation will be scaled by the absolute values of the corresponding eigenvalues. For example, consider the following matrix A and the complex zonotope $\mathcal{C}(V, 0)$ generated by the complex eigenvectors of A.

$$A = \begin{bmatrix} 0.1502 & -0.0438 & 0.1366 \\ 0.7482 & 0.1470 & 0.1251 \\ -0.8436 & -0.7027 & 0.0418 \end{bmatrix}$$

$$V = \begin{bmatrix} -0.2226 & -0.1335+0.1769\imath & -0.1335-0.1769\imath \\ 0.3615 & 0.2713+0.3991\imath & 0.2713-0.3991\imath \\ 0.2446 & -0.8473 & -0.8473 \end{bmatrix}$$

The eigenvalues of A are -0.2291, $0.1339+0.5071\imath$ and $0.1339-0.5071\imath$, whose absolute values are 0.2291, 0.5245, and 0.5245, respectively. After the transformation by A, the set generated by V_1^T gets scaled down to 0.2291 times its size and that of V_2^T and V_3^T to 0.5245 times its their size. So, the complex zonotope, which is a Minkowski sum of these sets, contracts after the transformation. This is illustrated in Figure 2.2, which shows the contraction of each of the sets formed by the generators and the consequent contraction of the complex zonotope. This property of contraction of complex zonotope by a linear transformation based on the eigenstructure of a matrix is explained mathematically in the following proposition.

Proposition 2.1.2 (Eigenstructure based invariance)**.** *Let us consider $\mathcal{V} \in \mathbb{M}_{n\times n}(\mathbb{C})$ consists of the complex eigenvectors of a matrix $A \in \mathbb{M}_{n\times n}(\mathbb{R})$ as its column vectors and $\mu \in \mathbb{C}^n$ be the vector of complex eigenvalues, i.e., $A\mathcal{V} = \mathcal{V}\,\mathrm{diag}(\mu)$. Then*

$$A(\mathcal{C}(\mathcal{V}, 0)) = \mathcal{C}(\mathcal{V}\,\mathrm{diag}(\mu), 0).$$

If $\|\mu\|_\infty \leq 1$, then $A(\mathcal{Z}(\mathcal{V}, 0)) \subseteq \mathcal{Z}(\mathcal{V}, 0)$.

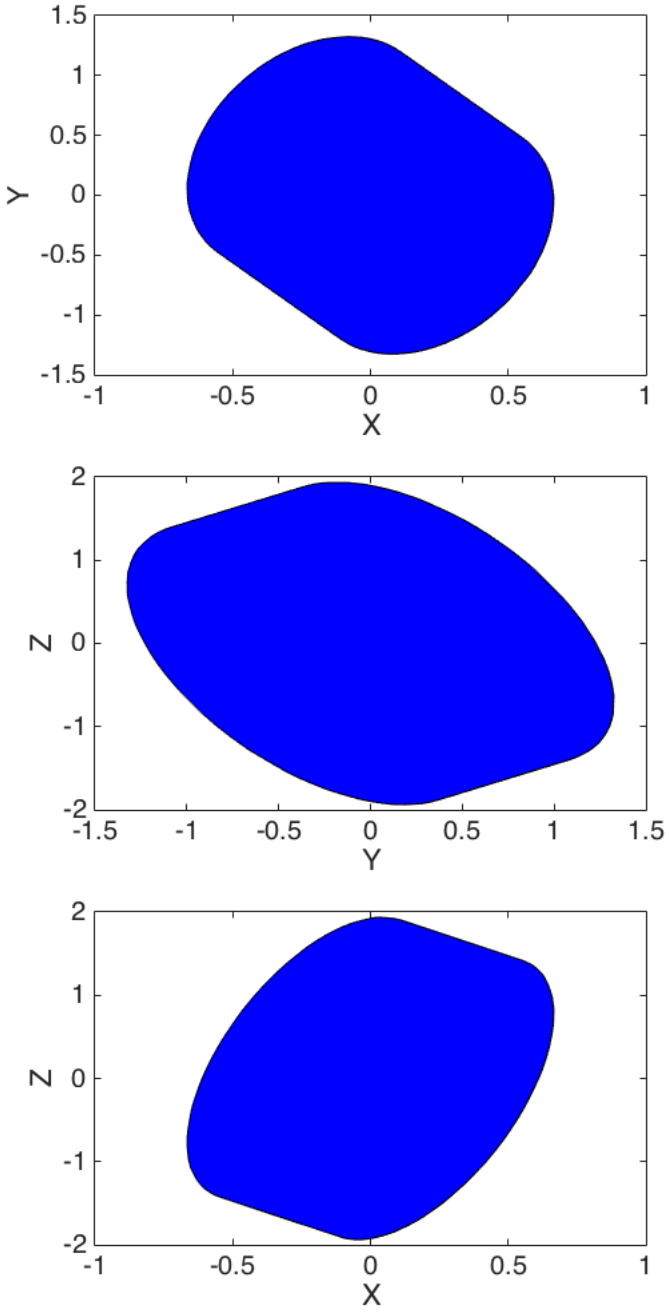

Figure 2.1: Real projection of complex zonotope on axis oriented hyperplanes

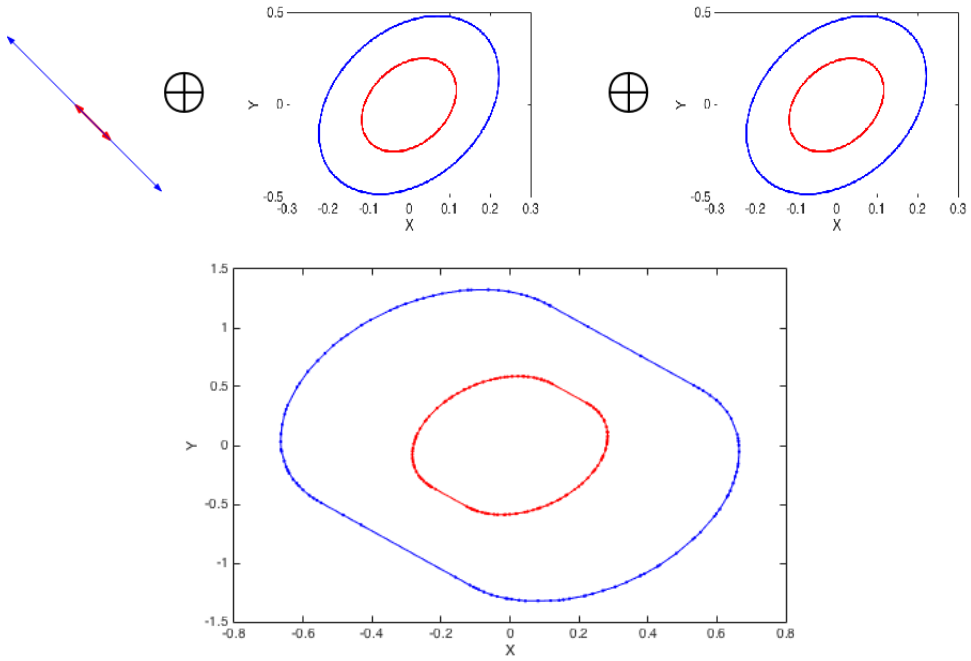

Figure 2.2: Contraction of complex zonotope along eigenvectors

Proof. We derive

$$\begin{aligned} &A\left(\mathcal{C}\left(\mathcal{V},0\right)\right) = A\left\{\mathcal{V}\zeta:\ \zeta\in\mathbb{C}^n, \left\|\zeta\right\|_\infty \leq 1\right\} \\ &= \left\{A\mathcal{V}\zeta:\ \zeta\in\mathbb{C}^n, \left\|\zeta\right\|_\infty \leq 1\right\} = \mathcal{C}\left(A\mathcal{V},0\right) = \mathcal{C}\left(\mathcal{V}\,\mathrm{diag}\left(\mu\right),0\right). \end{aligned}$$

which proves the first part of the Proposition.

For the second part, we are given that $\left\|\mu\right\|_\infty \leq 1$. Consider a point

$$\begin{aligned} &y \in A\mathcal{C}\left(\mathcal{V},0\right) = \mathcal{C}\left(\mathcal{V}\,\mathrm{diag}\left(\mu\right),0\right) \quad \text{where} \\ &y = \mathcal{V}\,\mathrm{diag}\left(\mu\right)\delta : \left\|\delta\right\|_\infty \leq 1. \end{aligned}$$

Let $\zeta = \mathrm{diag}\left(\mu\right)\delta$. Then $\left\|\zeta\right\|_\infty \leq \left\|\mu\right\|_\infty \left\|\delta\right\|_\infty \leq 1$. So,

$$y = \mathcal{V}\zeta \quad \text{where} \quad \left\|\zeta\right\|_\infty \leq 1.$$

So, we get $y \in \mathcal{C}\left(\mathcal{V},0\right)$. As this is true for all $y \in \mathcal{C}\left(\mathcal{V},0\right)$, we have $A\left(\mathcal{C}\left(\mathcal{V},0\right)\right) \subseteq \mathcal{C}\left(\mathcal{V},0\right)$ when $\left\|\mu\right\|_\infty \leq 1$. □

If we add more generators to the above representation of a complex zonotope, it would increase the size of the complex zonotope. Therefore, we can not find

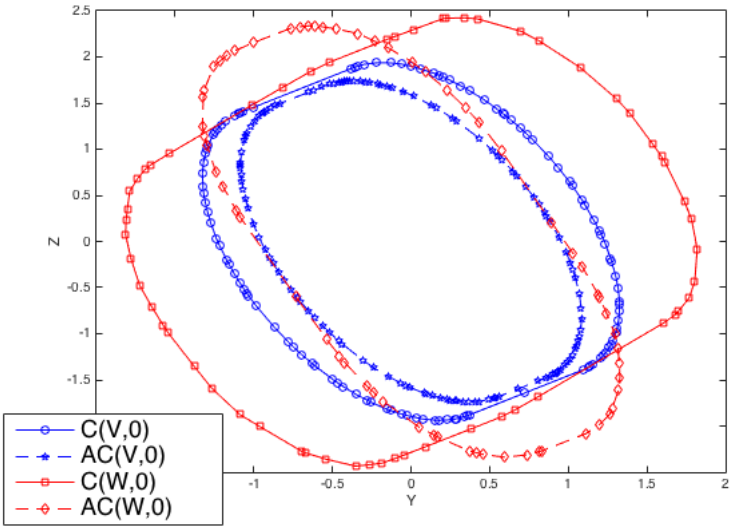

Figure 2.3: Violation of positive invariance and size increase after adding a generator to the basic representation.

better approximations of a given set by only adding more generators to the complex zonotope. Moreover, adding a generator can violate positive invariance. For example, consider the complex zonotope $\mathcal{C}(\mathcal{V}, 0)$, where

$$\mathcal{V} = \begin{bmatrix} -0.2226 & -0.1335 + 0.1769\imath & -0.1335 - 0.1769\imath \\ 0.3615 & 0.2713 + 0.3991\imath & 0.2713 - 0.3991\imath \\ 0.2446 & -0.8473 & -0.8473 \end{bmatrix}.$$

The above complex zonotope contracts after transformation by the matrix

$$A = \begin{bmatrix} -0.2766 & -0.0806 & 0.2516 \\ 1.3779 & 0.2707 & 0.2304 \\ -1.5536 & -1.2942 & 0.0769 \end{bmatrix}$$

as shown in Figure 2.3. On the other hand, when we add another generator $\begin{bmatrix} 0 & 0.5 & 0.5 \end{bmatrix}^T$, then the complex zonotope, $\mathcal{C}(W, 0)$, where

$$W = \begin{bmatrix} -0.2226 & -0.1335 + 0.1769\imath & -0.1335 - 0.1769\imath & 0 \\ 0.3615 & 0.2713 + 0.3991\imath & 0.2713 - 0.3991\imath & 0.5 \\ 0.2446 & -0.8473 + 0.0000\imath & -0.8473 & 0.5 \end{bmatrix}$$

does not contract as illustrated in Figure 2.3.

Alternatively, to refine a complex zonotope, we can adjust the magnitude of contribution of each generator to the size of the set while also preserving the

positive invariance. This way, we can also add more generators and increase approximation accuracy by adjusting the magnitudes of each generator. In order to conveniently perform algebraic manipulations on the magnitude of each generator, we can explicitly specify variable bounds on the combining coefficients. This gives us a more general representation, which we call as *template complex zonotope*, where the magnitude of each combining coefficient is bounded in its absolute value by a *scaling factor*. We call the matrix whose column vectors generate a template complex zonotope as a *template*. This representation is similar in spirit to the known template based set representations [SDI08a, Min06] in abstract interpretation, where for some fixed template, subsets of metric spaces are mapped to points in a lattice. In the case of a template complex zonotope, for a fixed template, subsets of the complex vector space can be mapped to the *scaling factors*.

Definition 2.1.3 (Template complex zonotope)**.** Let us consider $\mathcal{V} \in \mathbb{M}_{n\times m}(\mathbb{C})$ called the template, $s \in \mathbb{R}^m_{\geq 0}$ called scaling factors and $c \in \mathbb{R}^n$ called the center. Then the following is a template complex zonotope.

$$\mathcal{T}(\mathcal{V}, c, s) = \{\mathcal{V}\zeta + c : \ |\zeta_i| \leq s_i \ \forall i \in \{1, ..., m\}\}. \tag{2.2}$$

In further discussion, we use the term *representation size* of a template complex zonotope to refer to the size of the template matrix. In the rest of this chapter, we consider the following notation, unless otherwise specified.

$$\mathcal{V} \in \mathbb{M}_{n\times m}(\mathbb{C}), \quad c \in \mathbb{C}^n, \quad s \in \mathbb{R}^m_{\geq 0}.$$

A template complex zonotope can be converted to the basic representation of the complex zonotope by multiplying the diagonal matrix of scaling factors to the template. This is described in the following lemma.

Lemma 2.1.4 (Normalization)**.** *Let us consider* $\mu \in \mathbb{C}^m$.

$$\begin{aligned} \textit{Then} \qquad & \mathcal{T}(\mathcal{V}\,\mathrm{diag}(\mu), c, s) = \mathcal{T}(\mathcal{V}, c, \mathrm{diag}(|\mu|)\, s). \\ \textit{Therefore}, \qquad & \mathcal{T}(\mathcal{V}, c, s) = \mathcal{C}(\mathcal{V}\,\mathrm{diag}(s), c). \end{aligned} \tag{2.3}$$

Proof. Consider a point $x \in \mathcal{T}(\mathcal{V}\,\mathrm{diag}(\mu), c, s)$, where

$$x = c + \mathcal{V}\,\mathrm{diag}(\mu)\,\zeta : |\zeta| \leq s.$$

Let $\zeta' = \mathrm{diag}(\mu)\,\zeta$. Then, $x = c + \mathcal{V}\zeta'$. We get

$$|\zeta'| = \mathrm{diag}(|\mu|)\,|\zeta| \leq \mathrm{diag}(|\mu|)\, s.$$

Therefore, $x \in \mathcal{T}(\mathcal{V}, c, \text{diag}(\mu)\, s)$. This means,

$$\mathcal{T}(\mathcal{V}\,\text{diag}(\mu), c, s) \subseteq \mathcal{T}(\mathcal{V}, c, \text{diag}(|\mu|)\, s)$$

Next consider a point $y \in \mathcal{T}(\mathcal{V}, c, \text{diag}(|\mu|\, s))$ where

$$y = c + \mathcal{V}\epsilon : \ |\epsilon| \leq \text{diag}(|\mu|)\, s.$$

Let us consider $\epsilon' \in \mathbb{C}^m$, such that

$$\forall i \in \{1, ..., m\}, \ \ \epsilon_i = \begin{cases} \frac{\epsilon_i}{\mu_i} \text{ if } \mu_i \neq 0 \\ 0 \text{ if } \mu_i = 0. \end{cases}$$

We shall show that $\epsilon = \epsilon' \,\text{diag}(\mu)$, i.e., for any $i \in \{1, ..., m\}$, $\epsilon_i = \epsilon'_i \mu_i$. We prove it in the following two cases.

1. Let us consider $\epsilon_i \neq 0$. As $|\epsilon| \leq |\text{diag}(\mu_i)|\, s$, so $\mu_i \neq 0$. Therefore,

$$\epsilon_i = \frac{\epsilon_i}{\mu_i}\mu_i = \epsilon'_i \mu_i.$$

2. Let us consider $\epsilon_i = 0$. As $|\epsilon| \leq |\text{diag}(\mu_i)|\, s$, so $\mu_i = 0$. This implies

$$0 = \epsilon = \epsilon'_i \times 0 = \epsilon'_i \mu_i.$$

So, we get $y = c + \mathcal{V}\,\text{diag}(\mu_i)\,\epsilon'$. By the definition of ϵ', we get

$$\forall i \in \{1, ..., m\} \quad |\epsilon'_i| \leq \begin{cases} \left|\frac{\epsilon_i}{\mu_i}\right| \leq \frac{|\mu_i| s_i}{|\mu_i|} = s_i \text{ if } \mu_i \neq 0 \\ 0 \text{ if } \mu_i = 0 \end{cases}$$

Therefore, $|\epsilon'| \leq s$. So, $y \in \mathcal{T}(\mathcal{V}\,\text{diag}(\mu), c, s)$. Therefore,

$$\mathcal{T}(\mathcal{V}, c, \text{diag}(|\mu|)\, s) \subseteq \mathcal{T}(\mathcal{V}\,\text{diag}(\mu), c, s).$$

Combining the previous two conclusions, we get Equation 2.3.

By definition,

$$\begin{aligned} &\mathcal{C}(\mathcal{V}\,\text{diag}(s), c) = \mathcal{T}\left(\mathcal{V}\,\text{diag}(s), c, [1]_{m\times 1}\right) \\ &\%\% \text{ by Equation 2.3} \\ &= \mathcal{T}\left(\mathcal{V}, c, \text{diag}(s)\,[1]_{m\times 1}\right) = \mathcal{T}(\mathcal{V}, c, s). \end{aligned}$$ □

2.2 Basic operations

We shall discuss the computation of some basic operations on template complex zonotopes like linear transformation, Minkowski sum and intersection in special cases. In the next section, we shall discuss how to check inclusion between two template complex zonotopes. The set of template complex zonotopes is closed under linear transformation and Minkowski sum operations, which are straightforward algebraic computations just like in the case of simple (real) zonotopes.

Lemma 2.2.1 (Linear transformation)**.** *Let* $A \in \mathbb{M}_{n\times n}(\mathbb{R})$ *and* $\mathcal{V} \in \mathbb{M}_{n\times m}(\mathbb{C})$.

$$\textit{Then} \quad A\mathcal{T}(\mathcal{V}, c, s) = \mathcal{T}(A\mathcal{V}, Ac, s).$$

Proof. We derive

$$\begin{aligned} &A\mathcal{T}(\mathcal{V}, c, s) = A\{c + \mathcal{V}\zeta : \ \zeta \in \mathbb{C}^m, \ |\zeta| \leq s\} \\ &= \{Ac + A\mathcal{V}\zeta : \ \zeta \in \mathbb{C}^m, \ |\zeta| \leq s\} = \mathcal{T}(A\mathcal{V}, Ac, s). \end{aligned} \qquad \square$$

In the above lemma, we see that the template of a complex zonotope can change after a linear transformation. But when the column vectors of the template are the eigenvectors of the linear transformation we can represent the transformed complex zonotope using the same template by multiplying the scaling factors with the magnitudes of eigenvalues. Therefore, when the magnitudes of eigenvalues are less than one and the center is the origin, the transformed template complex zonotope contains the original template complex zonotope. This result can be seen as an extension of Proposition 2.1.2 to the case of template complex zonotopes.

Lemma 2.2.2 (Eigenstructure based scaling)**.** *Let us consider* $\mathcal{V} \in \mathbb{M}_{n\times n}(\mathbb{C})$ *consists of the complex eigenvectors of a matrix* $A \in \mathbb{M}_{n\times n}(\mathbb{R})$ *as the column vectors. Let* $\mu \in \mathbb{C}^n$ *be the vector of eigenvalues such that* $A\mathcal{V} = \mathcal{V}\,\mathrm{diag}(\mu)$.

$$\textit{Then} \ \ A\mathcal{T}(\mathcal{V}, 0, s) = \mathcal{T}(\mathcal{V}, 0, \mathrm{diag}(|\mu|)\, s). \tag{2.4}$$

Proof. Based on Equation 2.2.1 and the fact that $A\mathcal{V} = \mathcal{V}\,\mathrm{diag}(\mu)$, we get

$$A\mathcal{T}(\mathcal{V}, 0, s) = \mathcal{T}(A\mathcal{V}, 0, s) = \mathcal{T}(\mathcal{V}\,\mathrm{diag}(\mu), 0, s).$$

Then using Equation 2.3, we get

$$\mathcal{T}(\mathcal{V}\,\mathrm{diag}(\mu), 0, s) = \mathcal{T}(\mathcal{V}, 0, \mathrm{diag}(|\mu|)\, s). \qquad \square$$

The Minkowski sum of two template complex zonotopes is another template complex zonotope, which is computed as follows.

Lemma 2.2.3 (Minkowski sum)**.** *Let us consider two templates $\mathcal{V} \in \mathbb{M}_{n\times m}(\mathbb{C})$ and $\mathcal{V}' \in \mathbb{M}_{n\times r}(\mathbb{C}^r)$. We get*

$$\mathcal{T}(\mathcal{V}, c, s) \oplus \mathcal{T}(\mathcal{V}', c', s') = \mathcal{T}\left(\begin{bmatrix}\mathcal{V} & \mathcal{V}'\end{bmatrix}, c + c', \begin{bmatrix} s \\ s' \end{bmatrix}\right) \tag{2.5}$$

Proof. We derive the following.

$$\begin{aligned}
&\mathcal{T}(\mathcal{V}, c, s) \oplus \mathcal{T}(\mathcal{V}', c', s') \\
&= \{c + \mathcal{V}\zeta : \zeta \in \mathbb{C}^m, \ |\zeta| \leq s\} \oplus \{c' + \mathcal{V}\zeta' : \zeta' \in \mathbb{C}^r, \ |\zeta'| \leq s'\} \\
&= \{(c + c') + \mathcal{V}\zeta + \mathcal{V}'\zeta' : \zeta \in \mathbb{C}^m, \ \zeta' \in \mathbb{C}^r, \ |\zeta| \leq s, \ |\zeta'| \leq s'\} \\
&= \left\{(c + c') + \begin{bmatrix}\mathcal{V} & \mathcal{V}'\end{bmatrix}\begin{bmatrix}\zeta \\ \zeta'\end{bmatrix} : \begin{bmatrix}\zeta \\ \zeta'\end{bmatrix} \in \mathbb{C}^{m+r}, \ \left|\begin{bmatrix}\zeta \\ \zeta'\end{bmatrix}\right| \leq \begin{bmatrix} s \\ s' \end{bmatrix}\right\} \\
&= \mathcal{T}\left(\begin{bmatrix}\mathcal{V} & \mathcal{V}'\end{bmatrix}, c + c', \begin{bmatrix} s \\ s' \end{bmatrix}\right). \qquad \square
\end{aligned}$$

In the above lemma, we see that that the representation size of a template complex zonotope can increase after a Minkowski sum with another template complex zonotope. But when two template complex zonotopes have the same template, their Minkowski sum results in a complex zonotope with the same template, i.e., the representation size does not increase. This is described in the following Proposition.

Proposition 2.2.4 (Minkowski sum with common template)**.** *The following is true.*

$$\mathcal{T}(\mathcal{V}, c, s) \oplus \mathcal{T}(\mathcal{V}, c', s') = \mathcal{T}(\mathcal{V}, c + c', s + s') \tag{2.6}$$

Proof. We have $\mathcal{T}(\mathcal{V}, c, s) \oplus \mathcal{T}(\mathcal{V}, c', s') =$

$$\begin{aligned}
&\{(c + \mathcal{V}\zeta) + (c' + \mathcal{V}\zeta') : \zeta, \zeta' \in \mathbb{C}^m, \ |\zeta| \leq s, \ |\zeta'| \leq s'\} \\
&= \{(c + c') + \mathcal{V}(\zeta + \zeta') : \zeta, \zeta' \in \mathbb{C}^m, \ |\zeta| \leq s, \ |\zeta'| \leq s'\}
\end{aligned} \tag{2.7}$$

We shall show that

$$\{\zeta + \zeta' : \zeta, \zeta' \in \mathbb{C}^m, \ |\zeta| \leq s, \ |\zeta'| \leq s'\} = \{\zeta'' : |\zeta''| \leq s + s'\}. \tag{2.8}$$

First we shall show that the L.H.S of Equation 2.8 is contained within the R.H.S of Equation 2.8, as follows. Let us consider

$$\zeta, \zeta' \in \mathbb{C}^m : \quad |\zeta| \leq s, \ |\zeta'| \leq s'.$$

Then using the triangular inequality, we get

$$|\zeta_i + \zeta_i'| \leq |\zeta_i| + |\zeta_i'| = s + s'$$

First we shall show that the R.H.S of Equation 2.8 is contained within the L.H.S of Equation 2.8, as follows. Let us consider

$$\zeta'' \in \mathbb{C} : \ |\zeta''| \leq s + s'.$$

Let us consider

$$\zeta = s\frac{\zeta''}{s+s'}, \ \ \zeta' = s'\frac{\zeta''}{s+s'}.$$

So, $\zeta'' = \zeta + \zeta'$. As $\left|\frac{\zeta''}{s+s'}\right| \leq 1$, we get $|\zeta| \leq s$ and $|\zeta'| \leq s'$. This proves that the R.H.S of Equation 2.8 is contained inside the L.H.S of Equation 2.8.

Hence, we have proved Equation 2.8. Then the proposition follows from Equations 2.7 and 2.8. □

We denote the value of the support function of a set $\Psi \in \mathbb{R}^n$ at a vector $v \in \mathbb{R}^n$ as $\rho(v, \Psi)$, which is defined as follows.

$$\rho(v, \Psi) = \sup_{x \in \Psi} v^T x.$$

The support function of a template complex zonotope is an affine expression of the scaling factors and the center, as described in the following lemma.

Lemma 2.2.5 (Support function)**.** *Let $v \in \mathbb{R}^n$. Then*

$$\rho(v, \mathrm{Re}(\mathcal{T}(\mathcal{V}, c, s))) = v^T c + \left|v^T \mathcal{V}\right| s.$$

Proof. We derive

$$\begin{aligned}
\rho(v, \mathrm{Re}(\mathcal{T}(\mathcal{V}, c, s))) &= \sup_{x \in \mathrm{Re}(\mathcal{T}(\mathcal{V},c,s))} v^T x \\
&= v^T c + \sup_{\zeta \in \mathbb{C}^m:\ |\zeta| \leq s} \mathrm{Re}\left(v^T \mathcal{V} \zeta\right) \qquad (2.9) \\
&\leq v^T c + \sup_{\zeta \in \mathbb{C}^m:\ |\zeta| \leq s} \left|v^T \mathcal{V}\right| |\zeta| \\
&\leq v^T c + \sup_{y \in \mathbb{R}^m_{\geq 0}: y \leq s} \left|v^T \mathcal{V}\right| y = v^T c + \left|v^T \mathcal{V}\right| s. \qquad (2.10)
\end{aligned}$$

Let us consider $\epsilon \in \mathbb{C}^m$ where

$$\forall i \in \{1, ..., m\}, \ \epsilon_i = \frac{\left|v^T \mathcal{V}\right|_i}{\left(v^T \mathcal{V}\right)_i} s_i.$$

Then we derive the following.

$$\forall i \in \{1, ..., m\}, \ |\epsilon_i| = \frac{\left|v^T\mathcal{V}\right|_i}{\left|v^T\mathcal{V}\right|_i} |s_i| = s_i. \tag{2.11}$$

$$\begin{aligned} v^T\epsilon &= \sum_{i=1}^{m} \left(v^T\mathcal{V}\right)_i \frac{\left|v^T\mathcal{V}\right|_i}{\left(v^T\mathcal{V}\right)_i} s_i \\ &= \left|v^T\mathcal{V}\right| s. \end{aligned} \tag{2.12}$$

By Equations 2.9, 2.11, and 2.12, we get

$$\rho\left(v, \mathrm{Re}\left(\mathcal{T}\left(\mathcal{V}, c, s\right)\right)\right) \geq v^T c + \left|v^T\mathcal{V}\right| s \tag{2.13}$$

The Lemma follows from Equations 2.10 and 2.13. □

Like real zonotopes, complex zonotopes are also not closed under mutual intersection. Even the intersection between template complex zonotopes with a common template and center need not be a closed. But when the common template is a non-singular (invertible) matrix and the center is common, then the intersection is a closed operation and can be expressed algebraically.

Example 2.2.6. Let us consider two template complex zonotopes having a common template as $\mathcal{T}\left(\mathcal{V}, 0, s\right)$ and $\mathcal{T}\left(\mathcal{V}, 0, s'\right)$ where

$$V = \begin{bmatrix} 1+\iota & 1 & 0 \\ 1 & 0 & 1 \end{bmatrix}, \ s = \begin{bmatrix} 1 \\ 0.5 \\ 1 \end{bmatrix} \text{ and } s' = \begin{bmatrix} 1 \\ 1 \\ 0.5 \end{bmatrix}.$$

The template complex zonotope $\mathcal{T}\left(V, 0, s \bigwedge s'\right)$, where $s \bigwedge s' = \begin{bmatrix} 1 & 0.5 & 0.5 \end{bmatrix}^T$, can not be an over-approximation of the intersection of the previous two template complex zonotopes as shown in Figure 2.4.

On the other hand, let us consider the following invertible matrix W and two vectors of scaling factors r and r', respectively.

$$W = \begin{bmatrix} 0.5+\iota & 0 \\ 0.5 & 1 \end{bmatrix}, \ r = \begin{bmatrix} 1 \\ 0.5 \end{bmatrix}, \ r' = \begin{bmatrix} 0.5 \\ 1 \end{bmatrix}.$$

Since W is invertible, we can exactly express the intersection between the two complex zonotopes as another complex zonotope given below and illustrated in Figure 2.5.

$$\mathcal{T}\left(W, 0, r\right) \bigcap \mathcal{T}\left(W, 0, r'\right) = \mathcal{T}\left(W, 0, r \bigwedge r'\right).$$

Figure 2.4: Non-closure of intersection between complex zonotopes for a non-invertible template.

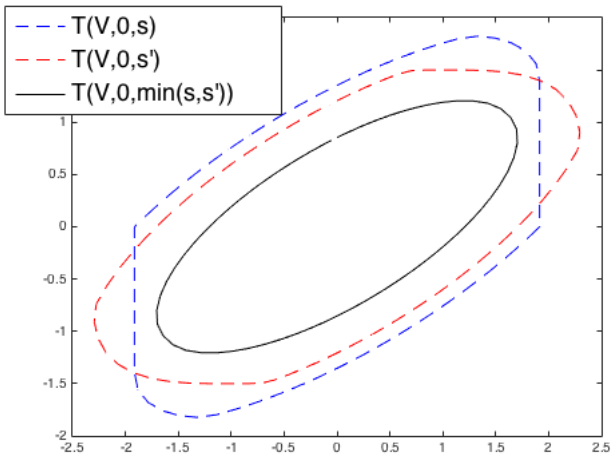

Figure 2.5: Closure of intersection between complex zonotopes for an invertible template.

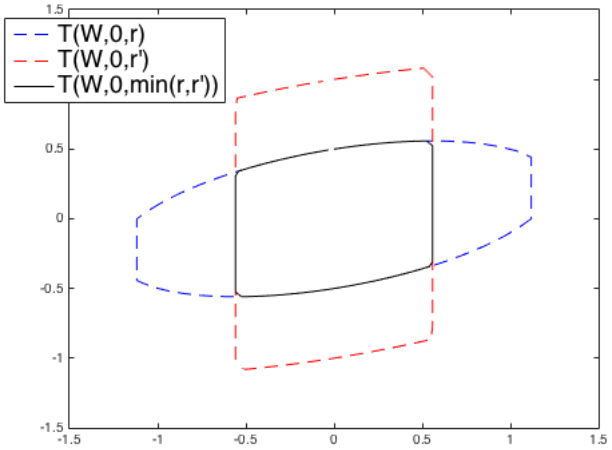

The observation in the above example about intersection between complex zonotopes is mathematically explained for a general case in the following lemma.

Lemma 2.2.7 (Mutual intersection)**.** *Let $\mathcal{V} \in \mathbb{M}_{n\times n}(\mathbb{C})$ be a non-singular matrix.*

$$\textit{Then} \quad \mathcal{T}(\mathcal{V}, c, s) \bigcap \mathcal{T}(\mathcal{V}, c, s') = \mathcal{T}\left(\mathcal{V}, c, s \bigwedge s'\right). \tag{2.14}$$

Proof. Let us consider a point $z \in \mathcal{T}(\mathcal{V}, c, s \bigwedge s')$ where

$$z = c + \mathcal{V}\zeta : \ |\zeta| \leq s \bigwedge s'. \text{Then} \quad |\zeta| \leq s, \quad |\zeta| \leq s'$$
$$\implies z \in \mathcal{T}(\mathcal{V}, c, s) \ \wedge \ z \in \mathcal{T}(\mathcal{V}, c, s') \implies z \in \mathcal{T}(\mathcal{V}, c, s) \bigcap \mathcal{T}(\mathcal{V}, c, s').$$

This proves that the L.H.S of Equation 2.14 is contained inside the R.H.S.

Now let us consider a point $x \in \mathcal{T}(\mathcal{V}, c, s) \bigcap \mathcal{T}(\mathcal{V}, c, s')$. Let us express x as

$$x = c + \mathcal{V}\zeta.$$

Since $\mathcal{V}$ is an invertible matrix, we have a unique solution for ζ, i.e., $\zeta = \mathcal{V}^{-1}(x - c)$. As $x \in \mathcal{T}(\mathcal{V}, c, s) \bigcap \mathcal{T}(\mathcal{V}, c, s')$ and ζ has unique solution, we get

$$|\zeta| \leq s \ \wedge \ |\zeta| \leq s'.$$
$$\implies |\zeta| \leq s \bigwedge s' \implies x \in \mathcal{T}\left(\mathcal{V}, c, s \bigwedge s'\right).$$

The above means that the R.H.S of Equation 2.14 is contained inside the L.H.S. The converse was proved earlier. So, we have proved the Lemma. □

Since template complex zonotopes are not closed under intersection, generally there is no smallest over-approximation of a given set by a template complex zonotope. But according to Lemma 2.2.7, template complex zonotopes with a fixed invertible template matrix and fixed center are closed under mutual intersection. Therefore, for a fixed invertible template and fixed center, there exists a smallest template complex zonotope approximation of a given set, expressed as follows.

Theorem 2.2.8. *Let $\Psi \subseteq \mathbb{C}^n$ be a bounded set and $\mathcal{V} \in \mathbb{M}_{n\times n}(\mathbb{C})$ be an invertible square matrix. Let us consider*

$$S = \left\{s \in \mathbb{R}^n_{\geq 0} : \Psi \subseteq \mathcal{T}(\mathcal{V}, c, s)\right\}$$

Then all of the following is true.

$$\Psi \subseteq \bigcap_{s\in S} \mathcal{T}(\mathcal{V}, c, s) = \mathcal{T}\left(\mathcal{V}, c, \bigwedge_{s\in S} s\right). \tag{2.15}$$

$$\bigwedge_{s\in S} s = \bigvee_{x\in\Psi} \left|\mathcal{V}^{-1}(x - c)\right|. \tag{2.16}$$

Proof. First, we shall prove Equation 2.15. Based on Lemma 2.2.7, it follows that

$$\bigcap_{s\in S} \mathcal{T}\left(\mathcal{V}, c, s\right) = \mathcal{T}\left(\mathcal{V}, c, \bigwedge_{s\in S} s\right).$$

As S is the set of all scaling factors whose corresponding template complex zonotope is an over-approximation of Ψ, we also get

$$\Psi \subseteq \bigcap_{s\in S} \mathcal{T}\left(\mathcal{V}, c, s\right) = \mathcal{T}\left(\mathcal{V}, c, \bigwedge_{s\in S} s\right).$$

So, we have proved Equation 2.15.

Now we shall prove Equation 2.16. We shall first prove

$$\Psi \subseteq \mathcal{T}\left(\mathcal{V}, c, \bigvee_{x\in\Psi} \left|\mathcal{V}^{-1}\left(x-c\right)\right|\right). \tag{2.17}$$

Let us consider a point $x \in \Psi$. Since $\mathcal{V}$ is invertible, x can be written as a linear combination of template column vectors of $\mathcal{V}$ plus the center c as

$$x = c + \mathcal{V}\left(\mathcal{V}^{-1}\left(x-c\right)\right),$$

where the vector of combining coefficients is $(\mathcal{V}^{-1}\left(x-c\right))$. Since

$$\left|\mathcal{V}^{-1}\left(x-c\right)\right| \leq \bigvee_{x\in\Psi} \left|\mathcal{V}^{-1}\left(x-c\right)\right|,$$

$$\text{we get,} \quad x \in \mathcal{T}\left(\mathcal{V}, c, \bigvee_{x\in\Psi} \left|\mathcal{V}^{-1}\left(x-c\right)\right|\right).$$

As the above is true for any $x \in \Psi$, we have proved Equation 2.17. By Equation 2.17 and the definition of S, we get $\bigvee_{x\in\Psi} \left|\mathcal{V}^{-1}\left(x-c\right)\right| \in S$. Therefore,

$$\bigwedge_{s\in S} s \leq \bigvee_{x\in\Psi} \left|\mathcal{V}^{-1}\left(x-c\right)\right|. \tag{2.18}$$

By Equation 2.15, which we have proved earlier, and the fact that $x \in \Psi$, we get

$$x \in \mathcal{T}\left(\mathcal{V}, c, \bigwedge_{s\in S} s\right).$$

Since $\mathcal{V}^{-1}(x-c)$ is the unique vector of combining coefficients when x is expressed as a linear combination of column vector of $\mathcal{V}$, the above implies

$$\left|\mathcal{V}^{-1}(x-c)\right| \leq \bigwedge_{s\in S} s.$$

As the above equation is true for any x in Ψ, we get

$$\bigvee_{x\in\Psi} \left|\mathcal{V}^{-1}(x-c)\right| \leq \bigwedge_{s\in\Psi} s.$$

Based on the above equation and Equation 2.18, we get Equation 2.16. □

2.3 Checking inclusion

While computing positive invariants using a set representation, ascertaining the positive invariance of a set requires deciding the inclusion of the next reachable set inside the given set. In the case of complex zonotopes, we shall show that checking the exact inclusion amounts to solving a non-convex optimization problem. Therefore, we later find a sufficient condition expressed by convex constraints for checking the inclusion. The convex constraints we derive later are specifically second order conic constraints, which are described below.

Definition 2.3.1 (Second order conic constraint)**.** A second order conic constraint on a variable x taking values in $\mathbb{R}^n$ is one of the following expressions.

1. $\|Ax+b\|_2 \leq c^T x + d$ where $A \in \mathbb{M}_{r\times n}(\mathbb{R})$, $b \in \mathbb{R}^r$, $c \in \mathbb{R}^n$ and $d \in \mathbb{R}$.
2. $p^T x = q$ where $p \in \mathbb{R}^n$ and $q \in \mathbb{R}$.

Example 2.3.2. An inequality like $x^2 + 4y^2 + 25z^2 - 3x - 4y + z + 3 \leq 0$ is a second order conic constraint because it can be written as

$$\left\| \begin{bmatrix} 1 & 0 & 0 \\ 0 & 2 & 0 \\ 0 & 0 & 5 \end{bmatrix} \begin{bmatrix} x \\ y \\ z \end{bmatrix} \right\|_2 \leq \begin{bmatrix} 3 & 4 & -1 \end{bmatrix} \begin{bmatrix} x \\ y \\ z \end{bmatrix} - 3.$$

A linear equality like $3x + 2y - 4z = 5$ is also a second order conic constraint.

In the case of complex zonotope, we shall later derive a set of second order conic constraints, which have to be collectively satisfied to guarantee inclusion. Given a set of second order conic constraints on a variable $x \in \mathbb{R}^n$, solving the constraints refers to finding a value $x^* \in \mathbb{R}^n$ that satisfies the constraints. A

value $x' \in \mathbb{R}^n$ is called an approximate solution within a precision $\epsilon \in \mathbb{R}_{\geq 0}$ if there exists a solution $x^* \in \mathbb{R}^n$ such that $\|x' - x^*\|_2 \leq \epsilon$. There are tools based on interior point methods (see [GBY08]) that can efficiently find approximate solutions with very high precision to second order conic constraints (SOCC).

Checking inclusion of a single point inside a template complex zonotope is equivalent to solving SOCC, as described below.

Lemma 2.3.3 (Inclusion of a point)**.** *Let us consider a point $x \in \mathbb{C}^n$. Then $x \in \mathcal{T}(\mathcal{V}, c, s) \subset \mathbb{C}^n$ if and only if all of the following is collectively true.*

$$\exists \zeta \in \mathbb{C}^m :$$
$$\mathcal{V}\zeta = x - c \tag{2.19}$$
$$|\zeta| \leq s. \tag{2.20}$$

Proof. The above result follows from the fact that any point $x \in \mathcal{T}(\mathcal{V}, c, s)$ is of the form $x = c + \mathcal{V}\zeta$ for some $\zeta \in \mathbb{C}^m$ such that $|\zeta| \leq s$. □

Example 2.3.4. Let us consider the template complex zonotope $\mathcal{T}(\mathcal{V}, c, s) \subset \mathbb{C}^2$ and a point $x \in \mathbb{C}^2$, where

$$\mathcal{V} = \begin{bmatrix} 1+\iota & 1 & 0 \\ 1 & 0 & 1 \end{bmatrix}, \quad c = \begin{bmatrix} \iota \\ 1 \end{bmatrix}, \quad s = \begin{bmatrix} 1 \\ 1 \\ 1 \end{bmatrix} \text{ and } x = \begin{bmatrix} 2\iota - 2 \\ \iota + 2 \end{bmatrix}.$$

To prove that $x \in \mathcal{T}(\mathcal{V}, c, s)$, let us consider $\zeta = \begin{bmatrix} \iota & -1 & 1 \end{bmatrix}^T$. Then we get

$$\mathcal{V}\zeta = \begin{bmatrix} \iota - 2 \\ \iota + 1 \end{bmatrix} = \begin{bmatrix} 2\iota - 2 \\ \iota + 2 \end{bmatrix} - \begin{bmatrix} \iota \\ 1 \end{bmatrix} = x - c.$$

Therefore, Equation 2.19 is satisfied. Furthermore, $|\zeta| = \begin{bmatrix} 1 & 1 & 1 \end{bmatrix}^T$. So, Equation 2.20 is also satisfied. Henceforth, $x \in \mathcal{T}(\mathcal{V}, c, s)$.

Equation 2.19 is an equality constraint on ζ, which is therefore an SOCC. We know that the absolute value of a complex number is the square norm of a two dimensional vector. So, Equation 2.20 is equivalent to a set of square norm constraints on the real and imaginary components of ζ, which are therefore SOCC constraints. Hence, the inclusion of a point inside a template complex zonotope can be checked by solving second order conic constraints.

Now we state the necessary and sufficient condition for checking inclusion between two template complex zonotopes.

Lemma 2.3.5 (Exact inclusion between template complex zonotopes)**.** *Let us consider* $\mathcal{V} \in \mathbb{M}_{n\times m}(\mathbb{C})$ *and* $\mathcal{V}' \in \mathbb{M}_{n\times r}(\mathbb{C})$*. The inclusion* $\mathcal{T}(\mathcal{V}', c', s') \subseteq \mathcal{T}(\mathcal{V}, c, s)$ *holds if and only if*

$$\sup_{\{\zeta'\in\mathbb{C}^r:|\zeta'|\leq s'\}} \inf_{\{\zeta\in\mathbb{C}^m:\mathcal{V}\zeta=\mathcal{V}'\zeta'+c'-c\}} \sup_{i=1}^{m} (|\zeta_i| - s_i) \leq 0 \tag{2.21}$$

Proof. We have

$$\mathcal{T}(\mathcal{V}, c, s) = \{c + \mathcal{V}\zeta :\ \zeta \in \mathbb{C}^m,\ |\zeta| \leq s\},$$
$$\mathcal{T}(\mathcal{V}', c', s') = \{c' + \mathcal{V}'\zeta' :\ \zeta' \in \mathbb{C}^r,\ |\zeta'| \leq s'\}.$$

Therefore, we get $\mathcal{T}(\mathcal{V}', c', s') \subseteq \mathcal{T}(\mathcal{V}, c, s)$ if and only if for every $\zeta' \in \mathbb{C}^r : |\zeta'| \leq s'$, there exists $\zeta \in \mathbb{C}^m : \mathcal{V}\zeta + c = \mathcal{V}'\zeta' + c' \wedge |\zeta| \leq s$. This is equivalently expressed as the constraint in Equation 2.21. □

The reason solving Equation 2.21 requires non-convex optimization is explained as follows. Let us consider that $\mathcal{V}$ has a pseudo-inverse $\mathcal{V}^\dagger$. Then by the rank-nullity theorem

$$\{\zeta :\ \mathcal{V}\zeta = \mathcal{V}\zeta' + c' - c\} = \left\{\mathcal{V}^\dagger(\zeta' - c) + v :\ v \in \mathrm{null}(\mathcal{V})\right\}$$

So,

$$\inf_{\{\zeta\in\mathbb{C}:\mathcal{V}\zeta=\mathcal{V}'\zeta'+c'-c\}} \sup_{i=1}^{m} (|\zeta_i| - s_i)$$
$$= \inf_{\{v\in\mathrm{null}(\mathcal{V})\}} \sup_{i=1}^{m} \left(\left|\mathcal{V}^\dagger(\zeta' - c) + v\right| - s_i\right)$$

The absolute value of a complex variable is a convex quadratic function of the real and imaginary components of the variable. So, the above function is a point-wise minimum (for points v in the null space $\mathcal{V}$) of a set of convex quadratic functions over ζ', which is therefore a non-concave function of ζ'. So the maximization

$$\sup_{\{\zeta'\in\mathbb{C}^r:|\zeta'|\leq s'\}} \inf_{\{\zeta\in\mathbb{C}^m:\mathcal{V}\zeta=\mathcal{V}'\zeta'+c'-c\}} \sup_{i=1}^{m} (|\zeta_i| - s_i)$$

is equivalent to maximizing a non-concave function of ζ'. Maximizing a non-concave function is a non-convex optimization problem.

Alternatively, we shall now derive a sufficient condition, equivalent to a set of second order conic constraints, for checking inclusion between two template complex zonotopes. The following result is used to later derive the sufficient condition.

Lemma 2.3.6. *Let us consider* $s \in \mathbb{R}^m_{\geq 0}$, $s' \in \mathbb{R}^r_{\geq 0}$, $\zeta' \in \mathbb{C}^r$, $c, c' \in \mathbb{C}^n$,$\mathcal{V} \in \mathbb{M}_{n\times m}(\mathbb{C})$, $\mathcal{V}' \in \mathbb{M}_{n\times r}(\mathbb{C})$ $|\zeta'| \leq s'$, $X \in \mathbb{M}_{m\times r}(\mathbb{C})$ *and* $y \in \mathbb{C}^m$ *such that*

$$\mathcal{V}X = \mathcal{V}' \operatorname{diag}(s'), \quad \mathcal{V}y = (c' - c). \tag{2.22}$$

Then
$$\inf_{\{\zeta\in\mathbb{C}:\mathcal{V}\zeta=\mathcal{V}'\zeta'+c'-c\}} \sup_{i=1}^{m} (|\zeta_i| - s_i) \leq \sup_{i=1}^{m} \left(|y_i| + \sum_{j=1}^{r} |X_{ij}| - s_i \right). \tag{2.23}$$

Proof. Let us consider $\epsilon \in \mathbb{C}^r$, such that for any $i \in \{1, ..., r\}$,

$$\begin{cases} \epsilon_i = \frac{\zeta'_i}{s'_i} \text{ if } s'_i \neq 0 \\ \epsilon_i = 0 \text{ otherwise} \end{cases}.$$

From the above definition and the fact that $|\zeta'| \leq s'$, we get $\zeta' = \operatorname{diag}(s')\,\epsilon$ and $\sup_{j=1}^{r} |\epsilon_j| \leq 1$. Then we derive

$$\mathcal{V}'\zeta' + c - c' = \mathcal{V}' \operatorname{diag}(s')\,\epsilon + c - c' = \mathcal{V}X\epsilon + \mathcal{V}y = \mathcal{V}(X\epsilon + y)$$

According the above equation,

$$\begin{aligned}
&X\epsilon + y \in \{\zeta \in \mathbb{C} : \mathcal{V}\zeta = \mathcal{V}'\zeta' + c' - c\}. \\
&\implies \inf_{\{\zeta\in\mathbb{C}:\mathcal{V}\zeta=\mathcal{V}'\zeta'+c'-c\}} \sup_{i=1}^{m} (|\zeta_i| - s_i) \leq \sup_{i=1}^{m} (|(X\epsilon + y)_i| - s_i) \\
&\%\% \text{ Using triangular inequality} \\
&\leq \sup_{i=1}^{m} \left(|y_i| + \sum_{j=1}^{r} |X_{ij}|\,|\epsilon_j| - s_i \right) \\
&\%\% \text{ Since } \sup_{j=1}^{r} |\epsilon_j| \leq 1 \\
&\leq \sup_{i=1}^{m} \left(|y_i| + \sum_{j=1}^{r} |X_{ij}| - s_i \right). \qquad \square
\end{aligned}$$

We define the following relation between two template complex zonotopes, which we shall prove is a sufficient condition for the inclusion between them.

Definition 2.3.7 (Relation for inclusion-checking)**.** Let us consider $\mathcal{V} \in \mathbb{M}_{n\times m}(\mathbb{C})$ and $\mathcal{V}' \in \mathbb{M}_{n\times r}(\mathbb{C})$. We say $\mathcal{T}(\mathcal{V}', c', s') \sqsubseteq \mathcal{T}(\mathcal{V}, c, s)$ iff all of the following is collectively true.

$$\begin{aligned}
&\exists X \in \mathbb{M}_{m\times r}(\mathbb{C}), y \in \mathbb{C}^m \text{ such that} \\
&\mathcal{V}X = \mathcal{V}' \operatorname{diag}(s'), \ \ \mathcal{V}y = c' - c \\
&\sup_{i=1}^{m} \left(|y_i| + \sum_{j=1}^{r} |X_{ij}| - s_i \right) \leq 0.
\end{aligned} \tag{2.24}$$

Theorem 2.3.8 (Inclusion checking)**.** *If* $\mathcal{T}(\mathcal{V}', c', s') \sqsubseteq \mathcal{T}(\mathcal{V}, c, s)$ *then* $\mathcal{T}(\mathcal{V}', c', s') \subseteq \mathcal{T}(\mathcal{V}, c, s)$.

Proof. The theorem follows from Lemmas 2.3.5 and 2.3.6. By Lemma 2.3.5, the inclusion $\mathcal{T}(\mathcal{V}, c, s) \subseteq \mathcal{T}(\mathcal{V}', c', s')$ holds iff the L.H.S of Equation 2.21 is bounded above by zero. According to Lemma 2.3.6, if there exists a X and y satisfying Equation 2.22, then the R.H.S of Equation 2.23 is an upper bound on the L.H.S of Equation 2.21. So, if there exist X and y satisfying Equation 2.22 such that the R.H.S of Equation 2.23 is bounded above by zero, then the inclusion holds. The relation $\mathcal{T}(\mathcal{V}, c, s) \sqsubseteq \mathcal{T}(\mathcal{V}', c', s')$ implies that there exists X and y satisfying Equations 2.22 such that the R.H.S of Equation 2.23 is bounded above by zero. □

Remark 2.3.9. For a complex variable $x \in \mathbb{C}$, a constraint of the form $|x| \leq \epsilon$ is equivalent to

$$\left\| \begin{bmatrix} \mathrm{Re}(x) \\ \mathrm{Im}(x) \end{bmatrix} \right\|_2 \leq \epsilon.$$

The above is a second order conic constraint. Accordingly, Equation 2.24 for checking inclusion can be rewritten as polynomial number of second order conic constraints on a variable whose size is $\mathcal{O}(mr + n)$.

When the template of the complex zonotope inside which containment is checked is invertible, and the centers of the template complex zonotopes are same, then the above sufficient condition for inclusion checking is also a necessary condition. This is described in the following theorem.

Theorem 2.3.10. *Let us consider* $\mathcal{V} \in \mathbb{M}_{n\times n}(\mathbb{C})$ *and* $\mathcal{V}' \in \mathbb{M}_{n\times m}(\mathbb{C})$ *such that* $\mathcal{V}$ *is a non-singular matrix. Then* $\mathcal{T}(\mathcal{V}', c', s') \subseteq \mathcal{T}(\mathcal{V}, c, s)$ *if and only if* $\mathcal{T}(\mathcal{V}', c, s') \sqsubseteq \mathcal{T}(\mathcal{V}, c, s)$.

Proof. By Theorem 2.3.8, we know that if $\mathcal{T}(\mathcal{V}', c, s') \sqsubseteq \mathcal{T}(\mathcal{V}, c, s)$ is true, then we get $\mathcal{T}(\mathcal{V}', c, s') \subseteq \mathcal{T}(\mathcal{V}, c, s)$. So, we have to prove the converse that if $\mathcal{T}(\mathcal{V}', c, s') \subseteq \mathcal{T}(\mathcal{V}, c, s)$, then $\mathcal{T}(\mathcal{V}', c, s') \sqsubseteq \mathcal{T}(\mathcal{V}, c, s)$.

Let us consider $\mathcal{T}(\mathcal{V}', c, s') \subseteq \mathcal{T}(\mathcal{V}, c, s)$. Using Lemma 2.1.4, we get

$$\begin{aligned}
&\mathcal{T}(\mathcal{V}', c, s') = \mathcal{C}(\mathcal{V}' \operatorname{diag}(s'), c) \subseteq \mathcal{T}(\mathcal{V}, c, s) \\
&\quad \Leftrightarrow \ \{c + \mathcal{V}' \operatorname{diag}(s')\zeta' : \ \zeta' \in \mathbb{C}^m, \ \|\zeta'\|_\infty \leq 1\} \subseteq \{c + \mathcal{V}\zeta : \ \zeta \in \mathbb{C}^n, \ |\zeta| \leq s\} \\
&\quad \%\% \text{ since } \mathcal{V} \text{ is non-singular} \\
&\Leftrightarrow \{\mathcal{V}^{-1}(c - c) + \mathcal{V}^{-1}\mathcal{V}' \operatorname{diag}(s')\zeta' : \ \zeta' \in \mathbb{C}^m, \ \|\zeta'\|_\infty \leq 1\} \\
&\quad \subseteq \{\zeta : \zeta \in \mathbb{C}^n, \ |\zeta| \leq s\} \\
&\quad \Leftrightarrow \ \{\mathcal{V}^{-1}\mathcal{V}' \operatorname{diag}(s')\zeta' : \ \zeta' \in \mathbb{C}^m, \ \|\zeta'\|_\infty \leq 1\} \subseteq \{\zeta : \zeta \in \mathbb{C}^n, \ |\zeta| \leq s\}
\end{aligned} \tag{2.25}$$

Let $X = \mathcal{V}^{-1}\mathcal{V}' \operatorname{diag}(s')$ and $y = 0$. Then by Equation 2.25, we get for any $i \in \{1, ..., n\}$

$$\sup_{\zeta' \in \mathbb{C}^m:\ \|\zeta\|_\infty \leq 1} \left| \sum_{j=1}^{m} X_{ij}\zeta_i \right| \leq s_i. \quad \therefore \sum_{j=1}^{m} \left| X_{ij} \frac{|X_{ij}|}{X_{ij}} \right| \leq s_i$$

%% since $y_i = 0$

$$\therefore \sum_{i=1}^{n} |X_{ij}| + |y_i| \leq s_i. \tag{2.26}$$

Furthermore, we have

$$\begin{aligned} &\mathcal{V}X = \mathcal{V}\mathcal{V}^{-1}\mathcal{V}' \operatorname{diag}(s) = \mathcal{V}' \operatorname{diag}(s') \quad \text{and} \\ &\mathcal{V}y = 0 = c - c. \end{aligned} \tag{2.27}$$

By Equations 2.26 and 2.27, we get $\mathcal{T}(\mathcal{V}', c, s') \sqsubseteq \mathcal{T}(\mathcal{V}, c, s)$. □

CHAPTER 3

Augmented Complex Zonotopes

In hybrid dynamical systems, a transition can be controlled by constraints on the state variables which act as preconditions for the transition. In an affine hybrid system, the preconditions are linear constraints on the state variables. So, computing an overapproximation of a reachable set in a set representation would involve computing accurate overapproximation for the intersection with linear constraints. In case of complex zonotopes, similar to simple zonotopes they are not closed under intersection with sub-level sets of linear inequalities. To address this problem, we shall introduce a more general representation of a complex zonotopic set, called augmented complex zonotope, by which we can over-approximate the intersection with a particular class of linear constraints, called *sub-parallelotopic*. Furthermore, we can control the error in overapproximation by adjusting the scaling factors. First we shall motivate the need for a novel extension of complex zonotope to handle the intersection, by explaining a drawback in extending the known approches for real zonotope and halfspace intersection to complex zonotopes. In this regard, a brief description of the related approaches is given below. However, a more detailed discussion was given in the introductory chapter.

Related set representations and problem with their extension to complex zonotopes: To accurately represent the intersection with linear sub-level sets, real zonotopes have been extended to constrained zonotopes [SRMB16] or more generally constrained affine sets [GGP10]. Constrained zonotopes are briefly described in the introductory chapter. In these representations, in addition to the interval constraints on the combining coefficients, there can be more general linear constraints. This permits exact representation of the intersection with hyperplanes, in the case of constrained zonotopes, and half-spaces, in the case of con-

strained affine sets. In these extended representations, the support function can still be computed efficiently by linear programming because there are only linear constraints on the combining coefficients. Similarly, in our complex zonotope representation, although there are quadratic constraints (absolute value bounds) on the combining coefficients, the support function can be computed by a simple affine expression given in Lemma 2.2.5. However, if we introduce linear constraints on the complex combining coefficients in addition to the quadratic absolute value bounds, computing the support function becomes intractable. But accurate computation of the support function is required in verifying bounds on the reachable set. In other words, extending the idea of constrained zonotope or constrained affine set to a complex zonotope will make the computation of support function intractable.

Our solution: We observe that in certain cases, intersection of a version of the real zonotope representation, called *interval zonotope*, with a particular class of linear sub-level sets, called *sub-parallelotopes*, can be computed efficiently. Motivated by this, we introduce a more general representation of complex zonotope, called *augmented complex zonotope*, which denotes the Minkowski sum of a complex zonotope and an interval zonotope. We show that the interval zonotope part of an augmented complex zonotope can be used to over-approximate the intersection. On the other hand, we can still compute the support function efficiently because an augmented complex zonotope is geometrically equivalent to a template complex zonotope. Furthermore, we show that the error in overapproximation can be regulated by adjusting the scaling factors and the center of the template complex zonotope part.

This chapter has three main sections. In Section 3.1, we introduce the interval zonotope and sub-parallelotope set representations, and describe the intersection between them. We also discuss other operations on interval zonotopes like linear transformation, Minkowski sum and computation of the support function. In Section 3.2, we introduce the augmented complex zonotope representation and discuss the over-approximation of its intersection with a sub-parallelotope. We compute a bound on the error in over-approximation of the intersection, which can be regulated by changing the scaling factors and the center. In Section 3.3, we shall discuss other operations on augmented complex zonotopes like linear transformation, Minkowski sum and computation of the support function.

3.1 Interval zonotope and sub-parallelotope

Before we introduce an augmented complex zonotope, we shall describe a particular case when real zonotopes are closed under intersection with sub-level sets of linear inequalities. We introduce a slight variation of the representation of a

real zonotope, called an *interval zonotope*, so as to express the intersection by a succinct algebraic expression. In an interval zonotope, we specify interval bounds on the combining coefficients, without explicitly specifying the center. However, we note that an interval zonotope is geometrically the same as a real zonotope.

Definition 3.1.1 (Interval Zonotope)**.** Let us consider $\mathcal{W} \in \mathbb{M}_{n\times k}(\mathbb{R})$, called the *template*, and $l, u \in \mathbb{R}^k$ such that $l \leq u$, called the upper and lower interval bounds, respectively. The following is the representation of an interval zonotope.

$$\mathcal{I}(\mathcal{W}, l, u) := \left\{\mathcal{W}\zeta : \zeta \in \mathbb{R}^k,\ l \leq \zeta \leq u\right\}.$$

We consider a particular type of sub-level set of linear inequalities, which we call as *sub-parallelotope*, for which the intersection with a suitably aligned interval zonotope gives another interval zonotope. Furthermore, the intersection can be computed by a simple algebraic expression. A sub-parallelotope can be seen as a generalization of parallelotopes to possibly unbounded sets, which is defined as follows.

Definition 3.1.2 (Sub-parallelotope)**.** Let us consider $\mathcal{K} \in \mathbb{M}_{k\times n}(\mathbb{R})$ such that $\left(\mathcal{K}\mathcal{K}^T\right)$ is non-singular. We call such a matrix $\mathcal{K}$ as a *sub-paralleotopic template*. Let us consider $\widehat{l}, \widehat{u} \in \left(\mathbb{R}\bigcup\{-\infty, \infty\}\right)^k$ such that $\widehat{l} \leq \widehat{u}$, called *lower and upper offsets*, respectively. The following is the representation of a sub-parallelotope.

$$\mathcal{P}\left(\mathcal{K}, \widehat{l}, \widehat{u}\right) := \left\{x \in \mathbb{R}^n : \widehat{l} \leq \mathcal{K}x \leq \widehat{u}\right\}.$$

In other words, a sub-level set of a set of linear inequalities is a sub-parallelotope when the linear functions on which the inequalities are defined are linearly independent. For example, because the row vectors $\begin{bmatrix}1 & 1 & -1\end{bmatrix}$ and $\begin{bmatrix}1 & -1 & 1\end{bmatrix}$ are linearly independent, the sub-level set of the linear inequalities

$$\begin{aligned} -1 \leq x + y - z &\leq 1 \\ x - y + z &\leq 3 \end{aligned}$$

can be specified as a sub-parallelotope

$$\mathcal{P}\left(\begin{bmatrix}1 & 1 & -1\\ 1 & 1 & 1\end{bmatrix}, \begin{bmatrix}-1\\ -\infty\end{bmatrix}, \begin{bmatrix}1\\ 3\end{bmatrix}\right).$$

On the other hand, the sub-level set of

$$\begin{aligned} -1 \leq x + y - z &\leq 1 \\ x + y + z &\leq 2 \\ -1 &\leq x + y \end{aligned}$$

is not a sub-parallelotope, because there is linear dependence among the row vectors $\begin{bmatrix}1 & 1 & -1\end{bmatrix}$, $\begin{bmatrix}1 & 1 & 1\end{bmatrix}$, and $\begin{bmatrix}1 & 1 & 0\end{bmatrix}$.

A sub-parallelotope can be represented as a union of possibly inifinite set of interval zonotopes, as described in the following lemma.

Lemma 3.1.3. *Let $\mathcal{K} \in \mathbb{M}_{k\times n}(\mathbb{R})$ be a sub-parallelotopic template. Then,*

$$\mathcal{P}\left(\mathcal{K}, \widehat{l}, \widehat{u}\right) = \left\{c + \mathcal{K}^\dagger\zeta :\ c \in \mathbb{R}^n, \zeta \in \mathbb{R}^k,\ \mathcal{K}c = 0,\ \widehat{l} \le \zeta \le \widehat{u}\right\}.$$

Proof. Let $\zeta \in \mathbb{R}^k$. As $\mathcal{K}\mathcal{K}^\dagger\zeta = \zeta$, by the rank-nullity theorem we get

$$\begin{aligned}
&\{x \in \mathbb{R}^n : \mathcal{K}x = \zeta\} = \left\{c + \mathcal{K}^\dagger\zeta : \mathcal{K}c = 0\right\}.\\
&\text{So, } \{x \in \mathbb{R}^n : \mathcal{K}x = \zeta\} = \left\{c + \mathcal{K}^\dagger\zeta :\ \mathcal{K}c = 0\right\}.\\
&\text{Then, } \mathcal{P}\left(\mathcal{K}, \widehat{l}, \widehat{u}\right) = \left\{x \in \mathbb{R}^n :\ \widehat{l} \le \mathcal{K}x \le \widehat{u}\right\}\\
&= \left\{x \in \mathbb{R}^n : \mathcal{K}x = \zeta, \widehat{l} \le \zeta \le \widehat{u}\right\}\\
&= \left\{c + \mathcal{K}^\dagger\zeta : \mathcal{K}c = 0,\ \widehat{l} \le \zeta \le \widehat{u}\right\}. \qquad \square
\end{aligned}$$

The above similarity between sub-parallelotopes and interval zonotopes provides an intuition that interval zonotopes can be closed under intersection with suitably aligned sub-parallelotopes. In fact, we observe that when a sub-parallelotope has its template aligned with that of an interval zonotope, their intersection can be exactly represented by another interval zonotope. As an example, the intersection of

$\mathcal{I}\left(\begin{bmatrix}1 & 0\\ 0 & 1\end{bmatrix}, \begin{bmatrix}-1\\ -1\end{bmatrix}, \begin{bmatrix}2\\ 2\end{bmatrix}\right)$
with the sub-level sets of: $x_1 \le 1, \quad x_2 \ge 0.5,$
which is the sub-parallelotope $\mathcal{P}\left(\begin{bmatrix}1 & 0\\ 0 & 1\end{bmatrix}, \begin{bmatrix}-\infty & 0.5\end{bmatrix}, \begin{bmatrix}1 & \infty\end{bmatrix}\right)$
gives $\mathcal{I}\left(\begin{bmatrix}1 & 0\\ 0 & 1\end{bmatrix}, \begin{bmatrix}-1\\ 0.5\end{bmatrix}, \begin{bmatrix}1\\ 2\end{bmatrix}\right)$.

In the general case, we express the intersection between a a sub-parallelotope and a possibly translated interval zonotope as follows.

Lemma 3.1.4. *Let $\mathcal{K} \in \mathbb{M}_{k\times n}(\mathbb{R})$ be a sub-parallelotopic template and $c \in \mathbb{R}^n$.*

$$\begin{aligned}
&\textit{Then } \left(c + \mathcal{I}\left(\mathcal{K}^\dagger, l, u\right)\right) \bigcap \mathcal{P}\left(\mathcal{K}, \widehat{l}, \widehat{u}\right)\\
&= c + \mathcal{I}\left(\mathcal{K}^\dagger, l \bigvee \left(\widehat{l} - \mathcal{K}c\right), u \bigwedge \left(\widehat{u} - \mathcal{K}c\right)\right). \qquad (3.1)
\end{aligned}$$

Proof. Let us denote $S_1 = \left(c + \mathcal{I}\left(\mathcal{K}^\dagger, l, u\right)\right) \bigcap \mathcal{P}\left(\mathcal{K}, \widehat{l}, \widehat{u}\right)$ and $S_2 = c + \mathcal{I}\left(\mathcal{K}^\dagger, l \bigvee \left(\widehat{l} - \mathcal{K}c\right), u \bigwedge \left(\widehat{u} - \mathcal{K}c\right)\right)$. We shall first prove that $S_1 \subseteq S_2$. Let us consider that $x \in S_1$. So, $x \in \mathcal{P}\left(\mathcal{K}, \widehat{l}, \widehat{u}\right)$ and

$$\exists \zeta \in \mathbb{R}^k : \; x = c + \mathcal{K}^\dagger \zeta, \; l \leq \zeta \leq u.$$

Then we get

$$\begin{aligned} &\widehat{l} \leq \mathcal{K}x \leq \widehat{u} \;\; \Leftrightarrow \;\; \widehat{l} \leq \mathcal{K}\left(c + \mathcal{K}^\dagger \zeta\right) \leq \widehat{u} \\ &\Leftrightarrow \;\; \widehat{l} - \mathcal{K}c \leq \zeta \leq \widehat{u} - \mathcal{K}\zeta. \end{aligned}$$

Also, we have $l \leq \zeta \leq u$ as given previously. Therefore,

$$l \bigvee \left(\widehat{l} - \mathcal{K}c\right) \leq \zeta \leq u \bigwedge \left(\widehat{u} - \mathcal{K}c\right).$$

As $x = c + \mathcal{K}^\dagger \zeta$, the above constraint implies $x \in S_2$. This shows that $S_1 \subseteq S_2$.

Now, we shall prove $S_2 \subseteq S_1$. Since

$$\begin{aligned} &l \leq l \bigvee \left(\widehat{l} - \mathcal{K}c\right) \;\text{ and }\; u \bigwedge \left(\widehat{u} - \mathcal{K}c\right) \leq u, \;\text{ we derive} \\ &S_2 = c + \mathcal{I}\left(\mathcal{K}^\dagger, l \bigvee \left(\widehat{l} - \mathcal{K}c\right), u \bigwedge \left(\widehat{u} - \mathcal{K}c\right)\right) \subseteq c + \mathcal{I}\left(\mathcal{K}^\dagger, l, u\right) \end{aligned} \tag{3.2}$$

Now, let us consider a point $y \in S_2$. So, $\exists \zeta' \in \mathbb{R}^k$:

$$\begin{aligned} &y = c + \mathcal{K}^\dagger \zeta', \; l \bigvee \left(\widehat{l} - \mathcal{K}c\right) \leq \zeta' \leq u \bigwedge \left(\widehat{u} - \mathcal{K}c\right). \\ &\text{Then } \; \mathcal{K}y = \mathcal{K}\left(c + \mathcal{K}^\dagger \zeta'\right) = \mathcal{K}c + \zeta' \\ &\%\% \;\text{ since } l \bigvee \left(\widehat{l} - \mathcal{K}c\right) \leq \zeta' \leq u \bigwedge \left(\widehat{u} - \mathcal{K}c\right) \\ &\implies \mathcal{K}c + \left(\widehat{l} - \mathcal{K}c\right) \leq \mathcal{K}y \leq \mathcal{K}c + \left(\widehat{u} - \mathcal{K}c\right) \\ &\implies \widehat{l} \leq \mathcal{K}y \leq \widehat{u}. \end{aligned}$$

Therefore, $y \in \mathcal{P}\left(\mathcal{K}, \widehat{l}, \widehat{u}\right)$. This shows that $S_2 \subseteq \mathcal{P}\left(\mathcal{K}, \widehat{l}, \widehat{u}\right)$. Using this result along with Equation 3.2, we get that $S_2 \subseteq S_1$. We have also shown earlier that $S_1 \subseteq S_2$. Therefore, $S_1 = S_2$. □

Now, we shall derive an over-approximation of intersection of a sub-parallelotope with the Minkowski sum of an interval zonotope and a general convex set. Before that, we describe the following result about convex sets which is latter used in the

proof of the over-approximation. We use the following notation for the rest of this chapter, unless otherwise specified.

$$l, u \in \mathbb{R}^k : k \leq n, \quad \widehat{l} \in \left(\mathbb{R} \bigcup \{-\infty\}\right)^k, \quad \widehat{u} \in \left(\mathbb{R} \bigcup \{\infty\}\right)^k$$
$$\mathcal{K} \in \mathbb{M}_{k \times n}(\mathbb{R}) : \quad \left(\mathcal{K}\mathcal{K}^T\right) \text{ is non-singular}$$

For any $i \in \{1, ..., k\}$, we consider $\boldsymbol{\alpha}_i \in \mathbb{R}^k$ such that for any $j \in \{1, ..., k\}$, $(\boldsymbol{\alpha}_i)_j = 0$ if $i = j$ and $(\boldsymbol{\alpha}_i)_j = 1$ otherwise.

Lemma 3.1.5. *Let $\Psi \subseteq \mathbb{R}^k$ be a convex set such that $\operatorname{diag}(\boldsymbol{\alpha}_i)\Psi \in \Psi$ for all $i \in \{1, ..., k\}$. Let $v \in \Psi$. Then*

$$\prod_{i=1}^{k} \boldsymbol{Conv}(\{0, v_i\}) \subseteq \Psi.$$

Proof. We prove the above by induction. We have

$\operatorname{diag}(\boldsymbol{\alpha}_1) v = 0 \times \prod_{i=2}^{k} \{v_i\} \subseteq \Psi$. As Ψ is a convex set and $v \in \Psi$, we get

$$\boldsymbol{Conv}(\{0, v_1\}) \times \prod_{i=2}^{k} \{v_i\} \subseteq \Psi\ . \tag{3.3}$$

$$\text{If for } j < k \prod_{i=1}^{j} \boldsymbol{Conv}(\{0, v_i\}) \times \prod_{i=j+1}^{k} \{v_i\} \subseteq \Psi, \tag{3.4}$$

$$\text{then } \operatorname{diag}(\boldsymbol{\alpha}_{j+1}) \prod_{i=1}^{j} \boldsymbol{Conv}(\{0, v_i\}) \times \prod_{i=j+1}^{k} \{v_i\} \subseteq \operatorname{diag}(\boldsymbol{\alpha}_{j+1})\Psi \subseteq \Psi$$
$$\Leftrightarrow \prod_{i=1}^{j} \boldsymbol{Conv}(\{0, v_i\}) \times \{0\} \times \prod_{i=j+2}^{k} \{v_i\} \subseteq \Psi$$

As Ψ is a convex set, by the above equation and Equation 3.4, we get

$$\implies \prod_{i=1}^{j+1} \boldsymbol{Conv}(\{0, v_i\}) \times \prod_{i=j+2}^{k} \{v_i\} \subseteq \Psi. \tag{3.5}$$

Using Equations 3.3 and 3.5, the lemma follows by induction. □

Now we state a result about over-approximating the intersection of a sub-parallelotope with the Minkowski sum of a convex set and interval zonotope. We

also find an under-approximation of the former so that we can bound the error in over-approximation. We use the following notation for the rest of this chapter.

If $k < n$, then we consider $Y \in \mathbb{M}_{n\times(n-k)}(\mathbb{R})$ such that the column vectors of Y form the basis of $\mathcal{K}$. Otherwise when $k = n$, we consider $Y = 0$.

Lemma 3.1.6 (Intersection with Minkowski sum)**.** *Let $S \in \mathbb{R}^n$ be a convex set and*

$$\forall i \in \{1, ..., k\} \quad \text{diag}(\boldsymbol{\alpha}_i)\,\mathcal{K}S \subseteq \mathcal{K}S, \tag{3.6}$$

$$l \leq l \bigvee \widehat{l} \leq u \bigwedge \widehat{u} \leq u\,. \tag{3.7}$$

$$\textit{Then} \quad \begin{bmatrix} 0 \\ Y^T \end{bmatrix} S \oplus \begin{bmatrix} \mathcal{K} \\ Y^T \end{bmatrix} \mathcal{I}\left(\mathcal{K}^\dagger, l \bigvee \widehat{l}, u \bigwedge \widehat{u}\right)$$

$$\subseteq \begin{bmatrix} \mathcal{K} \\ Y^T \end{bmatrix} \left(\left(S \oplus \mathcal{I}\left(\mathcal{K}^\dagger, l, u\right)\right) \bigcap \mathcal{P}\left(\mathcal{K}, \widehat{l}, \widehat{u}\right)\right) \tag{3.8}$$

$$\subseteq \begin{bmatrix} \mathcal{K} \\ Y^T \end{bmatrix} \left(S \oplus \mathcal{I}\left(\mathcal{K}^\dagger, l \bigvee \widehat{l}, u \bigwedge \widehat{u}\right)\right). \tag{3.9}$$

Proof. First we shall prove Equation 3.8. By Equation 3.6, we get $0 \in \mathcal{K}S$. So,

$$\begin{bmatrix} 0 \\ Y^T \end{bmatrix} S \subseteq \begin{bmatrix} \mathcal{K} \\ Y^T \end{bmatrix} S. \tag{3.10}$$

By Equation 3.7 we get

$$\begin{bmatrix} \mathcal{K} \\ Y^T \end{bmatrix} \mathcal{I}\left(\mathcal{K}^\dagger, l \bigwedge \widehat{l}, u \bigvee \widehat{u}\right) \subseteq \begin{bmatrix} \mathcal{K} \\ Y^T \end{bmatrix} \mathcal{I}\left(\mathcal{K}^\dagger, l, u\right). \tag{3.11}$$

Then, Equation 3.8 follows from Equations 3.10 and 3.11.

Now we shall prove Equation 3.9.

Let us consider $x \in \left(S \oplus \mathcal{I}\left(\mathcal{K}^\dagger, l, u\right)\right) \bigcap \mathcal{P}\left(\mathcal{K}, \widehat{l}, \widehat{u}\right)$ where

$$x = v + \mathcal{K}^\dagger\zeta : \; v \in S, \; l \leq \zeta \leq u.$$

$$\text{As } x \in \mathcal{P}\left(\mathcal{K}, \widehat{l}, \widehat{u}\right), \text{ we get } \widehat{l} \leq \mathcal{K}\left(v + \mathcal{K}^\dagger\zeta\right) \leq \widehat{u}$$

$$\implies \widehat{l} \leq \mathcal{K}v + \zeta \leq \widehat{u}. \tag{3.12}$$

Let us consider

$$\epsilon \in \mathbb{R}^k : \; \epsilon_i = \begin{cases} \inf\{u_i, \widehat{u}_i\} \text{ if } \zeta_i > \inf\{u_i, \widehat{u}_i\} \\ \sup\left\{l_i, \widehat{l}_i\right\} \text{ if } \zeta_i < \sup\left\{l_i, \widehat{l}_i\right\} \\ \zeta_i \text{ otherwise.} \end{cases}$$

By the above definition, we get

$$l \bigvee \widehat{l} \leq \epsilon \leq u \bigwedge \widehat{u}. \tag{3.13}$$

Let $w = x - \mathcal{K}^{\dagger}\epsilon = v + \mathcal{K}^{\dagger}\zeta - \mathcal{K}^{\dagger}\epsilon$.

For any $i \in \{1, ..., k\}$, we analyze the following cases.

Case 1: Let us consider $\zeta_i > \inf\{u_i, \widehat{u}_i\}$. Then $\epsilon_i = \inf\{u_i, \widehat{u}_i\}$. Since $\zeta_i \leq u_i$, we get $\inf\{u_i, \widehat{u}_i\} = \widehat{u}_i = \epsilon_i$. Then by using Equation 3.12, we derive

$$\begin{aligned} \mathcal{K}_i w &= \mathcal{K}_i x - \epsilon_i \\ &\leq \widehat{u}_i - \widehat{u}_i = \widehat{u}_i - \widehat{u}_i = 0. \end{aligned}$$

Also by using Equation 3.13, we get

$$\begin{aligned} \mathcal{K}_i w &= \mathcal{K}_i v + \zeta_i - \epsilon_i \\ &\geq \mathcal{K}_i v + \inf\{u_i, \widehat{u}_i\} - \inf\{u_i, \widehat{u}_i\} = \mathcal{K} v_i. \end{aligned}$$

$$\text{Therefore } \mathcal{K}_i w \in \boldsymbol{Conv}\left(\{0, \mathcal{K}_i v\}\right). \tag{3.14}$$

Case 2: Let us consider that $\zeta_i < \sup\left\{l_i, \widehat{l}_i\right\}$. Then $\epsilon_i = \sup\left\{l_i, \widehat{l}_i\right\}$. Since $\zeta_i \geq l_i$, we get $\sup\left\{l_i, \widehat{l}_i\right\} = \widehat{l}_i = \epsilon_i$. Then by using Equation 3.12, we derive

$$\begin{aligned} \mathcal{K}_i w &= \mathcal{K}_i x - \epsilon_i \\ &\geq \widehat{l}_i - \widehat{l}_i = \widehat{l}_i - \widehat{l}_i = 0. \end{aligned}$$

Also by using Equation 3.13, we derive

$$\begin{aligned} \mathcal{K}_i w &= \mathcal{K}_i v + \zeta_i - \epsilon_i \\ &\leq \mathcal{K}_i v + \sup\left\{l_i, \widehat{l}_i\right\} - \sup\left\{l_i, \widehat{l}_i\right\} = \mathcal{K} v_i. \end{aligned}$$

$$\text{Therefore } \mathcal{K}_i w \in \boldsymbol{Conv}\left(\{0, \mathcal{K}_i v\}\right). \tag{3.15}$$

Case 3: Let us consider that the above two cases are not true. Then $\epsilon_i = \zeta_i$. So,

$$\mathcal{K}_i w = \mathcal{K}_i v + \zeta_i - \epsilon_i = \mathcal{K}_i v + 0 = v_i. \tag{3.16}$$

From Equations 3.14–3.16, we get

$$\mathcal{K} w \in \prod_{i=1}^{k} \boldsymbol{Conv}\left(\{0, v_i\}\right). \tag{3.17}$$

As S is a convex set and $v \in S$, using Lemma 3.1.5 and Equations 3.6, we get

$$\prod_{i=1}^{k} \boldsymbol{Conv}\left(\{0, v_i\}\right) \subseteq \mathcal{K}S$$
$$\%\% \text{ by Equation 3.17}$$
$$\implies \mathcal{K}w \in \mathcal{K}S.$$

As Y^T is orthogonal to $\mathcal{K}$, we get

$$Y^T w = Yv + Y\mathcal{K}^\dagger(\zeta - \epsilon) = Y^T v + 0 = Y^T v \in Y^T S.$$
$$\text{So, } \begin{bmatrix}\mathcal{K}\\ Y^T\end{bmatrix} w \in \begin{bmatrix}\mathcal{K}\\ Y^T\end{bmatrix} S.$$

By Equation 3.13, we get $\mathcal{K}^\dagger\epsilon \in \mathcal{I}\left(\mathcal{K}^\dagger, l \bigvee \widehat{l}, u \bigwedge \widehat{u}\right)$. So, we get

$$\begin{bmatrix}\mathcal{K}\\ Y^T\end{bmatrix} x = \begin{bmatrix}\mathcal{K}\\ Y^T\end{bmatrix}\left(w + \mathcal{K}^\dagger\epsilon\right) \in \begin{bmatrix}\mathcal{K}\\ Y^T\end{bmatrix}\left(S \oplus \mathcal{I}\left(\mathcal{K}^\dagger, l \bigvee \widehat{l}, u \bigwedge \widehat{u}\right)\right).$$

As the above is true for any $x \in S \oplus \mathcal{I}\left(\mathcal{K}^\dagger, l \bigvee \widehat{l}, u \bigwedge \widehat{u}\right)$, we have proved Equation 3.9. □

Other computations on interval zonotopes

An interval zonotope can be equivalently specified as the real projection of a template complex zonotope, as described in the following lemma. We use this result to compute other operations on interval zonotopes, like linear transformation, Minkowski sum, inclusion-checking and support function.

Lemma 3.1.7. *The following is true.*

$$\mathcal{I}\left(\mathcal{W}, l, u\right) = \mathrm{Re}\left(\mathcal{T}\left(\mathcal{W}, \mathcal{W}\frac{u+l}{2}, \frac{u-l}{2}\right)\right).$$

Proof. Let us consider a point $x \in \mathcal{I}\left(\mathcal{W}, l, u\right)$ expressed as

$$x = \mathcal{W}\zeta : \zeta \in \mathbb{R}^n, l \leq \zeta \leq u.$$

Let $\zeta' = \zeta - \frac{u+l}{2}$. Then we get,

$$\begin{aligned} x = \mathcal{W}\zeta &= \mathcal{W}\frac{u+l}{2} + \mathcal{W}\left(\zeta - \frac{u+l}{2}\right) \\ &= \mathcal{W}\frac{u+l}{2} + \mathcal{W}\zeta' \text{ and} \\ |\zeta'| &= \left|\zeta - \frac{u+l}{2}\right| \\ &\%\% \text{ As } \zeta \text{ is a real vector and } l \leq \zeta \leq u \\ &\leq \left|l - \frac{u+l}{2}\right| \bigvee \left|u - \frac{u+l}{2}\right| = \left|\frac{u-l}{2}\right|. \end{aligned}$$

So, $x \in \mathrm{Re}\left(\mathcal{T}\left(\mathcal{W}, \mathcal{W}\frac{u+l}{2}, \frac{u-l}{2}\right)\right)$. Therefore,

$$\mathcal{I}(\mathcal{W}, l, u) \subseteq \mathrm{Re}\left(\mathcal{T}\left(\mathcal{W}, \mathcal{W}\frac{u+l}{2}, \frac{u-l}{2}\right)\right).$$

Next consider $y \in \mathrm{Re}\left(\mathcal{T}\left(\mathcal{W}, \mathcal{W}\frac{u+l}{2}, \frac{u-l}{2}\right)\right)$, expressed as

$$y = \mathcal{W}\zeta + \mathcal{W}\frac{u+l}{2} : \ |\zeta| \leq \frac{u-l}{2}.$$

Let $\zeta'' = \zeta + \frac{u+l}{2}$. As $|\zeta| \leq \frac{u-l}{2}$, so we get

$$\begin{aligned} &\frac{u+l}{2} - \frac{u-l}{2} \leq \zeta'' \leq \frac{u-l}{2} + \frac{u+l}{2} \\ &\Leftrightarrow l \leq \zeta'' \leq u \end{aligned}$$

Furthermore, $y = \mathcal{W}\zeta + \mathcal{W}\frac{u+l}{2} = \mathcal{W}\zeta''$. So, $y \in \mathcal{I}(\mathcal{W}, l, u)$. Therefore,

$$\mathcal{I}(\mathcal{W}, l, u) \supseteq \mathrm{Re}\left(\mathcal{T}\left(\mathcal{W}, \mathcal{W}\frac{u+l}{2}, \frac{u-l}{2}\right)\right).$$

Combining the previous two conclusions about the set inclusions, we get

$$\mathcal{I}(\mathcal{W}, l, u) = \mathrm{Re}\left(\mathcal{T}\left(\mathcal{W}, \mathcal{W}\frac{u+l}{2}, \frac{u-l}{2}\right)\right). \quad \square$$

An interval zonotope can be equivalently represented as a simple zonotope, which is stated in the following lemma.

Lemma 3.1.8. *The following is true.*

$$\mathcal{I}(\mathcal{W}, l, u) = \mathcal{Z}\left(\mathcal{W}\,\mathrm{diag}\left(\frac{u-l}{2}\right), \mathcal{W}\frac{u+l}{2}\right).$$

Proof. Based on Lemma 3.1.7, we have

$$\mathcal{I}\left(\mathcal{W}, l, u\right) = \mathrm{Re}\left(\mathcal{T}\left(\mathcal{W}, \mathcal{W}\frac{u+l}{2}, \frac{u-l}{2}\right)\right).$$

Next based on Lemma 2.1.4, we have

$$\mathcal{T}\left(\mathcal{W}, \mathcal{W}\frac{u+l}{2}, \frac{u-l}{2}\right) = \mathcal{C}\left(\mathcal{V}\,\mathrm{diag}\left(\frac{u-l}{2}\right), \mathcal{W}\frac{u-l}{2}\right).$$

As $\mathcal{V}$ is real, so

$$\mathrm{Re}\left(\mathcal{C}\left(\mathcal{V}\,\mathrm{diag}\left(\frac{u-l}{2}\right), \mathcal{W}\frac{u-l}{2}\right)\right) = \mathcal{Z}\left(\mathcal{V}\,\mathrm{diag}\left(\frac{u-l}{2}\right), \mathcal{W}\frac{u-l}{2}\right).$$

Combining the above results, we get

$$\mathcal{I}\left(\mathcal{W}, l, u\right) = \mathcal{Z}\left(\mathcal{W}\,\mathrm{diag}\left(\frac{u-l}{2}\right), \mathcal{W}\frac{u+l}{2}\right). \quad \square$$

Interval zonotopes are closed under linear transformation and Minkowski sum operations. The parameters of the resultant interval zonotopes are an affine transformation of the original parameters. This is described in the following lemmas.

Lemma 3.1.9 (Linear transformation)**.** *Let us consider* $A \in \mathbb{M}_{n\times n}\left(\mathbb{R}^n\right)$*. Then,*

$$A\mathcal{I}\left(\mathcal{W}, l, u\right) = \mathcal{I}\left(A\mathcal{W}, l, u\right).$$

Proof. Based on Lemma 3.1.8, we get

$$\begin{aligned}
&A\mathcal{I}\left(\mathcal{W}, l, u\right) = A\mathcal{Z}\left(\mathcal{W}\,\mathrm{diag}\left(\frac{u-l}{2}\right), \frac{u+l}{2}\right)\\
&\%\% \text{ by Lemma 1.1.3}\\
&= \mathcal{Z}\left(A\mathcal{W}\,\mathrm{diag}\left(\frac{u-l}{2}\right), \frac{u+l}{2}\right)\\
&\%\% \text{ by Lemma 3.1.8}\\
&= \mathcal{I}\left(A\mathcal{W}, l, u\right). \quad \square
\end{aligned}$$

Lemma 3.1.10 (Minkowski sum)**.** *The following is true.*

$$\mathcal{I}\left(\mathcal{W}, l, u\right) \oplus \mathcal{I}\left(\mathcal{W}', l', u'\right) = \mathcal{I}\left(\begin{bmatrix}\mathcal{W} & \mathcal{W}'\end{bmatrix}, \begin{bmatrix}l\\ l'\end{bmatrix}, \begin{bmatrix}u\\ u'\end{bmatrix}\right).$$

Proof. By Lemma 3.1.8, we get

$$
\begin{aligned}
&\mathcal{I}\left(\mathcal{W}, l, u\right) \oplus \mathcal{I}\left(\mathcal{W}', l', u'\right) \\
&= \mathcal{Z}\left(\mathcal{W}\,\mathrm{diag}\left(\frac{u-l}{2}\right), \frac{u+l}{2}\right) \oplus \mathcal{Z}\left(\mathcal{W}\,\mathrm{diag}\left(\frac{u'-l'}{2}\right), \frac{u'+l'}{2}\right) \\
&\%\% \text{ by Lemma 1.1.4} \\
&= \mathcal{Z}\left(\left[\mathcal{W}\,\mathrm{diag}\left(\tfrac{u-l}{2}\right) \quad \mathcal{W}'\,\mathrm{diag}\left(\tfrac{u'-l'}{2}\right)\right], \frac{u+l}{2} + \frac{u'+l'}{2}\right) \\
&= \mathcal{Z}\left(\begin{bmatrix}\mathcal{W} & \mathcal{W}'\end{bmatrix}\mathrm{diag}\left(\frac{\begin{bmatrix}u\\u'\end{bmatrix} - \begin{bmatrix}l\\l'\end{bmatrix}}{2}\right), \frac{\begin{bmatrix}u\\u'\end{bmatrix} + \begin{bmatrix}l\\l'\end{bmatrix}}{2}\right) \\
&\%\% \text{ by Lemma 3.1.8} \\
&= \mathcal{I}\left(\begin{bmatrix}\mathcal{W} & \mathcal{W}'\end{bmatrix}, \begin{bmatrix}l\\l'\end{bmatrix}, \begin{bmatrix}u\\u'\end{bmatrix}\right). \qquad \square
\end{aligned}
$$

The support of an interval zonotope along a vector is an affine function of the lower and upper interval bounds, which is stated in the following proposition.

Lemma 3.1.11 (Support of a vector)**.** *Let* $v \in \mathbb{R}^n$*. Then*

$$\rho\left(v, \mathcal{I}\left(\mathcal{W}, l, u\right)\right) = v^T\mathcal{W}\left(\frac{u+l}{2}\right) + \left|v^T\mathcal{W}\right|\left(\frac{u-l}{2}\right).$$

Proof. By Lemma 3.1.7, we get

$$
\begin{aligned}
&\rho\left(v, \mathcal{I}\left(\mathcal{W}, l, u\right)\right) = \rho\left(v, \mathrm{Re}\left(\mathcal{T}\left(\mathcal{W}, \frac{u+l}{2}, \frac{u-l}{2}\right)\right)\right) \\
&\%\% \text{ by Lemma 2.2.5} \\
&v^T\mathcal{W}\left(\frac{u+l}{2}\right) + \left|v^T\mathcal{W}\right|\left(\frac{u-l}{2}\right). \qquad \square
\end{aligned}
$$

3.2 Augmented complex zonotope and intersection

We shall now introduce the augmented complex zonotope set representation and describe the over-approximation of its intersection with a sub-parallelotope. In Lemma 3.1.4, we have shown that the intersection of a suitably aligned interval zonotope with a sub-parallelotope can be computed exactly by a simple algebraic formula. Afterwards, in Lemma 3.1.6, we gave an over-approximation and also an under-approximation of the intersection between a sub-parallelotope and the

Minkowski sum of a convex set with interval zonotope. Motivated by this, we specify an augmented complex zonotope as a Minkowski sum of a template complex zonotope and an interval zonotope. The idea behind such a representation is that the interval zonotope part is used to compute the intersection with a sub-parallelotope, while the template complex zonotope may capture positive invariance based on complex eigenstructure.

Definition 3.2.1. Let us consider a template complex zonotope $\mathcal{T}(\mathcal{V}, c, s) \subseteq \mathbb{C}^n$ and an interval zonotope $\mathcal{I}(\mathcal{W}, l, u) \subseteq \mathbb{R}^n$. Then the following is the representation of an augmented complex zonotope.

$$\mathcal{G}(\mathcal{V}, c, s, \mathcal{W}, l, u) = \mathcal{T}(\mathcal{V}, c, s) \oplus \mathcal{I}(\mathcal{W}, l, u).$$

Now we state an over-approximation by an augmented complex zonotope for the the intersection between an augmented complex zonotope and a sub-parallelotope. We also derive a bound on the over-approximation error expressed in terms of the Hausdorff distance.

We recall the notation used in Lemma 3.1.6. We define the Hausdorff distance as follows.

$$\delta_H(S_1, S_2) = \sup\left(\sup_{x\in S_1}\inf_{y\in S_2}\|x-y\|_2, \sup_{x\in S_2}\inf_{y\in S_1}\|x-y\|_2\right).$$

Theorem 3.2.2. *Let us denote* $\Psi_1 = \mathcal{G}\left(\mathcal{V}, c, s, \mathcal{K}^\dagger, l, u\right) \bigcap \mathcal{P}\left(\mathcal{K}, \widehat{l}, \widehat{u}\right)$, $\Psi_2 = \mathcal{P}\left(\mathcal{K}, \widehat{l}, \widehat{u}\right)$ *and* $\Psi_3 = \mathcal{G}\left(\mathcal{V}, c, s, \mathcal{K}^\dagger, l \bigvee \widehat{l}, u \bigwedge \widehat{u}\right)$. *Let us consider that*

$$l \leq l \bigvee \widehat{l} \leq u \bigwedge \widehat{u} \leq u \text{ and } \forall i \in \{1, ..., k\}$$
$$\mathcal{T}(\operatorname{diag}(\boldsymbol{\alpha}_i)\mathcal{K}\mathcal{V}, \operatorname{diag}(\boldsymbol{\alpha}_i)\mathcal{K}c, s) \sqsubseteq \mathcal{T}(\mathcal{K}\mathcal{V}, \mathcal{K}c, s). \tag{3.18}$$

Then $\Psi_1 \bigcap \Psi_2 \subseteq \Psi_3$ *and* (3.19)

$$\delta_H\left(\Psi_1 \bigcap \Psi_2, \Psi_3\right) \leq \left\|\begin{bmatrix}\mathcal{K}^\dagger & Y^\dagger\end{bmatrix}\right\|_2 \delta_H(\mathcal{T}(\mathcal{K}\mathcal{V}, \mathcal{K}c, s), 0). \tag{3.20}$$

Proof. Let us denote $S = \mathcal{T}(\mathcal{V}, c, s)$. We get by Equation 3.18 and Theorem 2.3.8 that $\forall i \in \{1, ..., k\}$, $\operatorname{diag}(\boldsymbol{\alpha}_i)\mathcal{K}S \subseteq \mathcal{K}S$.

Then by Lemma 3.1.6, we get

$$\text{Then } \begin{bmatrix}0\\ Y^T\end{bmatrix} S \oplus \begin{bmatrix}\mathcal{K}\\ Y^T\end{bmatrix} \mathcal{I}\left(\mathcal{K}^\dagger, l \bigvee \widehat{l}, u \bigwedge \widehat{u}\right)$$
$$\subseteq \begin{bmatrix}\mathcal{K}\\ Y^T\end{bmatrix} \left(\left(S \oplus \mathcal{I}\left(\mathcal{K}^\dagger, l, u\right)\right) \bigcap \mathcal{P}\left(\mathcal{K}, \widehat{l}, \widehat{u}\right)\right) \tag{3.21}$$
$$\subseteq \begin{bmatrix}\mathcal{K}\\ Y^T\end{bmatrix} \left(S \oplus \mathcal{I}\left(\mathcal{K}^\dagger, l \bigvee \widehat{l}, u \bigwedge \widehat{u}\right)\right). \tag{3.22}$$

By the definition of an augmented complex zonotope, we have

$$\Psi_1 = S \oplus \mathcal{I}\left(\mathcal{K}^\dagger, l, u\right), \quad \Psi_3 = S \oplus \mathcal{I}\left(\mathcal{K}^\dagger, l \bigvee \widehat{l}, u \bigwedge \widehat{u}\right).$$

Then by Equation 3.22 we get

$$\begin{bmatrix} \mathcal{K} \\ Y^T \end{bmatrix} \left(\Psi_1 \bigcap \Psi_2\right) \subseteq \begin{bmatrix} \mathcal{K} \\ Y^T \end{bmatrix} \Psi_3.$$

As $\begin{bmatrix} \mathcal{K} \\ Y^T \end{bmatrix}$ is a non-singular (invertible) matrix, we get Equation 3.19.

Next, we shall prove Equation 3.20. By Equation 3.21 and 3.22 we get

$$\begin{aligned}
&\delta_H\left(\begin{bmatrix} \mathcal{K} \\ Y^T \end{bmatrix} \left(\Psi_1 \bigcap \Psi_2\right), \begin{bmatrix} \mathcal{K} \\ Y^T \end{bmatrix} (\Psi_3)\right) \leq \delta_H\left(\mathcal{K}S, 0\right). \\
&\implies \delta_H\left(\Psi_1 \bigcap \Psi_2, \Psi_3\right) \\
&\leq \left\| \begin{bmatrix} \mathcal{K}^\dagger & Y^\dagger \end{bmatrix} \right\|_2 \delta_H\left(\begin{bmatrix} \mathcal{K} \\ Y^T \end{bmatrix} \left(\Psi_1 \bigcap \Psi_2\right), \begin{bmatrix} \mathcal{K} \\ Y^T \end{bmatrix} (\Psi_3)\right) \\
&\leq \left\| \begin{bmatrix} \mathcal{K}^\dagger & Y^\dagger \end{bmatrix} \right\|_2 \delta_H\left(\mathcal{K}S, 0\right) = \left\| \begin{bmatrix} \mathcal{K}^\dagger & Y^\dagger \end{bmatrix} \right\|_2 \delta_H\left(\mathcal{T}\left(\mathcal{K}\mathcal{V}, \mathcal{K}c, s\right), 0\right). \qquad \square
\end{aligned}$$

In Theorem 3.2.2, the above bound on the over-approximation error is positively correlated with $\mathcal{K}\mathcal{V}$ and $\mathcal{K}c$, i.e., the orientation between the sub-parallelotopic template $\mathcal{K}$ the the primary template $\mathcal{V}$ and primary offset c. The bound is zero when the $\mathcal{K}$ is orthogonal to $\mathcal{V}$ and c, in which case the we can exactly specify the intersection by the augmented complex zonotope.

Example 3.2.3. Let us consider an augmented complex zonotope $S_1 = \mathcal{G}\left(V, 0, [1]_{3\times 1}, K^\dagger, 1, 1\right)$ and a sub-parallelotope $S_2 = \mathcal{P}\left(K, 0.5, 0.5\right)$ where

$$V = \begin{bmatrix} 1+2\iota & 1 & 0 \\ 1-\iota & 0 & 0 \\ 0 & 0 & e \end{bmatrix}, \quad K = \begin{bmatrix} 0 & 0 & 1 \end{bmatrix}.$$

for some $e \in \mathbb{R}$. Then

$$S_1 \bigcap S_2 \subseteq \mathcal{G}\left(V, 0, [1]_{3\times 1}, K, 0.5, 0.5\right).$$

Furthermore, the over-approximation error is proportional to $|e|$, which is equal to $\|KV\|_2$. For example, when $e = 0$, then the over-approximation error is zero, i.e., the above is an equality. On the other hand, when $e \neq 0$, then the Hausdorff distance between the intersected set and the over-approximation is equal to e. This is illustrated in Figures 3.1, 3.1 and 3.1 that display the projection of the intersected set and the over-approximation along the XY and YZ planes for $e = 0$, $e = 0.5$ and $e = 1$, respectively.

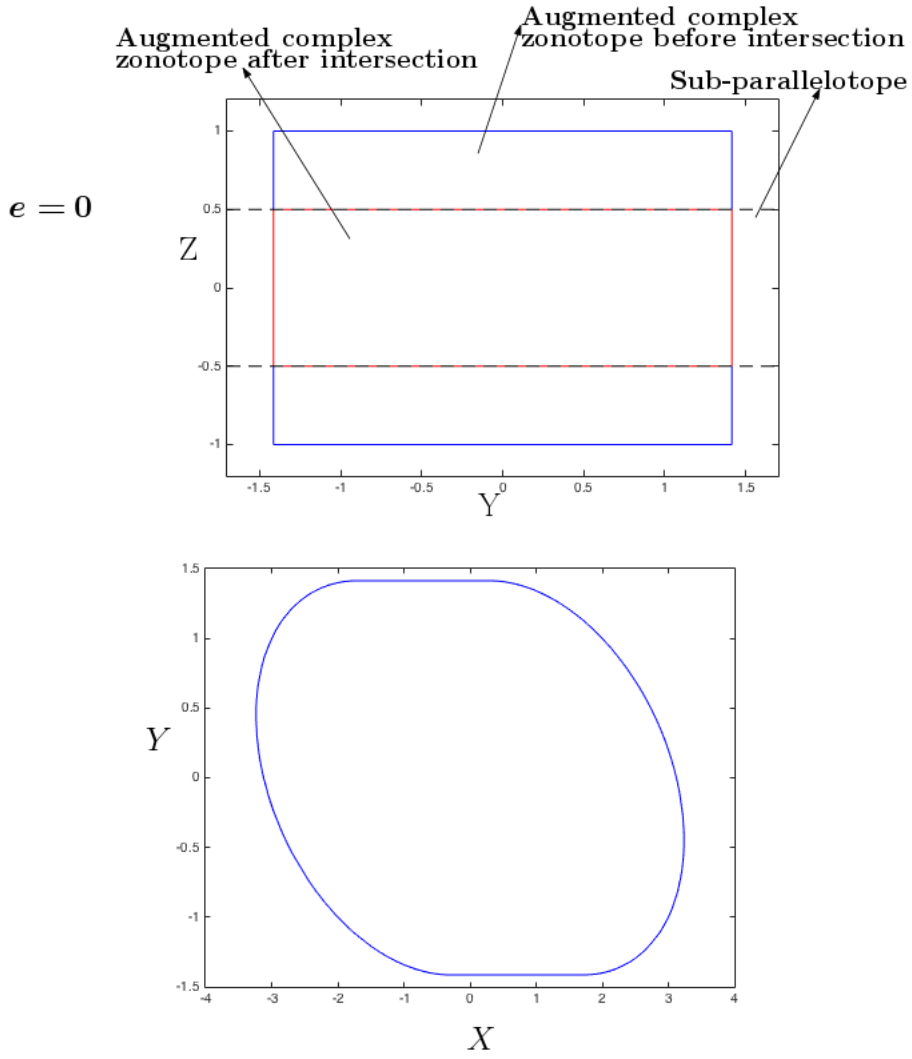

Figure 3.1: Over-approximation of intersection for $e = 0$.

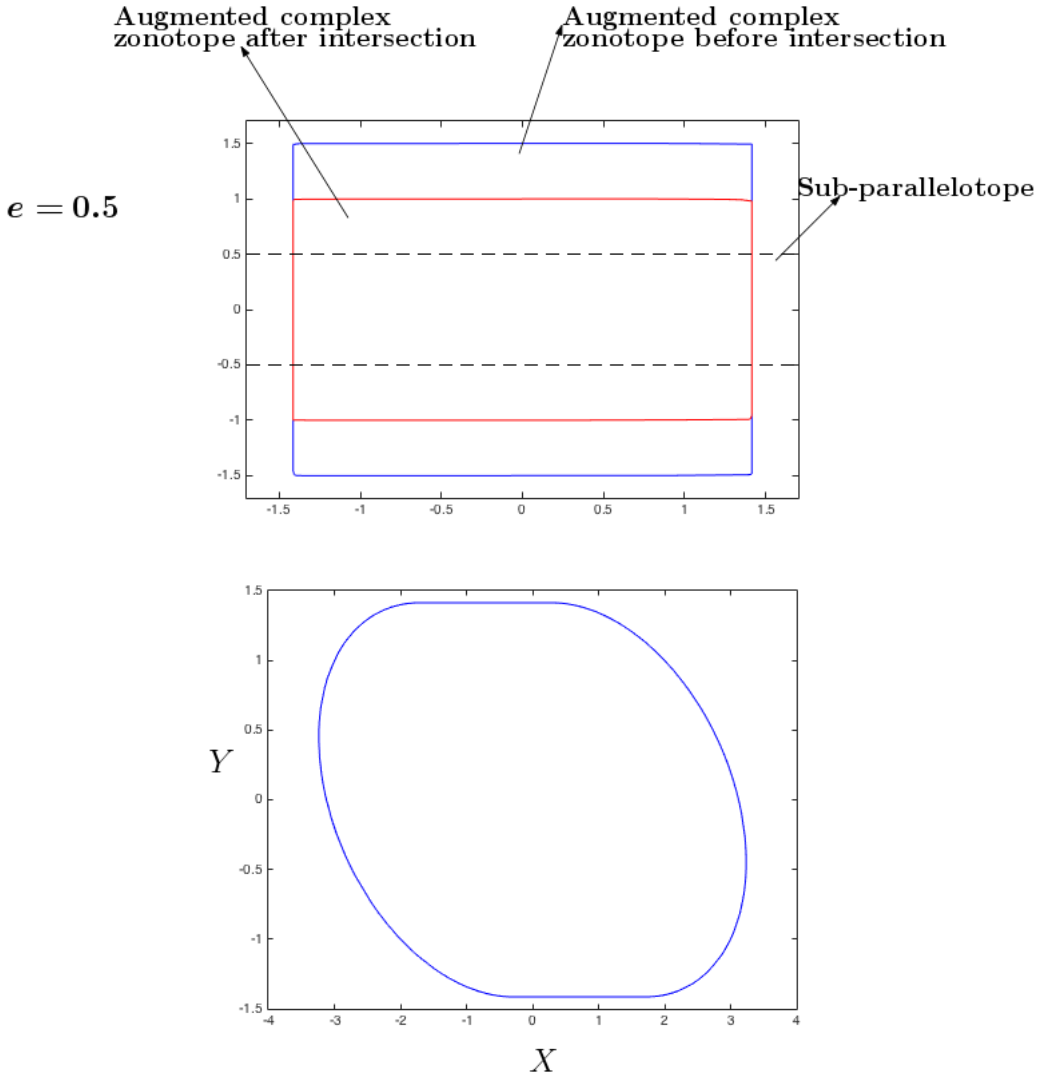

Figure 3.2: Over-approximation of intersection for $e = 0.5$.

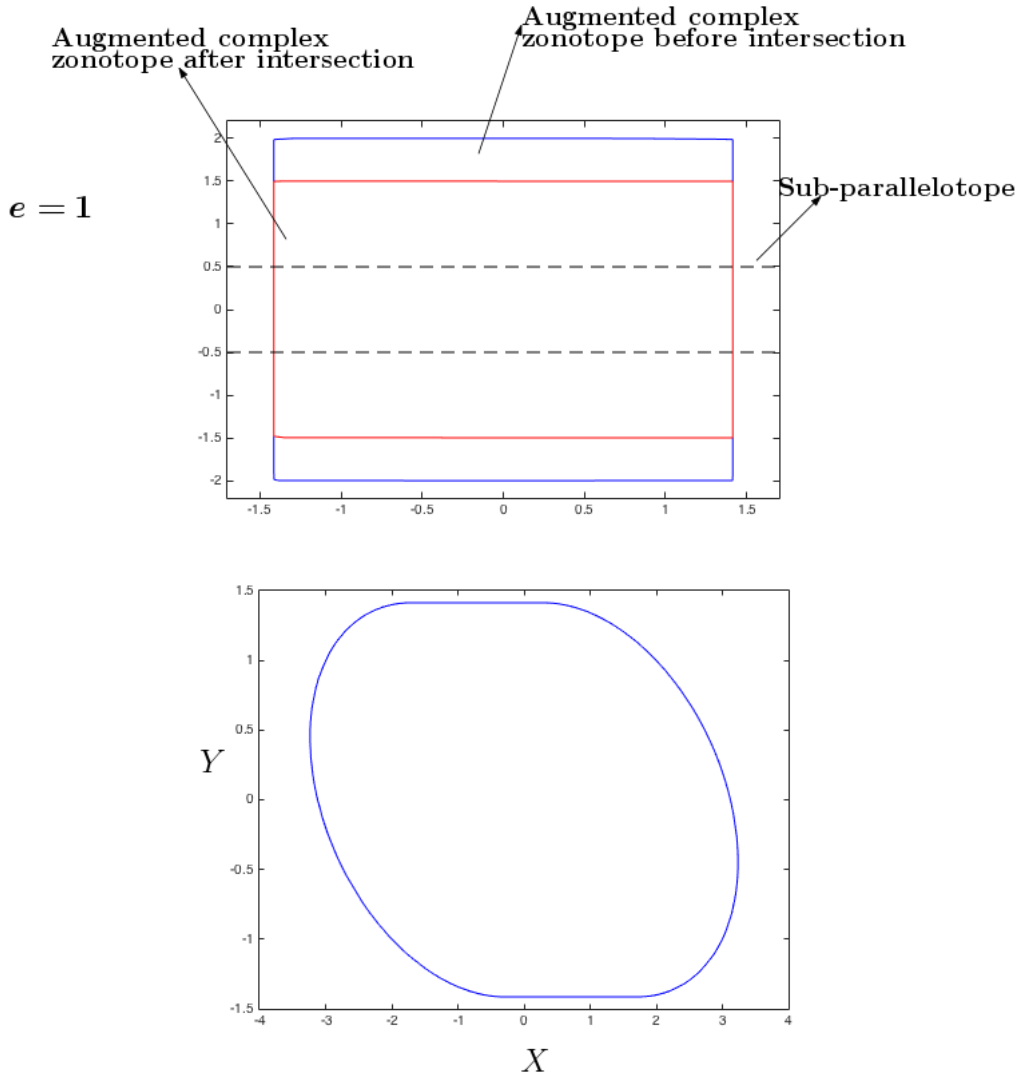

Figure 3.3: Over-approximation of intersection for $e = 1$.

3.3 Other operations on augmented complex zonotopes

We shall now describe other operations on augmented complex zonotopes like are linear transformation, Minkowski sum, support function and checking inclusion.

Augmented complex zonotopes are closed under linear transformation and Minkowski sum, as described in the following two lemmas. This is because an augmented complex is specified as a Minkowski sum of a template complex zonotope and an interval zonotope, both of which are closed under these operations.

Lemma 3.3.1 (Linear transformation)**.** *Let us consider* $A \in \mathbb{M}_{n\times n}(\mathbb{R})$. *Then*

$$A\mathcal{G}(\mathcal{V}, c, s, \mathcal{W}, l, u) = \mathcal{G}(A\mathcal{V}, Ac, s, A\mathcal{W}, l, u).$$

Proof. We derive the following.

$$\begin{aligned}
&A\mathcal{G}(\mathcal{V}, c, s, \mathcal{W}, l, u) = A(\mathcal{T}(\mathcal{V}, c, s) \oplus \mathcal{I}(\mathcal{W}, l, u)) \\
&\%\% \text{ by Lemmas 2.2.1 and 3.1.9} \\
&= \mathcal{T}(A\mathcal{V}, Ac, s) \oplus \mathcal{I}(A\mathcal{W}, l, u) \\
&= \mathcal{G}(A\mathcal{V}, Ac, s, A\mathcal{W}, l, u). \qquad \square
\end{aligned}$$

Lemma 3.3.2 (Minkowski sum)**.** *The following is true.*

$$\begin{aligned}
&\mathcal{G}(\mathcal{V}, c, s, \mathcal{W}, l, u) \oplus \mathcal{G}(\mathcal{V}', c', s', \mathcal{W}', l', u') \\
&= \mathcal{G}\left(\begin{bmatrix}\mathcal{V} & \mathcal{V}'\end{bmatrix}, c + c', \begin{bmatrix}s \\ s'\end{bmatrix}, \begin{bmatrix}\mathcal{W} & \mathcal{W}'\end{bmatrix}, \begin{bmatrix}l \\ l'\end{bmatrix}, \begin{bmatrix}u \\ u'\end{bmatrix}\right)
\end{aligned}$$

Proof. We derive the following.

$$\begin{aligned}
&\mathcal{G}(\mathcal{V}, c, s, \mathcal{W}, l, u) \oplus \mathcal{G}(\mathcal{V}', c', s', \mathcal{W}', l', u') \\
&= \mathcal{T}(\mathcal{V}, c, s) \oplus \mathcal{I}(\mathcal{W}, l, u) \oplus \mathcal{T}(\mathcal{V}', c', s') \oplus \mathcal{I}(\mathcal{W}', l', u') \\
&= (\mathcal{T}(\mathcal{V}, c, s) \oplus \mathcal{T}(\mathcal{V}', c', s')) \oplus (\mathcal{I}(\mathcal{W}, l, u) \oplus \mathcal{I}(\mathcal{W}', l', u')) \\
&\%\% \text{ by Lemmas 2.2.3 and 3.1.10} \\
&= \mathcal{T}\left(\begin{bmatrix}\mathcal{V} & \mathcal{V}'\end{bmatrix}, c + c', \begin{bmatrix}s \\ s'\end{bmatrix}\right) \oplus \mathcal{I}\left(\begin{bmatrix}\mathcal{W} & \mathcal{W}'\end{bmatrix}, \begin{bmatrix}l \\ l'\end{bmatrix}, \begin{bmatrix}u \\ u'\end{bmatrix}\right) \\
&= \mathcal{G}\left(\begin{bmatrix}\mathcal{V} & \mathcal{V}'\end{bmatrix}, c + c', \begin{bmatrix}s \\ s'\end{bmatrix}, \begin{bmatrix}\mathcal{W} & \mathcal{W}'\end{bmatrix}, \begin{bmatrix}l \\ l'\end{bmatrix}, \begin{bmatrix}u \\ u'\end{bmatrix}\right). \qquad \square
\end{aligned}$$

To problem of checking inclusion between two augmented complex zonotopes can be equivalently expressed as the problem of checking inclusion between two geometrically equivalent template complex zonotopes. For this, we use the following equivalence between the real projections of an augmented complex zonotope and a template complex zonotope.

Lemma 3.3.3. *The following is true.*

$$\mathrm{Re}\left(\mathcal{G}\left(\mathcal{V}, c, s, \mathcal{W}, l, u\right)\right) = \mathrm{Re}\left(\mathcal{T}\left(\begin{bmatrix}\mathcal{V} & \mathcal{W}\end{bmatrix}, c + \tfrac{u+l}{2}, \begin{bmatrix} s \\ \frac{u-l}{2}\end{bmatrix}\right)\right).$$

Proof. We derive the following.

$$\begin{aligned}
&\mathrm{Re}\left(\mathcal{G}\left(\mathcal{V}, c, s, \mathcal{W}, l, u\right)\right) = \mathrm{Re}\left(\mathcal{T}\left(\mathcal{V}, c, s\right)\right) \oplus \mathcal{I}\left(\mathcal{W}, l, u\right) \\
&\%\% \text{ By Lemma 3.1.7} \\
&= \mathrm{Re}\left(\mathcal{T}\left(\mathcal{V}, c, s\right)\right) \oplus \mathrm{Re}\left(\mathcal{T}\left(\mathcal{W}, \mathcal{W}\frac{u+l}{2}, \frac{u-l}{2}\right)\right) \\
&= \mathrm{Re}\left(\mathcal{T}\left(\begin{bmatrix}\mathcal{V} & \mathcal{W}\end{bmatrix}, c + \tfrac{u+l}{2}, \begin{bmatrix} s \\ \frac{u-l}{2}\end{bmatrix}\right)\right). \qquad \square
\end{aligned}$$

In Definition 2.3.7 of the previous chapter, we introduced a partial order "$\sqsubseteq$", as a sufficient convex condition for checking inclusion between two template complex zonotopes. We extend the relation for checking inclusion between two augmented complex zonotopes as follows.

Definition 3.3.4 (Ordering between augmented complex zonotopes)**.** We say that $\mathcal{G}\left(\mathcal{V}', c', s', \mathcal{W}', l', u'\right) \sqsubseteq \mathcal{G}\left(\mathcal{V}, c, s, \mathcal{W}, l, u\right)$ iff

$$\mathcal{T}\left(\begin{bmatrix}\mathcal{V}' & \mathcal{W}'\end{bmatrix}, c' + \tfrac{u'+l'}{2}, \begin{bmatrix} s' \\ \frac{u'-l'}{2}\end{bmatrix}\right) \sqsubseteq \mathcal{T}\left(\begin{bmatrix}\mathcal{V} & \mathcal{W}\end{bmatrix}, c + \tfrac{u+l}{2}, \begin{bmatrix} s \\ \frac{u-l}{2}\end{bmatrix}\right). \quad (3.23)$$

Theorem 3.3.5 (Inclusion-checking and partial order)**.** *All of the following is true.*

1. *Sufficient condition for inclusion:*

$$\begin{aligned}
&\mathcal{G}\left(\mathcal{V}', c', s', \mathcal{W}', l', u'\right) \sqsubseteq \mathcal{G}\left(\mathcal{V}, c, s, \mathcal{W}, l, u\right) \\
&\implies \mathrm{Re}\left(\mathcal{G}\left(\mathcal{V}', c', s', \mathcal{W}', l', u'\right)\right) \subseteq \mathrm{Re}\left(\mathcal{G}\left(\mathcal{V}, c, s, \mathcal{W}, l, u\right)\right).
\end{aligned}$$

2. *The relation "$\sqsubseteq$" is equivalent to a set of second order conic constraints on the primary offset, scaling factors and upper and lower interval bounds.*

Proof. We derive the following.

$$\begin{aligned}
&\mathcal{G}\left(\mathcal{V}', c', s', \mathcal{W}', l', u'\right) \sqsubseteq \mathcal{G}\left(\mathcal{V}, c, s, \mathcal{W}, l, u\right) \\
&\Leftrightarrow \mathcal{T}\left(\begin{bmatrix}\mathcal{V}' & \mathcal{W}'\end{bmatrix}, c' + \tfrac{u'+l'}{2}, \begin{bmatrix} s' \\ \frac{u'-l'}{2}\end{bmatrix}\right) \sqsubseteq \mathcal{T}\left(\begin{bmatrix}\mathcal{V} & \mathcal{W}\end{bmatrix}, c + \tfrac{u+l}{2}, \begin{bmatrix} s \\ \frac{u-l}{2}\end{bmatrix}\right) \\
&\%\% \text{ By Theorem 2.3.8} \\
&\implies \mathcal{T}\left(\begin{bmatrix}\mathcal{V}' & \mathcal{W}'\end{bmatrix}, c' + \tfrac{u'+l'}{2}, \begin{bmatrix} s' \\ \frac{u'-l'}{2}\end{bmatrix}\right) \subseteq \mathcal{T}\left(\begin{bmatrix}\mathcal{V} & \mathcal{W}\end{bmatrix}, c + \tfrac{u+l}{2}, \begin{bmatrix} s \\ \frac{u-l}{2}\end{bmatrix}\right) \\
&\%\% \text{ By Lemma 3.3.3} \\
&\implies \mathrm{Re}\left(\mathcal{G}\left(\mathcal{V}', c', s', \mathcal{W}', l', u'\right)\right) \subseteq \mathrm{Re}\left(\mathcal{G}\left(\mathcal{V}, c, s, \mathcal{W}, l, u\right)\right).
\end{aligned}$$

Since "$\sqsubseteq$" is equivalent to SOCC constraints on the center and scaling factors of template complex zonotope, Equation 3.23 translates them to SOCC on the primary offset, scaling factors and lower and upper interval bounds. □

Remark 3.3.6. We have explained for template complex zonotopes that the relation "$\sqsubseteq$" is equivalent to second order conic constraints on the center, scaling factors and some auxiliary variables. Therefore, according to Equation 3.23, the extension of "$\sqsubseteq$" to augmented complex zonotopes is equivalent to second order conic constraints on the primary offset, scaling factors, lower and upper interval bounds and some auxiliary variables.

The support function of an augmented complex zonotope is as an affine expression of the primary offset, scaling factors and the upper and lower interval bounds. This is described in the following lemma.

Lemma 3.3.7 (Support function)**.** *Let us consider* $v \in \mathbb{R}^n$*. Then*

$$\begin{aligned}&\rho\left(v, \operatorname{Re}\left(\mathcal{G}\left(\mathcal{V}, c, s, \mathcal{W}, l, u\right)\right)\right)\\ &= \operatorname{Re}\left(v^T \begin{bmatrix}\mathcal{V} & \mathcal{W}\end{bmatrix}\left(c + \frac{u+l}{2}\right)\right) + \left|v^T \begin{bmatrix}\mathcal{V} & \mathcal{W}\end{bmatrix}\right| \begin{bmatrix} s \\ \frac{u-l}{2}\end{bmatrix}.\end{aligned}$$

Proof. By using Lemmas 2.2.5 and 3.1.11, we get

$$\begin{aligned}&\rho\left(v, \operatorname{Re}\left(\mathcal{G}\left(\mathcal{V}, c, s, \mathcal{W}, l, u\right)\right)\right)\\ &= \rho\left(v, \operatorname{Re}\left(\mathcal{T}\left(\mathcal{V}, c, s\right)\right)\right) + \rho\left(v, \mathcal{I}\left(\mathcal{W}, l, u\right)\right)\\ &= v^T c + \left|v^T W\right| s + v^T\left(\frac{u+l}{2}\right) + \left|v^T W\right|\left(\frac{u-l}{2}\right)\\ &= \operatorname{Re}\left(v^T \begin{bmatrix}\mathcal{V} & \mathcal{W}\end{bmatrix}\left(c + \frac{u+l}{2}\right)\right) + \left|v^T \begin{bmatrix}\mathcal{V} & \mathcal{W}\end{bmatrix}\right| \begin{bmatrix} s \\ \frac{u-l}{2}\end{bmatrix}.\end{aligned}$$ □

CHAPTER 4

Invariance Verification for Discrete Time Affine Hybrid Systems

In many verification problems, the safe set can be given linear constraints. In this case, to verify safety, we have to verify the bounds on the reachable set of the system along the directions of the normals to the bounding hyperplanes. We shall call the boundedness of the reachable set along a given set of directions as a *linear invariance property*. In other words, a linear invariance property is a linear constraint that is true for all reachable states of the system at all time instants. We consider the problem of verifying a linear invariance property of a discrete time affine hybrid system. We show that a linear invariance property is equivalent to the existence of a positive invariant containing the initial set and satisfying the linear constraints of the invariance property. However, the smallest positive invariant satisfying the property can be computationally intractable to represent. Alternatively, we can use a set representation by which we can compute sufficiently accurate positive invariants that verify the property.

We shall use augmented complex zonotopes to compute the positive invariants. As discussed earlier, complex zonotopes have the advantage that they are closed under linear transformation and Minkowski sum, and efficiently capture positive invariants for linear systems using the complex eigenstructure. Their representation is generalized to augmented complex zonotopes to compute an over-approximation of the intersection with linear guards such that the support function can still be computed efficiently. The efficient computation of support function is crucial for verifying the satisfaction of linear constraints given in a linear invariance property. We shall derive a convex program for finding augmented complex

zonotope positive invariants to verify a linear invariance property. The derivation of the convex program uses the computations on augmented complex zonotopes that we have developed earlier.

This chapter is organized into four main sections. In Section 4.1, we describe a discrete time affine hybrid system and positive invariants of the system. In Section 4.2, we define a linear invariance property and show its equivalence to the existence of a certain positive invariant. In Section 4.3, we derive a convex program for computing a positive invariant that verifies a linear invariance property. We also explain heuristics for choosing the template of the augmented complex to leverage the efficiency of the verification procedure. In Section 4.4, we discuss experiments on three benchmark examples that demonstrate the efficiency of our approach.

4.1 Discrete time affine hybrid system

In a discrete time affine hybrid system, the state of the system is specified by a discrete valued variable, called location, and a continuous variable whose valuation is in the real Euclidean space of a finite dimension. The state of the system in each location has to stay within a polyhedral set, called the staying condition. The state of the system can change by two kinds of transitions, *continuous transition* and *discrete transit on*. In a continuous transition, the discrete state of the system remains constant while the continuous state changes by an affine transformation. The affine transformation has possible additive disturbance input, which is bounded. The parameters of the affine transformation of a continuous transition depend on the location in which the transition takes place. In a discrete transition, there is a change in the discrete variable accompanied by an affine transformation of the continuous variable. The transition is has precondition specified by a linear constraint, called a guard, while the post-condition is the staying condition in the location reached after transition. A set of edges specifies the possible discrete transitions, vis a vis, the locations between which a discrete transition takes place, the parameters of the affine transformation and the guard.

Sub-parallelotopic guards and staying conditions: In this paper, we consider hybrid systems where the guards and staying conditions can be specified by a sub-parallelotope with a common template. We note that the class of sub-parallelotopic constraints are quite general and can be used in the specification of many practical affine hybrid systems.

Model. We specify the discrete time affine hybrid system by a tuple

$$\mathbb{H} = (Q, \mathcal{K}, \gamma, \mathcal{A}, U, E)\,.$$

The finite set of locations is Q. The sub-parallelotopic template for specifying the guards and staying conditions is $\mathcal{K} \in \mathbb{M}_{k\times n}(\mathbb{R})$. The staying set in a location $q \in Q$ is a sub-parallelotope $\mathcal{P}\left(\mathcal{K}, \gamma_q^-, \gamma_q^+\right)$, whose pair of lower and upper interval bounds is $\gamma_q = \left(\gamma_q^-, \gamma_q^+\right)$. The parameters affine transformation in a location $q \in Q$ consist of a linear transformation, specified by a matrix $\mathcal{A}_q \in \mathbb{M}_{n\times n}(\mathbb{R})$, and a bounded additive disturbance input set $U_q \subset \mathbb{R}^n$. The set of edges is E. An edge $\sigma \in E$ is specified by a tuple

$$\sigma = \left(\sigma_1, \sigma_2, \sigma^+, \sigma^-, \mathcal{A}_\sigma, U_\sigma\right).$$

The before and after locations of a discrete transition along an edge σ are $\sigma_1, \sigma_2 \in Q$. The sub-parallelotope $\mathcal{P}(\mathcal{K}, \sigma^-, \sigma^+)$ is the guard on the transition along the edge σ, where (σ^-, σ^+) is the pair of lower and upper interval bounds of the sub-parallelotope. The parameters of the affine transformation for the discrete transition along the edge σ are specified by a matrix $\mathcal{A}_\sigma \in \mathbb{M}_{n\times n}(\mathbb{R})$ and a bounded additive disturbance input set $U_\sigma \subset \mathbb{R}^n$. The set of initial states is $\Psi \subseteq Q \times \mathbb{R}^n$.

Dynamics. A state of the hybrid system, called a *hybrid state*, is a pair (x, q), where $x \in \mathbb{R}^n$, called the *continuous state*, and $q \in Q$, called the *discrete state*. A *trajectory* is the evolution of the state of the system as a function of discrete time instants. A trajectory is a function $(\mathbf{x}, \mathbf{q}) : \mathbb{Z}_{\geq 0}^n \times Q$, such that $\forall t \in \mathbb{Z}_{\geq 0}$, one of the following conditions is true.

1. Continuous transition:

$$\begin{aligned}
&\exists u \in U_{\mathbf{q}(t)} \text{ such that all of the following are collectively true.}\\
&\mathbf{x}(t+1) = \mathcal{A}_{\mathbf{q}(t)} + u, \quad \text{(affine map with uncertain input)}\\
&\mathbf{q}(t+1) = \mathbf{q}(t) \quad \text{(location does not change)}\\
&\mathbf{x}(t), \mathbf{x}(t+1) \in \mathcal{P}\left(\mathcal{K}, \gamma_{\mathbf{q}(t)}^-, \gamma_{\mathbf{q}(t)}^+\right) \quad \text{(staying condition)}
\end{aligned} \tag{4.1}$$

2. Discrete transition:

$$\begin{aligned}
&\exists \sigma \in E \text{ and } u \in U_\sigma \text{ all the following are collectively true.}\\
&\mathbf{q}(t) = \sigma_1, \ \ \mathbf{q}(t+1) = \sigma_2 \quad \text{(possible change in location)}\\
&\%\% \text{ satisfaction of guard and staying condition before transition:}\\
&\mathbf{x}(t) \in \mathcal{P}\left(\mathcal{K}, \sigma^- \bigvee \gamma_{\mathbf{q}(t)}^-, \sigma^+ \bigwedge \gamma_{\mathbf{q}(t)}^+\right)\\
&\%\% \text{ satisfaction of staying condition after transition:}\\
&\mathbf{x}(t+1) \in \mathcal{P}\left(\mathcal{K}, \gamma_{\mathbf{q}(t+1)}^-, \gamma_{\mathbf{q}(t)}^+\right)
\end{aligned} \tag{4.2}$$

In the definition, we use the following notation for the set of continuous states corresponding to a set of hybrid states Ψ for a fixed location q.

$$\Psi_q = \{x \in \mathbb{R}^n : \ (x, q) \in \Psi\}.$$

We denote the set of all possible trajectories of the system as Γ. We denote the set of next reachable states by every possible transition from a set of states Ψ as $\mathcal{R}(\Psi)$, which is mathematically defined as follows.

Definition 4.1.1 (Next set of reachable states)**.** Let us consider a subset of states $\Psi \subset \mathbb{R}^n \times Q$. The next set of reachable states of Ψ is

$$\mathcal{R}(\Psi) = \{(\mathbf{x}(t), \mathbf{q}(t)) : \ (\mathbf{x}(0), \mathbf{q}(0)) \in \Psi, \ (\mathbf{x}, \mathbf{q}) \in \Gamma\} \subseteq .$$

So, we define the set of reachable states at a time t starting from an initial set of states Ψ, denoted $\mathcal{R}^t(\Psi)$, as follows.

Definition 4.1.2 (Reachable states at a time point)**.** Let us consider a subset of states $\Psi \subseteq \mathbb{R}^n \times Q$. For all $t \in \mathbb{Z}_{\geq 0}$, we define $\mathcal{R}^t(\Psi)$ inductively as follows.

1. $\mathcal{R}^0(\Psi) = \Psi$.
2. If $t \geq 1$, $\mathcal{R}^t(\Psi) = \mathcal{R}(\mathcal{R}^{t-1}(\Psi))$.

Based on Equation 4.1, the continuous projection of the set of reachable states of a system from a set of states Ψ, after a continuous transition in a location q, denoted $\mathcal{R}_q(\Psi)$, can be represented as follows.

$$\mathcal{R}_q(\Psi) = \left(\mathcal{A}_q\left(\Psi_q \bigcap \mathcal{P}\left(\mathcal{K}, \gamma_q^-, \gamma_q^+\right)\right) \oplus U_q\right) \bigcap \mathcal{P}\left(\mathcal{K}, \gamma_q^-, \gamma_q^+\right). \tag{4.3}$$

Similarly, based on Equation 4.2, the continuous projection of the set of reachable states of a system from a set of states Ψ, after a discrete transition along an edge σ, denoted $\mathcal{R}_\sigma(\Psi)$, can be represented as follows.

$$\mathcal{R}_\sigma(\Psi) = \left(\mathcal{A}_\sigma\left(\Psi_{\sigma_1} \bigcap \mathcal{P}\left(\mathcal{K}, \sigma^- \bigvee \gamma_{\sigma_1}^-, \sigma^+ \bigwedge \gamma_{\sigma_1}^+\right)\right) \oplus U_\sigma\right) \bigcap \mathcal{P}\left(\mathcal{K}, \gamma_{\sigma_2}^-, \gamma_{\sigma_2}^+\right). \tag{4.4}$$

Therefore, we can represented the set of reachable states of the system in one time step from a set of states Ψ as follows.

$$\mathcal{R}(\Psi) = \bigcup_{q \in Q} (\mathcal{R}_q(\Psi), q) \bigcup_{\sigma \in E} (\mathcal{R}_\sigma(\Psi), \sigma_2).$$

If a set of states of the system are such that its next set of states is contained within itself, then it is called a *positive invariant*.

Definition 4.1.3 (Positive invariant)**.** A subset of states $\Omega \subseteq \mathbb{R}^n \times Q$ is a positive invariant iff $\mathcal{R}(\Omega) \subseteq \Omega$.

The reachable set of states for all time instants can be over-approximated by computing a positive invariant which contains the initial set. This is described in the following lemma.

Lemma 4.1.4 (Positive invariant based over-approximation of reachable states)**.** *Let us consider a positive invariant Ω such that $\Psi \subseteq \Omega$. Then*

$$\forall t \in \mathbb{Z}_{\geq 0}\, \mathcal{R}^t(\Psi) \subseteq \Omega$$

Proof. We prove the result by induction. We have $\mathcal{R}^0(t) = \Psi \subseteq \Omega$ as given, which means that the result holds for $t = 0$. Assume that for a $t \geq 0$, $\mathcal{R}^t(\Psi) \subseteq \Omega$. Then we derive the following.

$$\begin{aligned}
&\mathcal{R}^{t+1}(\Psi) = \mathcal{R}\left(\mathcal{R}^t(\Psi)\right) \subseteq \mathcal{R}(\Omega)\\
&\%\% \text{ by the definition of positive invariant}\\
&\subseteq \Omega.
\end{aligned}$$

The lemma then follows by the principle of induction. □

The set of all reachable states of the system at all discrete time instants is itself a positive invariant. This is described in the following lemma.

Lemma 4.1.5. *Let us consider a subset of states $\Psi \subseteq \mathbb{R}^n \times Q$ and*

$$\Omega = \bigcup_{t=0}^{\infty} \mathcal{R}^t(\Psi).$$

Then Ω is a positive invariant.

Proof. We derive the following.

$$\begin{aligned}
&\mathcal{R}(\Omega) = \mathcal{R}\left(\bigcup_{t=0}^{\infty} \mathcal{R}^t(\Psi)\right) = \bigcup_{t=0}^{\infty} \mathcal{R}\left(\mathcal{R}^t(\Psi)\right)\\
&= \bigcup_{t=0}^{\infty} \mathcal{R}^{t+1}(\Psi) = \bigcup_{t=1}^{\infty} \mathcal{R}^t(\Psi)\\
&\subseteq \bigcup_{t=0}^{\infty} \mathcal{R}^t(\Psi) = \Omega. \qquad \square
\end{aligned}$$

4.2 Linear invariance property

A linear invariance property is a set of linear inequalities that are satisfied by the state of the system at all time instants for every trajectory starting in a given initial set. Mathematically, it is defined as follows.

Definition 4.2.1 (Linear Invariance)**.** Let us consider a set of states $\Psi \subseteq \mathbb{R}^n \times Q$, a real matrix $T \in \mathbb{M}_{r\times n}(\mathbb{R})$ and a real vector $d \in \mathbb{R}^r$. We say that

$$(\mathbb{H}, \Psi) \models (T, d) \text{ (Linear invariance property) iff}$$

$$\forall t \in \mathbb{Z}_{\geq 0}, \forall x \in \bigcup_{q\in Q} \left(\mathcal{R}^t(\Psi)\right)_q : \ Tx \leq d.$$

To prove that a set of initial states satisfies a linear invariance property, we can equivalently show the existence of a positive invariant containing the initial states and satisfying the linear constraints given in the property specification. This is described below.

Lemma 4.2.2. *We have $(\mathbb{H}, \Psi) \models (T, d)$ iff there exists a positive invariant Ω such that $\Psi \subseteq \Omega$ and $\forall q \in Q\ \forall x \in \Omega_q : \ Tx \leq d$.*

Proof. Case 1: Let us consider that there exists a positive invariant Ω such that $\Psi \subseteq \Omega$ and $\forall q \in Q\ \forall x \in \Omega_q : \ Tx \leq d$. Since Ω is a positive invariant, we have

$$\bigcup_{t\in\mathbb{Z}_{\geq 0}} \mathcal{R}^t(\Omega) \subseteq \Omega$$

$$\begin{aligned}
&\therefore \forall t \in \mathbb{Z}_{\geq 0}\ \forall q \in Q\ \forall x \in \left(\mathcal{R}^t(\Omega)\right)_q : \ Tx \leq d \\
&\%\% \text{ since } \Psi \subseteq \Omega \\
&\forall t \in \mathbb{Z}_{\geq 0}\ \forall q \in Q\ \forall x \in \left(\mathcal{R}^t(\Psi)\right)_q : \ Tx \leq d \\
&(\Psi, \mathbb{H}) \models (T, d).
\end{aligned}$$

Case 2: Let us consider that $(\mathbb{H}, \Psi) \models (T, d)$. Let us denote

$$\Omega = \bigcup_{t=0}^{\infty} \mathcal{R}^t(\Psi).$$

Then by Lemma 4.1.5, Ω is a positive invariant. By the definition of linear invariant property, we get

$$\begin{aligned}
&\forall t \in \mathbb{Z}_{\geq 0}, \forall x \in \bigcup_{q \in Q} \left(\mathcal{R}^t\left(\Psi\right)\right)_q : \;\; Tx \leq d \\
&\Leftrightarrow \forall q \in Q \; \forall x \in \left(\bigcup_{t=0}^{\infty} \mathcal{R}^t\left(\Psi\right)\right)_q : \;\; Tx \leq d \\
&\Leftrightarrow \forall q \in Q \; \forall x \in \Omega_q : \;\; Tx \leq d.
\end{aligned}$$

The lemma follows from the results in both the above cases. □

4.3 Verification using complex zonotope

By Lemma 4.2.2, to prove a linear invariance property, we can compute a positive invariant containing the initial set and which satisfies the property. We shall derive a convex program to compute a positively invariant satisfying a linear invariance property and containing an initial set, whose continuous projection in any location is represented as an augmented complex zonotope. Our procedure a priori fixes the templates of the augmented complex zonotope and synthesizes the set of scaling factors, and lower and upper interval bounds for verifying the property. We shall discuss in a latter section how to select a suitable primary template. But the secondary template has to be the pseudo-inverse of the sub-parallelotopic template of the system, so that we can over-approximate the intersection with the guards and staying conditions based on Theorem 3.2.2.

Let us consider a set of states Ω whose projection onto continuous states in a location q is an augmented complex zonotope specified as

$$\Omega_q = \mathcal{G}\left(\mathcal{V}, c_q, s_q, \mathcal{K}^{\dagger}, l_q, u_q\right).$$

where $\mathcal{V} \in \mathbb{M}_{n \times m}\left(\mathbb{C}\right)$. Furthermore, we have the following condition on the templates so as to compute a sound intersection with the guards and staying conditions, based on Theorem 3.2.2.

$$\begin{aligned}
&\forall i \in \{1, ..., k\}\,, \; \forall q \in Q \\
&\mathcal{T}\left(\mathrm{diag}\left(\boldsymbol{\alpha}_i\right)\mathcal{K}\mathcal{V}, \mathrm{diag}\left(\boldsymbol{\alpha}_i\right)\mathcal{K}c_q, s_q\right) \sqsubseteq \mathcal{T}\left(\mathcal{K}\mathcal{V}, \mathcal{K}c_q, s_q\right)
\end{aligned} \tag{4.5}$$

We consider an over-approximation of the input disturbance set in any transition function, by an augmented complex zonotope, as follows.

$$\forall q \in Q, \; U_q \subseteq \mathcal{G}\left(\mathcal{V}_q^{\mathrm{inp}}, c_q^{\mathrm{inp}}, s_q^{\mathrm{inp}}, \mathcal{W}_q^{\mathrm{inp}}, l_q^{\mathrm{inp}}, u_q^{\mathrm{inp}}\right) \tag{4.6}$$

$$\forall \sigma \in E, \; U_\sigma \subseteq \mathcal{G}\left(\mathcal{V}_\sigma^{\mathrm{inp}}, c_\sigma^{\mathrm{inp}}, s_\sigma^{\mathrm{inp}}, \mathcal{W}_\sigma^{\mathrm{inp}}, l_\sigma^{\mathrm{inp}}, u_\sigma^{\mathrm{inp}}\right). \tag{4.7}$$

Min and Max-approximation functions: The over-approximation of an intersection between an augmented complex zonotope and a sub-parallelotope, given in Theorem 3.2.2 requires computing component wise minimum (meet) and maximum (join) of two real vectors. The meet and join operations on real vectors are in general not affine functions of the arguments. Since we are interested in deriving a convex program, we want to find an affine expression for the meet and join operations. In this regard, we observe that under a certain affine constraint on the variables, the meet and join operations can be expressed as affine expressions of the variables. We consider two affine functions called *min-approximation* and *max-approximation* functions, defined as follows. A function $[\![\bigwedge]\!] : \mathbb{R}^k \times (\mathbb{R} \bigcup \{\infty\})^k$ is a min-approximation function if for all $i \in \{1, ..., k\}$

$$\left([\![\bigwedge]\!] (u, \widehat{u}) \right)_i = \begin{cases} u_i \text{ if } \widehat{u}_i = \infty \\ \widehat{u}_i \text{ if } \widehat{u}_i < \infty \end{cases}$$

By the above definition, $[\![\bigwedge]\!] (u, \widehat{u})$ is an affine function of its first argument u, and is a finite valued real vector.

$$[\![\bigwedge]\!] (u, \widehat{u}) \geq u \bigwedge \widehat{u}. \tag{4.8}$$

Similarly, a function $[\![\bigvee]\!] : \mathbb{R}^k \times (\mathbb{R} \bigcup \{-\infty\})^k$ is a max-approximation function if for all $i \in \{1, ..., k\}$

$$\left([\![\bigvee]\!] \left(l, \widehat{l}\right) \right)_i = \begin{cases} l_i \text{ if } \widehat{l}_i = -\infty \\ \widehat{l}_i \text{ if } \widehat{l}_i > -\infty \end{cases}$$

By the above definition, $[\![\bigvee]\!] \left(l, \widehat{l}\right)$ is an affine function of its first argument l, and is a finite valued real vector.

$$[\![\bigwedge]\!] \left(l, \widehat{l}\right) \geq l \bigvee \widehat{l}. \tag{4.9}$$

The following lemma states an affine condition when the meet and join operations can be equivalently computed by min and max-approximation functions, respectively.

Lemma 4.3.1. *Let us consider vectors $l, u \in \mathbb{R}^k$ and $\widehat{l}, \widehat{u} \in (\mathbb{R} \bigcup \{-\infty, \infty\})^k$. If $l \leq [\![\bigvee]\!] \left(l, \widehat{l}\right) \leq [\![\bigwedge]\!] (u, \widehat{u}) \leq u$, then*

$$l \bigvee \widehat{l} = [\![\bigvee]\!] \left(l, \widehat{l}\right) \tag{4.10}$$

$$u \bigwedge \widehat{u} = [\![\bigwedge]\!] (u, \widehat{u}) . \tag{4.11}$$

Proof. For any $i \in \{1, ..., k\}$, we derive results for the following four cases

Case 1: Let us consider that $\widehat{l}_i > -\infty$. So, $\left(\llbracket \bigvee \rrbracket \left(l, \widehat{l}\right)\right)_i = \widehat{l}_i$. Then by Equation 4.10, we get

$$\left(l \bigvee \widehat{l}\right)_i = \widehat{l}_i = \left(\left\llbracket \bigvee \right\rrbracket \left(l, \widehat{l}\right)\right)_i .$$

Case 2: Let us consider that $\widehat{l}_i = -\infty$. Then $\left(\llbracket \bigvee \rrbracket \left(l, \widehat{l}\right)\right)_i = l_i$. Then by Equation 4.10, we get

$$\left(l \bigvee \widehat{l}\right)_i = l_i = \left(\left\llbracket \bigvee \right\rrbracket \left(l, \widehat{l}\right)\right)_i .$$

Case 3: Let us consider that $\widehat{u}_i < \infty$. So, $\left(\llbracket \bigwedge \rrbracket (u, \widehat{u})\right)_i = \widehat{u}_i$. Then by Equation 4.11, we get

$$\left(u \bigwedge \widehat{u}\right)_i = \widehat{l}_i = \left(\left\llbracket \bigwedge \right\rrbracket (u, \widehat{u})\right)_i .$$

Case 4: Let us consider that $\widehat{u}_i = \infty$. Then $\left(\llbracket \bigwedge \rrbracket (u, \widehat{u})\right)_i = u_i$. Then by Equation 4.11, we get

$$\left(u \bigwedge \widehat{u}\right)_i = u_i = \left(\left\llbracket \bigwedge \right\rrbracket (u, \widehat{u})\right)_i .$$

□

Deriving sufficient conditions for positive invariance. We introduce the following condition, which along with Equation 4.5 is sufficient for the inclusion of the set of continuous reachable states $\mathcal{R}_q(\Omega)$ inside Ω_q. We shall prove this inclusion in Lemma 4.3.3.

Definition 4.3.2. For $q \in Q$, we say that $\Omega \sqsubseteq (\mathbb{H}, q)$ iff all of the following is collectively true.

$$\exists l', u', l'', u'' \in \mathbb{R}^k :$$

$$l_q \leq \left\llbracket \bigvee \right\rrbracket \left(l_q, \gamma_q^-\right) \leq \left\llbracket \bigwedge \right\rrbracket \left(u_q, \gamma_q^+\right) \leq u_q, \tag{4.12}$$

$$l' = \left\llbracket \bigvee \right\rrbracket \left(l_q, \gamma_q^-\right), \quad u' = \left\llbracket \bigwedge \right\rrbracket \left(u_q, \gamma_q^+\right), \tag{4.13}$$

$$\mathcal{G}\left(\begin{bmatrix}\mathcal{A}_q\mathcal{V}_q & \mathcal{V}_q^{\text{inp}}\end{bmatrix}, c_q + c_q^{\text{inp}}, \begin{bmatrix} s_q \\ s_q^{\text{inp}}\end{bmatrix}, \begin{bmatrix}\mathcal{A}_q\mathcal{K} & \mathcal{W}_q^{\text{inp}}\end{bmatrix}, \begin{bmatrix} l' \\ l_q^{\text{inp}}\end{bmatrix}, \begin{bmatrix} u' \\ u_q^{\text{inp}}\end{bmatrix}\right),$$

$$\sqsubseteq \mathcal{G}\left(\mathcal{V}_q, c_q, s_q, \mathcal{K}, l'', u''\right), \tag{4.14}$$

$$l'' \leq \left\llbracket \bigvee \right\rrbracket \left(l'', \gamma_q^-\right) \leq \left\llbracket \bigwedge \right\rrbracket \left(u'', \gamma_q^+\right) \leq u'', \tag{4.15}$$

$$l_q \leq \left\llbracket \bigvee \right\rrbracket \left(l'', \gamma_q^-\right), \quad \left\llbracket \bigwedge \right\rrbracket \left(u'', \gamma_q^+\right) \leq u_q . \tag{4.16}$$

Lemma 4.3.3. *For a location $q \in Q$, if $\Omega \sqsubseteq (\mathbb{H}, q)$, and Equation 4.5 holds, then $\mathcal{R}_q(\Omega) \subseteq \Omega$.*

Proof. By Theorem 3.2.2, Equations 4.12, 4.13, 4.5 and Lemma 4.3.1, we get

$$\Omega_q \bigcap \mathcal{P}\left(\mathcal{K}, \gamma_q^-, \gamma_q^+\right) \subseteq \mathcal{G}\left(\mathcal{V}_q, c_q, s_q, \mathcal{K}, l', u'\right).$$

Using the above over-approximation and the expressions for the linear transformation and Minkowski sum of augmented complex zonotopes, we get

$$\begin{aligned}
&A\left(\Omega_q \bigcap \mathcal{P}\left(\mathcal{K}, \gamma_q^-, \gamma_q^+\right)\right) \oplus U_q \\
&\subseteq \mathcal{G}\left(\left[\mathcal{A}_q\mathcal{V}_q \quad \mathcal{V}_q^{\text{inp}}\right], c_q + c_q^{\text{inp}}, \begin{bmatrix} s_q \\ s_q^{\text{inp}} \end{bmatrix}, \left[\mathcal{A}_q\mathcal{K} \quad \mathcal{W}_q^{\text{inp}}\right], \begin{bmatrix} l' \\ l_q^{\text{inp}} \end{bmatrix}, \begin{bmatrix} u' \\ u_q^{\text{inp}} \end{bmatrix}\right) \\
&\%\% \text{ by Theorem 3.3.5 and Equation 4.14} \\
&\subseteq \mathcal{G}\left(\mathcal{V}_q, c_q, s_q, \mathcal{K}, l'', u''\right). \qquad (4.17)
\end{aligned}$$

Again by Theorem 3.2.2, Equations 4.15, 4.5 and Lemma 4.3.1, we get

$$\begin{aligned}
&\mathcal{G}\left(\mathcal{V}_q, c_q, s_q, \mathcal{K}, l'', u''\right) \bigcap \mathcal{P}\left(\mathcal{K}, \gamma_{\sigma_2}^-, \gamma_{\sigma_2}^+\right) \\
&\subseteq \mathcal{G}\left(\mathcal{V}_q, c_q, s_q, \mathcal{K}, \left[\!\left[\bigvee\right]\!\right]\left(l'', \gamma_q^-\right), \left[\!\left[\bigwedge\right]\!\right]\left(u'', \gamma_q^+\right)\right) \\
&\%\% \text{ by Equation 4.16} \\
&\subseteq \mathcal{G}\left(\mathcal{V}_q, c_q, s_q, \mathcal{K}, l_q, u_q\right) = \Omega_q. \qquad (4.18)
\end{aligned}$$

Using Equations 4.3, 4.17, and 4.18, we get $\mathcal{R}_q(\Omega) \subseteq \Omega_q$. □

For the set of continuous states reached from Ω after a discrete transition, $\mathcal{R}_\sigma(\Omega)$, to be contained within Ω_{σ_2}, we introduce the following condition. We shall show in Lemma 4.3.5 that this condition is sufficient for $\mathcal{R}_\sigma(\Omega) \subseteq \Omega_{\sigma_2}$.

Definition 4.3.4. For an edge $\sigma \in E$, we say that $\Omega \sqsubseteq (\mathbb{H}, \sigma)$ iff all of the following is collectively true.

$$\begin{aligned}
&\exists l', u', l'', u'' \in \mathbb{R}^k : \\
&l_{\sigma_1} \leq \left[\!\left[\bigvee\right]\!\right]\left(l_{\sigma_1}, \sigma^- \bigvee \gamma_{\sigma_1}^-\right) \leq \left[\!\left[\bigwedge\right]\!\right]\left(u_{\sigma_1}, \sigma^+ \bigwedge \gamma_{\sigma_1}^+\right) \leq u_{\sigma_1} \qquad (4.19) \\
&l' = \left[\!\left[\bigvee\right]\!\right]\left(l_{\sigma_1}, \sigma^- \bigvee \gamma_{\sigma_1}^-\right), \quad u' = \left[\!\left[\bigwedge\right]\!\right]\left(u_{\sigma_1}, \sigma^+ \bigwedge \gamma_{\sigma_1}^+\right) \qquad (4.20) \\
&\mathcal{G}\left(\left[\mathcal{A}_\sigma\mathcal{V}_{\sigma_1} \quad \mathcal{V}_\sigma^{\text{inp}}\right], c_{\sigma_1} + c_\sigma^{\text{inp}}, \begin{bmatrix} s_{\sigma_1} \\ s_\sigma^{\text{inp}} \end{bmatrix}, \left[\mathcal{A}_\sigma\mathcal{K} \quad \mathcal{W}_\sigma^{\text{inp}}\right], \begin{bmatrix} l' \\ l_\sigma^{\text{inp}} \end{bmatrix}, \begin{bmatrix} u' \\ u_\sigma^{\text{inp}} \end{bmatrix}\right), \\
&\sqsubseteq \mathcal{G}\left(\mathcal{V}_{\sigma_2}, c_{\sigma_2}, s_{\sigma_2}, \mathcal{K}, l'', u''\right), \qquad (4.21) \\
&l'' \leq \left[\!\left[\bigvee\right]\!\right]\left(l'', \gamma_{\sigma_2}^-\right) \leq \left[\!\left[\bigwedge\right]\!\right]\left(u'', \gamma_{\sigma_2}^+\right) \leq u'', \qquad (4.22) \\
&l_{\sigma_2} \leq \left[\!\left[\bigvee\right]\!\right]\left(l'', \gamma_{\sigma_2}^-\right), \quad \left[\!\left[\bigwedge\right]\!\right]\left(u'', \gamma_{\sigma_2}^+\right) \leq u_{\sigma_2}. \qquad (4.23)
\end{aligned}$$

Lemma 4.3.5. *For an edge $\sigma \in E$, if $\Omega \sqsubseteq (\mathbb{H}, \sigma)$, then $\mathcal{R}_\sigma(\Omega) \subseteq \Omega_{\sigma_2}$.*

Proof. By Theorem 3.2.2, Equations 4.19, 4.20, 4.5, and Lemma 4.3.1 we get

$$\Omega_{\sigma_1} \bigcap \mathcal{P}\left(\mathcal{K}, \sigma^- \bigvee \gamma^-_{\sigma_1}, \sigma^+ \bigwedge \gamma^+_{\sigma_1}\right) \subseteq \mathcal{G}\left(\mathcal{V}_{\sigma_1}, c_{\sigma_1}, s_{\sigma_1}, \mathcal{K}, l', u'\right).$$

Using the above over-approximation and the expressions for the linear transformation and Minkowski sum of augmented complex zonotopes, we get

$$\begin{aligned}
&A\left(\Omega_{\sigma_1} \bigcap \mathcal{P}\left(\mathcal{K}, \sigma^- \bigvee \gamma^-_{\sigma_1}, \sigma^+ \bigwedge \gamma^+_{\sigma_1}\right)\right) \oplus U_\sigma \\
&\subseteq \mathcal{G}\left(\begin{bmatrix}\mathcal{A}_{\sigma_1}\mathcal{V}_{\sigma_1} & \mathcal{V}^{\text{inp}}_\sigma\end{bmatrix}, c_{\sigma_1} + c^{\text{inp}}_\sigma, \begin{bmatrix} s_{\sigma_1} \\ s^{\text{inp}}_\sigma \end{bmatrix}, \begin{bmatrix}\mathcal{A}_{\sigma_1}\mathcal{K} & \mathcal{W}^{\text{inp}}_\sigma\end{bmatrix}, \begin{bmatrix} l' \\ l^{\text{inp}}_\sigma \end{bmatrix}, \begin{bmatrix} u' \\ u^{\text{inp}}_\sigma \end{bmatrix}\right) \\
&\%\% \text{ by Theorem 3.3.5 and Equation 4.21} \\
&\subseteq \mathcal{G}\left(\mathcal{V}_{\sigma_2}, c_{\sigma_2}, s_{\sigma_2}, \mathcal{K}, l'', u''\right). \qquad (4.24)
\end{aligned}$$

Again by Theorem 3.2.2, Equations 4.22, 4.5 and Lemma 4.3.1, we get

$$\begin{aligned}
&\mathcal{G}\left(\mathcal{V}_{\sigma_2}, c_{\sigma_2}, s_{\sigma_2}, \mathcal{K}, l'', u''\right) \bigcap \mathcal{P}\left(\mathcal{K}, \gamma^-_{\sigma_2}, \gamma^+_{\sigma_2}\right) \\
&\subseteq \mathcal{G}\left(\mathcal{V}_{\sigma_2}, c_{\sigma_2}, s_{\sigma_2}, \mathcal{K}, \left[\!\left[\bigvee\right]\!\right]\left(l'', \gamma^-_{\sigma_2}\right), \left[\!\left[\bigwedge\right]\!\right]\left(u'', \gamma^+_{\sigma_2}\right)\right) \\
&\%\% \text{ by Equation 4.23} \\
&\subseteq \mathcal{G}\left(\mathcal{V}_{\sigma_2}, c_{\sigma_2}, s_{\sigma_2}, \mathcal{K}, l_{\sigma_2}, u_{\sigma_2}\right) = \Omega_{\sigma_2}. \qquad (4.25)
\end{aligned}$$

Using Equations 4.4, 4.24 and 4.25, we get $\mathcal{R}_\sigma(\Psi) \subseteq \Omega_{\sigma_2}$. □

The following condition is sufficient to check a linear invariance property.

Theorem 4.3.6. *We get $(\mathbb{H}, \Psi) \models (T, d)$ if all of the following is true.*

$$\begin{aligned}
&\forall i \in \{1, ..., k\}, \ \forall q \in Q, \ \forall \sigma \in E \\
&\mathcal{T}\left(\text{diag}\left(\boldsymbol{\alpha}_i\right)\mathcal{K}\mathcal{V}, \text{diag}\left(\boldsymbol{\alpha}_i\right)\mathcal{K}c_q, s_q\right) \sqsubseteq \mathcal{T}\left(\mathcal{K}\mathcal{V}, \mathcal{K}c_q, s_q\right), \\
&\Omega \sqsubseteq (\mathbb{H}, q) \ \wedge \ \Omega \sqsubseteq (\mathbb{H}, \sigma), \\
&T\left(c_q + \mathcal{K}^\dagger \frac{l_q + u_q}{2}\right) + \left|T\begin{bmatrix}\mathcal{V} & \mathcal{K}^\dagger\end{bmatrix}\right| \begin{bmatrix} s_q \\ \frac{u_q - l_q}{2} \end{bmatrix} \leq d. \qquad (4.26)
\end{aligned}$$

Proof. By Lemmas 4.3.3 and 4.3.5, we get that Ω is a positive invariant. According to the expression for support function in Lemma 3.3.7 which matches the last part of Equation 4.26, we get that all continuous states $x \in \Omega_q$ for all the locations satisfy $Tx \leq d$. By Lemma 4.2.2, the linear invariance property is satisfied. □

Algorithm for verification: For fixed primary template and the secondary template chosen as explained previously, the verification procedure is given in Algorithm 1. The algorithm if successful guarantees the verification of a linear invariance property. But it can not invalidate a linear invariance property because it is based on a sufficient but not necessary condition. It can be implemented by a single step of *second order conic programming*. This follows from the fact that min and max-approximation functions are affine and the relation "$\sqsubseteq$" between complex zonotopes is equivalent to a set of second order conic constraints on the center, scaling factors and lower and upper interval bounds.

Algorithm 1 Verification of linear invariance property

For all $q \in Q$, solve for c_q, s_q, l_q and u_q satisfying Equation 4.26.

Selecting the primary template: We note that adding any arbitrary vector to a primary template increases the accuracy of the verification procedure because the scaling factors are adjusted by the optimizer. However, there the computational cost also increases by adding more vectors to a template. Therefore, we have to select the primary template wisely. In this regard, we provide some suggestions for choosing the primary template, which are based on the properties of complex zonotopes that we derived earlier.

1. *Eigenvectors:* We can add eigenvectors of the linear transformation matrices and their products. This choice is based on Lemma 2.2.2 which states that a complex zonotope can capture the contraction by a linear transformation along the eigenvectors of the transformation.

2. *Orthonormal vectors and their projections:* We can add the orthonormal vectors in the null space of the secondary template and the projection of template vectors in the space orthogonal to the null space. This is based on Theorem 3.2.2 where the upper bound on the error in over-approximation of the intersection between an augmented complex zonotope and sub-parallelotope is proportional to the orientation between the primary template and the sub-parallelotopic template.

3. *Template of the input set and its transformations:* We can add the templates used to over-approximate the disturbance input set and its transformations by the system matrices. This is based on Proposition 2.2.4 which states that the template size of the resultant complex zonotope from the Minkowski sum of two complex zonotopes does not increase when their templates are the same. Since we take Minkowski sum with the disturbance input in our verification procedure, we expect to increase accuracy by incorporating the input template and its transformations in the primary template.

4. Adding any vector to the primary template will increase the accuracy because the scaling factors can be adjusted by the optimizer.

4.4 Experiments

We performed experiments on 3 benchmark examples from the literature and compared the results with that obtained by the tool SpaceEx [FLGD+11], which performs verification by step-by-step reachability computation. On one example, we compared the computational time with the reported results of the MPT tool [RGK+04]. For convex optimization, we used CVX (version 2.1) with MOSEK solver (version 7.1) and Matlab (version: 8.5/R2015a) on a computer with 1.4 GHz Intel Core i5 processor and 4 GB 1600 MHz DDR3. The precision of the solver is set to the default precision of CVX.

4.4.1 Robot with a saturated controller

Our first example is a verification problem for the model of a self-balancing two wheeled robot called NXTway-GS1[1] by Yorihisa Yamamoto, which was presented in the ARCH workshop [HOW14]. We consider the linearized sampled data (discrete time) networked control system model from the paper. The state of the plant is represented by a 6-dimensional vector $x_p = (\dot{\theta}, \theta, \dot{\psi}, \psi, \dot{\phi}, \phi)^T$, where θ is the average angle of the left and right wheel, ψ is the body pitch angle, ϕ is the body yaw angle, and the rest coordinates are their respective angular velocities. The output of the plant is represented by a 3-dimensional vector $\left(\dot{\psi}_{\text{out}}, \theta_{m_1}, \theta_{m_r}\right)^T$ such that $y_p = C_p x_p$. The input to the plant is a two dimensional vector u_p. The dynamics of the plant is given by the differential equation $\dot{x}_p = A_p x_p + B_p u_p$. In the sampled data system, the state of the plant is sampled every 4s.

The controller state is represented by a 6-dimensional vector x_c, and the input to the controller is denoted $u_c = (u'_c, u''_c)$. The controller inputs u'_c and u''_c are both 2-dimensional inputs. The input u'' is an uncertain input which is in the range $[-100, 100]$. The controller dynamics is given by the equations

$$\begin{aligned}
&\dot{\tau} = 1, \;\; \tau(4^+) = 0\\
&u'_c(\tau) = \hat{u}_c(0) \text{ if } \tau \in [0, 4)\\
&u'_c(4) = y_p(\tau)\\
&\dot{x_c}(\tau) = A_c x_c(\tau) + B_c u_c(\tau)\\
&y_c(\tau) = C_c x_c(\tau) + D_c u_c(\tau).
\end{aligned}$$

[1] http://www.mathworks.com/matlabcentral/fileexchange/19147-nxtway-gs-self-balancing-two-wheeled-robot-controller-design

$$F_1 = \begin{bmatrix} 3.6929 & 0 & 0.7302 & 7.9715 & 14.5019 & -0.0072 & 0.0720 & -2.7354 \\ 3.6929 & 0 & 0.7302 & 7.9715 & 14.5019 & -0.0072 & 0.0720 & -2.7354 \\ 0.9562 & 0 & 0.0019 & -0.0021 & -0.0022 & -0.0000 & -0.0001 & -0.0002 \\ 0 & 0.6910 & 0 & 0 & 0 & 0 & 0 & 0 \\ 0.8833 & 0 & -0.1154 & -1.2943 & -2.3520 & 0.0012 & -0.0118 & 0.4427 \\ -0.4712 & 0 & -0.0812 & 0.1151 & -1.4845 & 0.0007 & -0.0071 & 0.2819 \\ -0.1560 & 0 & -0.0459 & -0.3173 & 0.3650 & 0.0003 & -0.0023 & 0.1162 \\ -0.7719 & 0 & -0.1248 & -1.4264 & -2.5901 & 0.9973 & -0.0131 & 0.4869 \\ -0.7544 & 0 & -0.1243 & -1.4204 & -2.5792 & 0.0013 & 0.9825 & 0.4796 \\ -0.1905 & 0 & -0.0148 & -0.2081 & -0.3751 & 0.0002 & 0.0033 & 1.0651 \end{bmatrix}$$

$$F_2 = \begin{bmatrix} 0.2543 & 0.2543 \\ 0.2543 & 0.2543 \\ -0.0001 & -0.0001 \\ 0 & 0 \\ -0.0413 & -0.0413 \\ 0.0219 & 0.0219 \\ 0.0102 & 0.0102 \\ 0.0431 & 0.0431 \\ 0.0428 & 0.0428 \\ 0.0065 & 0.0065 \end{bmatrix}, \; F_3 = 10^{-2} \times \begin{bmatrix} 0.0000 & 0 & -0.0330 & 2.0218 \\ 0 & 0 & -0.0330 & -2.0218 \\ 0 & 0 & -0 & 0 \\ -0 & 0 & 0 & 0.0109 \\ -0.0118 & 0 & 0.0172 & 0 \\ 0.0436 & 0 & 0.0003 & 0 \\ -0.0478 & 0 & 0.0034 & 0 \\ -13.3924 & 0 & 0.0062 & 0 \\ 0.0909 & 0 & 0.0061 & 0 \\ -0.0798 & 0 & 0.0017 & 0 \end{bmatrix}$$

Table 4.1: Matrices of the transformed system dynamics

The controller has a 2-dimensional output y_c which is processed to provide input to the plant. The processor has a saturation limit on the output received from the controller. The saturated controller output is given by the equation

$$u_p = D_p \left(\left(y_c \bigwedge \begin{bmatrix} v \\ v \end{bmatrix} \right) \bigvee \begin{bmatrix} -v \\ -v \end{bmatrix} \right). \tag{4.27}$$

where $v = 100$ is a saturation limit. The sampled data dynamics with saturation can be modeled by an affine discrete time hybrid system, where the switching is controlled by relevant guards on u_p. However, if we consider the continuous state of the affine hybrid system as $(x_p, x_c, u_p)^T$, we observed that some of the directions are unbounded. Therefore, we decoupled some unbounded directions of the dynamics from the bounded directions by making appropriate linear transformation of the coordinates. The linear transformation is composed by two transformations, one of which involved Jordan decomposition in Matlab.

After decomposition, the bounded dynamics with saturation could be modeled in a 10-dimensional state space, which is described below.

$$\begin{bmatrix} x(t+1) \\ y(t+1) \end{bmatrix} = F_1 \mathbf{x}(t) + F_2 sat(\mathbf{y}(t)) + F_3 \mathbf{u}(t),$$

where $\mathbf{x}(t) \in \mathbb{R}^8$ is the transformed state of the composite system of plant and controller, $\mathbf{y}(t) \in \mathbb{R}^2$ is the input sent by the controller, $\mathbf{u}(t) \in [-100, 100]^4$ is

the bounded additive disturbance input and sat is the saturation function which limits the controller input received by the plant. The body pitch angle is the first co-ordinate, i.e., $\psi = x_1$. The matrices F_1, F_2 and F_3 are given in Table 4.1. The saturation function is defined as follows. The saturation function is given as follows.

$$\text{If saturated } \ \text{sat}\,(y_i) = max\,(-\delta d_p, min\,(y_i, \delta d_p))\,,\ \forall i \in \{1,2\},$$
$$\text{If unsaturated } \ sat\,(y_i) = y_i\ \forall i \in \{1,2\}.$$

where $\delta = 100$ and $d_p = 0.0807$.

Model complexity: The 2-dimensional input y on which the positive and negative saturation is defined can thus be divided into 9 different regions, where the system exhibits different dynamics. We model each of the discrete time dynamics by a self edge on a common location. Therefore, the saturated model consists of a single location with 9 self-edges having appropriate linear guards and transition matrices. On the other hand, the unsaturated model is a linear system having uncertain input, which is therefore modeled by only one location.

Size of saturated model: 10 dimensional, 1 location and 9 edges.

Size of unsaturated model: 10 dimensional, 1 location, 0 edges.

Linear invariance property to verify: The safety requirement is that the *body pitch angle* of the robot, which in our model is denoted by x_1, should be bounded within some value. In the benchmark, it was suggested that for the saturated system $x_1 \in \left[-\frac{\pi}{2} + \epsilon, \frac{\pi}{2} - \epsilon\right] : \epsilon > 0$, while $x_1 \in \left[\frac{-\pi}{2.26}, \frac{\pi}{2.26}\right]$ for the unsaturated system. The initial set is the origin. Therefore, we want to find a small bound d on the valued of $|\psi| = |x_1|$. As the model is symmetric, it is sufficient to find a bound along the positive direction. Therefore, we have to find a small enough d such that (T, d), where $T = \begin{bmatrix}1 & [0]_{1\times 9}\end{bmatrix}$, is a linear invariance property.

Experiment settings.

Augmented complex zonotope: The primary template for the hybrid system is chosen as the collection of the (complex) eigenvectors of linear matrices of all affine maps for the edge transitions, the orthonormal vectors to the guarding hyperplane normals and the projections of the eigenvectors on the subspace spanned by the orthonormal vectors. For the linear system, it consists of the eigenvectors of the linear map, the input set template and its multiplication by the linear matrix (related to affine map) and square of the linear matrix.

SpaceEx: Concerning the experiment using SpaceEx, we tested with the octagon template and a template with 400 uniformly sampled support vectors distributed uniformly in space.

Results. For both the hybrid and the linear systems, we could verify smaller magnitudes for the bounds on the pitch angle than what is proposed in the benchmark [HOW14]. But the SpaceEx tool could not find a finite bound for either of the above systems. The results are reported in the Tables 4.2 and 4.3.

Method		Bound on pitch angle	Comp. time (s)
SpaceEx	octagon template	> 1000	Not terminate in $< 180s$
	400 support vectors	> 1000	Not terminate in $< 180s$
Suggested in [HOW14]		1.39	n/a
Augmented complex zonotope		1.29	4

Table 4.2: Unsaturated robot model: results

Method		Bound on pitch angle	Comp. time (s)
SpaceEx	octagon template	> 1000	Not terminate in $< 180s$
	400 support vectors	> 1000	Not terminate in $< 180s$
Suggested in [HOW14]		$1.571 - \epsilon : \ \epsilon > 0$	n/a
Augmented complex zonotope		1.16	45

Table 4.3: Saturated robot model: results

Remark. We have discussed in the review of polytopes that although a linear system has a polytopic invariant, computing it can be difficult. The representation size of a polytopic invariant for a fixed dimension can be arbitrarily large. In our unsaturated model which is linear, some of the eigenvalues are complex and their magnitudes are close to one. Possibly this is the reason SpaceEx could not find an invariant even with 400 support vectors distributed uniformly in space. But in our approach, since we use the complex eigenstructure, we could find the desired invariant for the unsaturated (linear) model. Furthermore, we we also computed the invariant for the saturated (hybrid) model.

4.4.2 Networked platoon of vehicles

Our third example is a model of a networked cooperative platoon of vehicles, which is presented as a benchmark in the ARCH workshop [MK14]. The platoon consists of three vehicles M_1, M_2 and M_3 along with a leader board ahead M_4. The movement of the vehicles is dependent on the communication between them their relative distances, velocities and accelerations. The distance between a vehicle M_i and its next vehicle M_{i+1}, relative to a reference distances d_i^{ref} is denoted e_i. The acceleration of the leader vehicle is a_L which ranges between $[-9, 1]m/s$. The state of the system is denoted by a vector $x = [e_1, \dot{e}_1, \ddot{e}_1, e_2, \dot{e}_2, \ddot{e}_2, e_3, \dot{e}_3, \ddot{e}_3]$. The dynamics of the platoon is different in the two cases when there is full communication and when there is total failure of communication. These dynamics are described by differential equations,

$$\dot{x} = A_c x + B_c a_L \text{ when there is communication}$$
$$\dot{x} = A_n x + B_n a_L \text{ when there is failure of communication.}$$

where the pairs of matrices (A_c, B_c) and (A_n, B_n) are different. In any given mode, the dynamics of the system is exponentially stable. So, the lyapunov exponent (measure of stability) is higher in case of slow switching than fast switching. Therefore, in our evaluation of this example, we also consider a model having integer switching times, which is less stable.

Time discretized models: We could discretized the dynamics of both models with large minimum switching time and integer switching time. The time discretized model has 2 locations and 4 edges, as described in Figure 4.1. The continuous state is 9-dimensional. The matrices denoted in the figure are different for the case of slow switching and fast switching and are given in Tables 4.4 and 4.5, respectively.

Linear invariance property: The verification challenge proposed in [MK14] is to find the minimum possible reference distances d_i^{ref} $\forall i \in \{1, 2, 3\}$, such that the vehicles do not collide. Any set of upper bounds on $-e_1$, $-e_2$, and $-e_3$

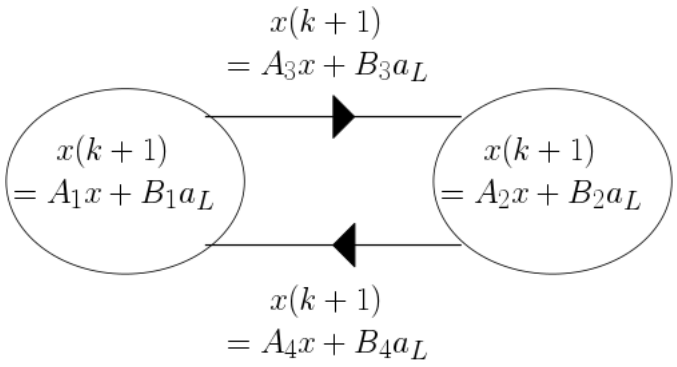

Figure 4.1: Time discretized model of networked platoon

Table 4.4: Matrices for discrete time slow switching model

$$A_1 = \begin{bmatrix} 0.2766 & 0.2855 & -0.0235 & 0.2550 & 0.2352 & -0.0429 & 0.1245 & 0.0956 & -0.0234 \\ -0.0917 & -0.0848 & 0.0392 & -0.0517 & 0.0134 & 0.0023 & 0.0003 & 0.0385 & -0.0166 \\ -0.0531 & -0.0485 & 0.0404 & 0.0434 & 0.0807 & -0.0172 & 0.0301 & 0.0363 & -0.0097 \\ 0.1406 & 0.1632 & 0.0002 & 0.0313 & 0.1166 & -0.0122 & 0.1017 & 0.1309 & -0.0431 \\ -0.0411 & -0.0589 & -0.0421 & -0.0512 & -0.1530 & 0.0575 & -0.0476 & -0.0321 & 0.0051 \\ -0.0393 & -0.0402 & -0.0111 & -0.0641 & -0.0754 & 0.0467 & 0.0497 & 0.0760 & -0.0251 \\ 0.0628 & 0.0763 & 0.0095 & 0.0634 & 0.0987 & 0.0081 & -0.0788 & 0.0489 & -0.0436 \\ -0.0088 & -0.0158 & -0.0081 & -0.0351 & -0.0452 & -0.0726 & -0.0621 & -0.2082 & 0.0863 \\ -0.0246 & -0.0235 & -0.0078 & -0.0572 & -0.0547 & -0.0183 & -0.1049 & -0.1146 & 0.0307 \end{bmatrix}$$

$$A_2 = \begin{bmatrix} 0.2398 & 0.2204 & -0.0715 & -0.0000 & 0.0000 & -0.0000 & -0.0000 & 0.0000 & -0.0000 \\ -0.1148 & -0.1083 & 0.0352 & -0.0000 & -0.0000 & 0.0000 & -0.0000 & -0.0000 & 0.0000 \\ -0.0565 & -0.0567 & 0.0176 & -0.0000 & -0.0000 & -0.0000 & -0.0000 & -0.0000 & 0.0000 \\ 0.0178 & 0.5068 & -0.0658 & 0.2410 & 0.3042 & -0.1113 & -0.0000 & 0.0000 & -0.0000 \\ -0.1056 & -0.3026 & 0.0327 & -0.1329 & -0.1627 & 0.05657 & -0.0000 & -0.0000 & 0.0000 \\ -0.1089 & -0.1100 & -0.0055 & -0.0675 & -0.0720 & 0.0204 & -0.0000 & -0.0000 & 0.0000 \\ 0.2386 & -0.0802 & 0.0965 & 0.1118 & 0.1544 & 0.0604 & 0.1197 & 0.2679 & -0.1103 \\ 0.0762 & 0.3143 & -0.0998 & -0.0213 & -0.0283 & -0.0726 & -0.1404 & -0.2191 & 0.0779 \\ -0.0043 & 0.0212 & -0.0122 & -0.0468 & -0.0413 & -0.0171 & -0.0991 & -0.0990 & 0.0251 \end{bmatrix}$$

$$B_1 = \begin{bmatrix} 1.8593 \\ 0.2855 \\ 1.0848 \\ 0.5394 \\ 0.1632 \\ 1.1437 \\ 0.1950 \\ 0.0763 \\ 1.1596 \end{bmatrix} \quad B_2 = \begin{bmatrix} 1.7651 \\ 0.2204 \\ 1.1083 \\ 2.1977 \\ 0.5068 \\ 1.4109 \\ -1.2748 \\ -0.0802 \\ 1.0966 \end{bmatrix} \quad B_3 = \begin{bmatrix} 2.8411 \\ 0.0019 \\ 1.0006 \\ 0.9508 \\ 0.0007 \\ 1.0009 \\ 0.3775 \\ 0.0003 \\ 1.0009 \end{bmatrix} \quad B_4 = \begin{bmatrix} 2.2276 \\ 0.0001 \\ 1.0001 \\ 2.7152 \\ -0.0005 \\ 1.0000 \\ -0.4469 \\ 0.0001 \\ 1.0000 \end{bmatrix} \quad A_3 = A_4 = [0]_{9\times 9}.$$

Table 4.5: Matrices for discrete time fast switching model

$$A_1 = A_3 = \begin{bmatrix} 0.8902 & 0.6370 & -0.1484 & 0.0588 & -0.0050 & 0.0001 & 0.0157 & -0.0148 & 0.0059 \\ -0.2340 & 0.1889 & -0.1119 & 0.1267 & 0.0147 & -0.0039 & 0.0363 & -0.0201 & 0.0104 \\ 0.1755 & 0.7560 & -0.2251 & -0.0959 & -0.0989 & 0.0181 & -0.0373 & -0.0273 & 0.0018 \\ 0.0462 & 0.0643 & 0.1514 & 0.8509 & 0.7076 & -0.1685 & 0.0303 & 0.0218 & -0.0038 \\ 0.0934 & 0.1271 & 0.1151 & -0.3284 & 0.2923 & -0.1466 & 0.0660 & 0.0517 & -0.0108 \\ 0.1262 & 0.6998 & 0.0092 & 0.1826 & 0.7469 & -0.2119 & -0.0885 & -0.0830 & 0.0189 \\ 0.0116 & 0.0170 & 0.0026 & 0.0241 & 0.0282 & 0.1719 & 0.8532 & 0.7238 & -0.1801 \\ 0.0256 & 0.0364 & 0.0064 & 0.0505 & 0.0619 & 0.1543 & -0.3320 & 0.3231 & -0.1730 \\ 0.1047 & 0.6724 & 0.0017 & 0.1502 & 0.6976 & 0.0119 & 0.2247 & 0.7581 & -0.1875 \end{bmatrix}$$

$$A_2 = A_4 = \begin{bmatrix} 0.8898 & 0.6325 & -0.1463 & 0.0000 & 0.0000 & 0.0000 & 0.0000 & 0.0000 & -0.0000 \\ -0.2348 & 0.1775 & -0.1094 & 0.0000 & 0.0000 & 0.0000 & 0.0000 & 0.0000 & -0.0000 \\ 0.1756 & 0.7674 & -0.2136 & 0.0000 & 0.0000 & 0.0000 & 0.0000 & 0.0000 & -0.0000 \\ 0.0939 & 0.3146 & 0.1064 & 0.9098 & 0.6995 & -0.1686 & 0.0000 & 0.0000 & -0.0000 \\ 0.1708 & 0.6120 & 0.0043 & -0.2012 & 0.2985 & -0.1533 & 0.0000 & 0.0000 & -0.0000 \\ 0.1687 & 0.5757 & 0.1151 & 0.1829 & 0.7569 & -0.1980 & 0.0000 & 0.0000 & -0.0000 \\ -0.0364 & -0.2331 & 0.0460 & 0.0254 & 0.0312 & 0.1721 & 0.9004 & 0.7304 & -0.1778 \\ -0.0529 & -0.4476 & 0.1169 & 0.0548 & 0.0704 & 0.1571 & -0.2263 & 0.3541 & -0.1728 \\ 0.1044 & 0.6771 & -0.0016 & 0.1418 & 0.6953 & 0.0121 & 0.2199 & 0.7571 & -0.1877 \end{bmatrix}$$

$$B_1 = B_3 = \begin{bmatrix} 0.3930 \\ 0.6370 \\ 0.8111 \\ 0.0200 \\ 0.0643 \\ 0.6840 \\ 0.0051 \\ 0.0170 \\ 0.6476 \end{bmatrix} \quad B_2 = B_4 = \begin{bmatrix} 0.3918 \\ 0.6325 \\ 0.8225 \\ 0.0979 \\ 0.3146 \\ 0.2105 \\ -0.0727 \\ -0.2331 \\ 0.6581 \end{bmatrix}$$

are safe lower limits on the respective reference distances. We express the verification problem in terms of three linear invariance properties, as follows. For each $T_i : 1 \leq i \leq 3$, where $T_1 = \begin{bmatrix} -1 & [0]_{1\times 8} \end{bmatrix}$, $T_2 = \begin{bmatrix} [0]_{1\times 3} & -1 & [0]_{5\times 3} \end{bmatrix}$ and $T_3 = \begin{bmatrix} [0]_{1\times 6} & -1 & [0]_{2\times 3} \end{bmatrix}$, find an upper bound on each $d_i : i \in \{1, 2, 3\}$ such that (T_i, d_i) is a linear invariance property of the system.

Experiment settings. We chose the primary template as the collection of the (complex) eigenvectors of linear matrices of the affine maps in the the two locations and their binary products, the axis aligned box template and the templates used for overapproximating the input sets. For the SpaceEx tool, we experimented with two templates, octagon and hundred uniformly sampled support vectors.

Results. For the large minimum dwell time of $20s$, the discrete time SpaceEx implementation and also a method based on using real zonotopes [MK14] could verify slightly smaller bounds compared to our approach. But for the small minimum dwell time ($1s$) model, SpaceEx could not even find a finite set of bounds, whereas our approach could verify a finite set of bounds. The reason is that the fast system model is more stable compared to the slow switching. Possibly because complex zonotope captures contraction along complex eigenvectors, we could find a finite invariant for even the less stable fast switching model. These results are reported in the Tables 4.6 and 4.7.

Method		Slow switching			
		$-e_1 \leq$	$-e_2 \leq$	$-e_3 \leq$	Comp. time (s)
SpaceEx	octagon template	28	27	10	$> 180s$
	100 support vectors	28	25	13	1.3
Real zonotope [MK14]		25	25	10	n/a
Augmented complex zonotope		28	26	12	12

Table 4.6: Experimental results: Slow switching networked platoon

Method		Fast switching			
		$-e_1 \leq$	$-e_2 \leq$	$-e_3 \leq$	Comp. time (s)
SpaceEx	octagon template	> 1000	> 1000	> 1000	$> 180s$
	100 support vectors	> 1000	> 1000	> 1000	$> 180s$
Augmented complex zonotope		46	54	57	12.6

Table 4.7: Experimental results: Fast switching networked Platoon

4.4.3 Perturbed double integrator

Our second example is a perturbed double integrator system given in [RGK+04]. The closed loop system with a feedback control is piecewise affine, having four different affine dynamics in four different regions of space, as

$$\mathbf{x}(t+1) = M_i \mathbf{x}(t) + w. \quad i = \begin{cases} 1, \text{ if } x_1 \geq 0 \text{ and } x_2 \geq 0 \\ 2, \text{ if } x_1 \leq 0 \text{ and } x_2 \leq 0 \\ 3, \text{ if } x_1 \leq 0 \text{ and } x_2 \geq 0 \\ 4, \text{ if } x_1 \geq 0 \text{ and } x_2 \leq 0 \end{cases},$$

$$M_1 = M_2 = \begin{bmatrix} 0.4103 & 0.0653 \\ -0.2949 & 0.5327 \end{bmatrix}, \; M_3 = M_4 = \begin{bmatrix} 0.4103 & -0.0653 \\ 0.2949 & 0.5327 \end{bmatrix}.$$

The additive disturbance input w is bounded as $\|w\|_\infty \leq 0.2$.

We perform two different experiments on this system. In the first experiment, we try to verify the smallest possible magnitude of bounds on the two coordinates, denoted x_1 and x_2. We compare these bounds with that found by the SpaceEx tool. In the second experiment, we try to quickly compute a large invariant for the system under the safety constraints given in [RGK+04]. The given safety constraints are $\|x\|_\infty \leq 5$. In the latter case, we maximize the sum of the scaling factors and differences of the upper and lower interval bounds of the augmented complex zonotopic invaraint. Furthermore, we decompose the given safety constraints as the intersection of four different sets of safety constraints. For each set of safety constraints, we compute a large augmented complex zonotopic invariant. Then the desired invariant is the intersection of four augmented complex zonotopic invariants. Although we may not find the largest possible (maximal) invariant by this approach, still the optimizer will try to maximize the size of the invariant. We draw comparison in terms of the computation time with the reported result for the MPT tool [RGK+04].

In our formalism, we model the system with 4 locations and 12 edges connecting all the locations. Appropriate staying conditions are specified in each location, reflecting the division of the state space into different regions where the dynamics is affine. The initial set is the origin. The same model is specified in SpaceEx.

Size of model: 2 dimensions, 4 locations and 12 edges.

Experiment settings. For the primary template, we collected the (complex) eigenvectors of all linear matrices of the affine maps and their binary products. For the SpaceEx tool, we experimented with two different templates, the octagon template and a template with 100 uniformly sampled support vectors.

Results. In the first experiment, we verified sligtly smaller bounds for x_1 than that of SpaceEx, while the bounds verified for x_2 were equal for both methods. In our second experiment on this example, the computation time for finding a large

Method		$\lvert x_1\rvert \leq$	$\lvert x_2\rvert \leq$	Comp. time (s)
SpaceEx	octagon template	0.38	0.43	1.7
	100 support vectors	0.38	0.43	23.6
ACZ invariant		0.37	0.43	5.1

Table 4.8: Small invariant computation: Perturbed double integrator

Method	Comp. time (s)
MPT tool [RGK+04]	107
ACZ	12

Table 4.9: Large invariant computation: Perturbed double integrator

invariant by our method is significantly smaller than that of the reported result for the MPT tool. The results are summarized in the Tables 4.8 and 4.9.

CHAPTER 5

Stability Verification of Nearly Periodic Linear Impulsive Systems

Since computers work with digital signals and the physical system they control operates in the analog world, sampling is required. Various parameters related to sampling of the system can be subject to uncertainty like the sampling period, delay, digital output of the controller, output feedback from the system, etc. These uncertainties can lead to instability of the system. Henceforth, we are faced with the challenge of verifying system stability in the presence of these uncertainties. We address this issue by considering the problem of verifying stability of nearly-periodic impulsive systems, which can be used to model sampled-data systems [NUoC07] and networked control systems [NHT08]. This problem has been tackled using control approaches, which mainly involve deriving stability conditions in terms of Lyapunov functions and checking these conditions using optimization (Linear Matrix Inequalities (LMI) or Sum of Squares (SOS)). In this work, we use a stability condition based on set contractiveness proposed in [AL14, FM14, KGD15] and propose a new method for checking it using computational techniques, inspired by hybrid systems verification techniques. Globally exponential stability (GES) of nearly-periodic linear impulsive systems can be proved by showing the contractiveness of a compact and convex set containing the origin in its interior, also called as a C-set [LDA13, AL14, FM14, KGD15]. The uncertainty in impulse times for which stability can be proved depends on the choice of the contractive C-set. A nearly-periodic linear impulsive system is stable only if all of its reachability operators, which compute the state reached

after an impulse, are stable. This motivates us to use complex zonotopes since we can find good candidate complex zonotope for contractive sets using the eigenvectors of the reachability operators. For proving stability condition, we consider complex zonotopes whose generator sets are chosen among the eigenvectors of reachability operators of the nearly-periodic linear impulsive system. We then derive a condition for the contractiveness of a complex zonotope that can be verified by convex optimization. Concerning experimental results, our approach is either competitive or better compared to the existing approaches, in terms of the largeness of uncertainty of sampling periods for which stability could be proved.

The chapter is organized into five main sections. We discuss the related work in Section 5.1. In Section 5.2, we describe the dynamics of a nearly-periodic linear impulsive system. In Section 5.3, we explain global exponential stability, the verification problem and its relation to finding a contractive C-set of the system. In Section 5.4, we explain our algorithm for stability verification based on complex zonotopes. The experiments on two benchmark examples are discussed in Section 5.5

5.1 Related work

A major approach to stability analysis of aperiodic sampling control uses time-delay systems, and stability can be proved using Lyapunov Krakovskii functional [YVE88, TNK98, LSF10, MMD13], or time-dependent Lyapunov functional [Fri10]. Using a continuous-time model, discrete-time Lyapunov functions is proposed for stability condition [Seu12], which can be checked using Sum of Squares (SOS) [SP13]. Robust stability with respect to time-varying input delay can also be handled by input/output approach [Mir07, Fuj, KW14, OHRLL13, OHRLL14]. Another important approach is based on the hybrid systems modeling framework, in particular time-varying impulsive systems [HLCS03, NT04, GST09, CGT08, BvLD+12] and employs Lyapunov-based methods in various forms including discontinuous time-independent [NHT08] or time-dependent Lyapunov functions [Fri10]. Another popular approach involves using convex embedding [HDI06, Fuj09, HKPR11, HDTP13, OHRLL14]. In this approach, stability tests can be formulated as parametric Linear Matrix Inequalities (LMIs) [HDI06], or as set contractiveness (such as, polytopic set contractiveness is equivalent to polyhedral Lyapunov functions) [FM14, Bri13, LDA13, AL14, KGD15]. In this work, we focus on exponential stability and are inspired by set theory conditions [FM14, AL14, KGD15] to derive a stability condition which is more conservative but can be efficiently verified. The novelty of our work lies in the use of complex zonotopes to efficiently find contractive sets. Computationally speaking, our approach is close in spirit to abstract interpretation and hybrid systems analysis. Indeed the

way we find contractive sets using such zonotopes is similar to the way invariant sets are computed using some zonotope [Gir05b, AK11a, GPV12] and template-polyhedral abstract domains [SDI08b, JM09].

5.2 Dynamics

A nearly periodic linear impulsive system is specified by a tuple

$$\mathbb{H} = (\mathbb{R}^n, A_r, A_c, \Delta)$$

where $\mathbb{R}^n$ is the state space with dimension $n \in \mathbb{Z}_{>0}$, A_r and A_c are $n \times n$ real matrices called the impulse matrix and the linear vector field matrix, respectively. The interval $\Delta = [\underline{\tau}, \overline{\tau}]$, such that $0 < \tau_m < \tau_M$, is called the *sampling interval*. A *trajectory* of the system is a function $\mathbf{x} : \mathbb{R}_{\geq 0} \to \mathbb{R}^n$, such that there exists a sequence of sampling times $(t_k)_{k=0}^{\infty}$ satisfying all the following for any $k \in \mathbb{Z}_{\geq 0}$.

$$\begin{aligned} \dot{\mathbf{x}}(t) &= A_c \mathbf{x}(t) \;\; \forall t \in [t_k, t_{k+1}) \\ \mathbf{x}\left(t_k^+\right) &= A_r \mathbf{x}(t_k^-) \\ t_{k+1} - t_k &\in \Delta \\ \mathbf{x}(0) &= \mathbf{x}_0 \end{aligned} \tag{5.1}$$

Here, $\mathbf{x}(t) \in \mathbb{R}^n$ is the state of the system at a time instant t. For any $k \in \mathbb{N}$, we shall denote the state reached just after the impulse at t_k as $\mathbf{x}_k = \mathbf{x}(t_k^+)$. When there is continuous evolution of a state x until time t, then the state reached at time t is $\mathbf{x}(t) = e^{A_c t}x$. If there is an impulse at time $t = 0$, then the state reached immediately afterwards is $A_r\mathbf{x}_0$. Therefore, using Equation 5.1, we get

$$\mathbf{x}_{k+1}t \in \left\{e^{A_c t} A_r \mathbf{x}_k : \; t \in \Delta\right\}.$$

We call the change in the state of the system from the time just before one impulse to the next impulse as *a step*. Therefore, for any set $\Psi \subset \mathbb{R}^n$, the set of all reachable points from a state x in one step is

$$R(\Psi) = \{e^{A_c t} A_r \mathbf{x}_0 : \mathbf{x}_0 \in \Psi, t \in \Delta\}.$$

Then, the set of all points reachable after k steps is

$$xR^k(\Psi) = \left\{\left(\Pi_{i=1}^{k} e^{A_c t_i} A_r\right)\mathbf{x}_0 : \mathbf{x}_0 \in \Psi, \forall i \in \{1, ..., k\} t_i \in \Delta\right\}.$$

Therefore, we define a *reachability operator* as follows.

$$\forall t \in \Delta, \; H_t = e^{A_c t} A_r.$$

As the the sampling period interval Δ is an uncountable set, there are uncountable number of reachability operators. For a sub-interval $[\tau_1, \tau_2] \subseteq \Delta$, we shall denote the set of reachability operators as

$$O([\tau_1, \tau_2]) = \{H_\tau : \tau \in [\tau_1, \tau_2]\}. \tag{5.2}$$

5.3 Globally exponential stability and set contraction

A nearly periodic linear impulsive system is globally exponentially stable (GES) if any point in the state space reaches arbitrarily close to the origin at an exponential rate. This property is mathematically stated as follows.

Definition 5.3.1. [Global exponential stability (GES)] The system $\mathbb{H}$ is globally exponentially stable (GES) if there exists $\lambda \in [0, 1)$ and $c > 0$ such that for all $\mathbf{x}_0 \in \mathbb{R}^n$ and $k \in \mathbb{Z}_+$, $||\mathbf{x}_k|| \leq c\lambda^k ||\mathbf{x}_0||$.

The following is the stability verification problem.

Problem 5.3.1. Given a sampling period interval $\Delta = [\underline{\tau}, \overline{\tau}]$, verify that the system $\mathbb{H}$ is globally exponentially stable.

The GES of a system is related to the reachable sets of the system. Indeed if all bounded sets containing the origin eventually contract to arbitrarily small sets around the origin, then every point eventually reaches close to the origin and the system is thus GES. Instead of verifying the contraction of all bounded sets containing the origin, we can verify the contraction of any compact and convex set containing the origin, because it can be scaled to include any bounded set. We call such sets as C-sets, defined as follows.

Definition 5.3.2. A set $\Psi \subset \mathbb{R}^n$ is called a C-set if it is compact, convex and contains the origin in its interior.

The contraction of a C-set is defined as follows.

Definition 5.3.3 ([FM14])**.** Given $\lambda \in [0, 1]$, a set C-set $\Psi \subset \mathbb{R}^n$ is λ-contractive for the system $\mathbb{H}$ iff

$$\forall x \in \Psi,\ \forall t \in \Delta,\ H_t x \in \lambda\Psi.$$

Remark 5.3.4. It has been shown previously in ([FM14, AL14, KGD15]) that globally exponentially stability of a nearly-periodic linear impulsive system is equivalent to the existence of a λ-contractive C-set for a $\lambda \in [0, 1)$. So, we can find a λ-contractive C-set for $\lambda < 1$ to prove global exponential stability.

A stability verification algorithm was proposed in [FM14] that definitely computes a contractive C-set for a globally exponentially stable system. But the algorithm involves iterative intersections. During iterative intersections, the complexity of representing the set can grow uncontrollably. So, the algorithm [FM14] can be costly, especially in higher dimensions. Alternatively, we propose a stability

verification algorithm using complex zonotope and convex optimization, where the size of the template is fixed a priori. Although the existence of a contractive complex zonotope is only a sufficient condition for global exponential stability, we demonstrate the efficiency of our procedure by experiments on some benchmark examples. Our algorithm, described in the next section, uses some properties of contraction of sets, which we shall discuss now.

As the state change of the system can be identified by the transformation by a reachability operator, we define contraction by a matrix as follows. From here on, we denote J as an $n \times n$ real matrix.

Definition 5.3.2. The amount of contraction of a set $\Psi \subset \mathbb{R}^n$ upon transformation by the matrix J, denoted as $\chi(\Psi, J)$, is

$$\chi(\Psi, J) = \inf\{a \in \mathbb{R}_{\geq 0} : J(\Psi) \subseteq a\Psi\}.$$

The amount of contraction being greater than one would indicate that the set is actually *expanding*, which will also be referred mathematically as "contraction" parameter, in a general sense. For any $\rho : 0 \leq \rho \leq \epsilon$, we want to derive a bound on the contraction of the operator $H_{t+\rho}$ as a function of H_t and ϵ. Using Taylor expansion of an order r, we can write

$$\begin{aligned} &H_{t+\rho} = e^{(A_c\rho)}H_t = P_r(\rho)H_t + E_r(\delta)H_t \text{ where} \\ &P_r(\rho) = \sum_{i=0}^{r} \frac{A_c^i\rho^i}{i!}, \qquad E_r(\delta) = \frac{A_c^{r+1}\delta^{r+1}}{(r+1)!} : \ \delta \in [0, \epsilon]. \end{aligned} \tag{5.3}$$

To use the above expansion for deriving the bound on contraction, we shall describe some of its properties. The following lemma states that the contraction upon transformation by the product of any two matrices is bounded by the product of the contractions by individual matrices. Also, the contraction upon transformation by the sum of two matrices is bounded by the sum of the contractions by the individual matrices.

Lemma 5.3.5. Let us consider $J_1, J_2 \in \mathbb{M}_{n\times n}(\mathbb{R}^n)$ and $\Psi \subset \mathbb{R}^n$. Then the all of the following is true.

1. $\chi(\Psi, J_1 + J_2) \leq \chi(\Psi, J_1) + \chi(\Psi, J_2)$.
2. $\chi(\Psi, J_1J_2) \leq \chi(\Psi, J_1)\chi(\Psi, J_2)$.

Proof. For proving the first part, we derive the following.

$$\begin{aligned} &\text{Since} \quad J_1\Psi \subseteq \chi(\Psi, J_1)\Psi \text{ and } J_2\Psi \subseteq \chi(\Psi, J_2), \text{ we get} \\ &(J_1 + J_2)\Psi \subseteq \chi(\Psi, J_1)\Psi \oplus \chi(\Psi, J_2)\Psi = (\chi(\Psi, J_1) + \chi(\Psi, J_2))\Psi. \end{aligned}$$

For proving the second part, we derive the following.

$$\begin{aligned} &J_1J_2\Psi = J_1(J_2\Psi) \subseteq J_1(\chi(\Psi, J_2)\Psi) \\ &= \chi(\Psi, J_2)\,(J_1\Psi) \subseteq \chi(\Psi, J_1)\chi(\Psi, J_2)\Psi. \end{aligned}$$ □

If a matrix is embedded inside the convex hull of a set of matrices, then we get the following bound on contraction by the matrix.

Lemma 5.3.6. *Let us consider that* $J \in \boldsymbol{Conv}(\{A_1, ..., A_r\})$ *and* $\Psi \subset \mathbb{R}^n$. *Then*

$$\chi(\Psi, J) \leq \sup_{i=1}^{r} \chi(\Psi, A_i).$$

Proof. As $J \in \boldsymbol{Conv}(\{A_1, ..., A_r\})$, there exists $\alpha_1, ..., \alpha_r \in \mathbb{R}_{\geq 0}$ such that $\sum_{i=1}^{r} \alpha_i = 1$ and $J = \sum_{i=1}^{r} \alpha_i A_i$. Then by using Lemma 5.3.5, we get

$$\begin{aligned} &\chi(\Psi, J) \leq \sum_{i=1}^{r} \alpha_i \chi(\Psi, A_i) \\ &\leq \left(\sum_{i=1}^{r} \alpha_i\right) \sup_{i=1}^{r} \chi(\Psi, A_i) = \sup_{i=1}^{r} \chi(\Psi, A_i). \end{aligned}$$ □

If we want to bound the contraction of a polynomial with matrix co-coefficients, where the variable has a bound, then the following lemma is useful. The set of all possible values of the polynomial can be embedded inside a convex hull of a finite set of matrices, as described below.

Lemma 5.3.7. [HDTP13] Let us consider $\{A_0, A_1, ..., A_r\} \subseteq \mathbb{M}_{n\times n}(\mathbb{R})$ where

$$\forall j \in \{0, ..., r\},\ U_j(\rho) = \sum_{i=0}^{j} A_i \rho^i.$$

If $0 \leq \rho \leq \epsilon$, then $U_r(\rho) \in \boldsymbol{Conv}(U_0(\epsilon), U_1(\epsilon), ..., U_r(\epsilon))$.

Proof. This has been proved in [HDTP13]. □

Using the above results, we derive the following bound on contraction by the operator $H_{t+\rho}$, when $\rho \in [0, \epsilon]$.

Lemma 5.3.8. *Let us consider* $\Psi \subset \mathbb{R}^n$ *and* $\rho \in [0, \epsilon]$. *If* $0 \leq \rho \leq \epsilon$, *then*

$$\chi(\Psi, H_{t+\rho}) \leq \sup_{i=1}^{r} \chi(\Psi, P_r(\epsilon)H_t) + \chi\left(\Psi, \frac{A_c^{r+1}}{(r+1)!}H_t\right)\epsilon^{r+1}.$$

Proof. Using Equation 5.3, there exists $\delta \in [0, \epsilon]$ such that,

$$\begin{aligned}
&\chi\left(\Psi, H_{t+\rho}\right) = \chi\left(\Psi, P_r(\rho) + E_r(\delta)\right) \\
&\%\% \text{ by Lemma 5.3.5} \\
&\leq \chi\left(\Psi, P_r(\rho) H_t\right) + \chi\left(\Psi, \frac{A_c^{r+1}}{(r+1)!} H_t\right) \delta^{r+1} \\
&\%\% \text{ by Lemmas 5.3.6 and 5.3.7} \\
&\leq \sup_{i=1}^{r} \chi\left(\Psi, P_r(\epsilon) H_t\right) + \chi\left(\Psi, \frac{A_c^{r+1}}{(r+1)!} H_t\right) \delta^{r+1} \\
&\leq \sup_{i=1}^{r} \chi\left(\Psi, P_r(\epsilon) H_t\right) + \chi\left(\Psi, \frac{A_c^{r+1}}{(r+1)!} H_t\right) \epsilon^{r+1}. \qquad \square
\end{aligned}$$

5.4 Stability verification using complex zonotope

We verify global exponential stability by finding a contractive complex zonotope that contains the origin in its interior. A motivation for considering complex zonotope for stability verification is that they can capture contraction along the complex eigenvectors of reachability operators, based on Lemma 2.2.2 described earlier. We find a complex zonotope by sampling the eigenvectors of some of the reachability operators, synthesizing suitable scaling factors and latter verifying that the complex zonotope contracts. Our algorithm for stability verification has two stages. In the first stage, we synthesize a complex zonotope that contracts with respect to a few sampled operators. In the next stage, we verify that the synthesized complex zonotope contracts with respect to all the sampled operators. We fix the template a priori by the collection of unit eigenvectors of a finite number of uniformly sampled reachability operators. Therefore, we have control over the representation size of the contractive set.

Synthesizing a candidate template complex zonotope. Let us sample uniform k time points in the interval Δ as

$$\begin{aligned}
\omega_i^k &= \underline{\boldsymbol{\tau}} + i\frac{(\overline{\boldsymbol{\tau}} - \underline{\boldsymbol{\tau}})}{k} : \ i \in \{0, ..., k-1\} \\
\Lambda_k &= \left\{\omega_i^k : i \in \{1, \ldots, k\}\right\}.
\end{aligned}$$

Let us denote Θ_i^k as a matrix with n columns consisting of all possible unit eigenvectors of $H_{\omega_i^k}$ with possible repetition. Let us consider Ξ_k as the matrix containing all the eigenvectors of k uniformly sampled operators, i.e.,

$$\Xi_k = \begin{bmatrix} \Theta_1^k & \ldots & \Theta_k^k \end{bmatrix}.$$

We fix Ξ_k as the template of the complex zonotope and synthesize suitable scaling factors based on the following theorem. The theorem uses the inclusion checking condition from Theorem 2.3.8.

Theorem 5.4.1. For a vector of scaling factors $s \in \mathbb{R}^m_{\geq 0}$, the template complex zonotope $\mathcal{T}(\Xi_k, 0, s)$ is λ-contractive with respect to all $H_t : t \in \Lambda_k$ and represents a C-set, if all of following is true.

$$\mathcal{T}\left(\boldsymbol{Id}_{n\times n}, 0, [1]_{n\times 1}\right) \sqsubseteq \mathcal{T}(\Xi_k, 0, s) \tag{5.4}$$

$$\forall t \in \Lambda_k,\ \mathcal{T}(H_t\Xi_k, 0, s) \sqsubseteq \mathcal{T}(\Xi, 0, \lambda s)\,. \tag{5.5}$$

Proof. A complex zonotope is a compact and convex set. Furthermore, the real projection of $\mathcal{T}\left(\boldsymbol{Id}_{n\times n}, 0, [1]_{n\times 1}\right)$ is the hypercube containing the origin. So, by Theorem 2.3.8 and Equation 5.4, $\mathcal{T}(\Xi_k, 0, s)$ contains the origin in its interior and hence a C-set. By Lemma 2.2.1, Theorem 2.3.8 and Equations 2.3 and 5.5, we get $H_t\mathcal{T}(\Xi_k, 0, s) \subseteq \lambda\mathcal{T}(\Xi_k, 0, s)$. □

Verifying contraction: To verify that the template complex zonotope synthesized in the first stage contracts with respect to all the reachability operators $H_t : t \in \Delta$, we divide the sampling interval into small enough sub-intervals and verify contraction in each interval. For this, we need to find a bound on contraction of a complex zonotope with respect to any reachability operator. When the synthesized complex zonotope contains the eigenvectors of only one reachability operator, then the contraction by the operator is bounded by the maximum magnitude of the eigenvalues of the operator. This is described in the following lemma.

Lemma 5.4.1. *Let us consider that* $H_{\omega_i^k}\Theta_i^k = \Theta_i^k \operatorname{diag}(\mu) : \mu \in \mathbb{C}^n$. *Let* $s \in \mathbb{R}^n_{\geq 0}$. *Then,*

$$\chi\left(\mathcal{T}(\Xi, 0, s), H_{\omega_i^k}\right) = \sup_{i=1}^{n} |\mu_i|\,.$$

Proof. By using Lemma 2.2.2, we get

$$H_{\omega_i^k}\mathcal{T}\left(\Theta_i^k, 0, s\right) = \mathcal{T}\left(\Theta_i^k, 0, \operatorname{diag}(|\mu|)\, s\right).$$
$$\therefore \chi\left(\mathcal{T}\left(\Theta_i^k, 0, s\right), H_{\omega_i^k}\right) \leq \sup_{i=1}^{n} |\mu_i|\,. \qquad \square.$$

However, when the eigenvectors of multiple reachability operators are sampled to form the template, the above lemma can not be used to compute the contraction bound. In the latter case, we compute the contraction bound using convex optimization, as follows. Let us define

$$\beta_k(s, J) = \inf\{\|X\|_\infty : X \in \mathbb{M}_{m\times m}(\mathbb{C}) \ \wedge\ \Xi_k \operatorname{diag}(s)\, X = J\Xi_k \operatorname{diag}(s)\}$$

Lemma 5.4.2. *We get* $\chi\left(J, \mathcal{T}\left(\Xi_k, 0, s\right)\right) \leq \beta_k(s, J)$.

Proof. Let us consider $J\Xi_k \operatorname{diag}\left(s\right) = \Xi_k \operatorname{diag}\left(s\right) X$. We have to prove that

$$J\mathcal{T}\left(\Xi_k, 0, s\right) = \mathcal{T}\left(J\Xi_k, 0, s\right) \subseteq \|X\|_\infty \mathcal{T}\left(\Xi_k, 0, s\right).$$

We derive the following. By using Lemma 2.1.4, we get

$$\begin{aligned}
&\mathcal{T}\left(J\Xi_k, 0, s\right) = \mathcal{C}\left(J\Xi_k \operatorname{diag}\left(s\right), 0\right) \\
&= \left\{J\Xi_k \operatorname{diag}\left(s\right)\zeta' : \|\zeta'\|_\infty \leq 1\right\} \\
&= \left\{J \operatorname{diag}\left(s\right) X\zeta' : \|\zeta'\|_\infty \leq 1\right\} \\
&\subseteq \|X\|_\infty \left\{\Xi_k \operatorname{diag}\left(s\right)\zeta' : \|\zeta'\|_\infty \leq 1\right\} \\
&= \|X\|_\infty \mathcal{C}\left(\Xi_k \operatorname{diag}\left(s\right), 0\right) = \|X\|_\infty \mathcal{T}\left(\Xi_k, 0, s\right). \qquad \square
\end{aligned}$$

In our verification procedure, we verify contraction in the neighborhoods of a finite set of time points in the sampling interval, such that the union of neighborhoods contains the time interval. Therefore, we derive a bound on the contraction in a neighborhood of a time point, as follows. For any $t \in \Delta$, $r \in \mathbb{Z}_{\geq 0}$ and $\epsilon \geq 0$, let us denote

$$\eta_k^r\left(s, t, \epsilon\right) = \sup_{i=1}^{k} \beta_k\left(s, P_i\left(\epsilon\right) H_t\right) + \beta_k\left(\frac{A_c^{r+1}}{(r+1)!} H_t\right) \epsilon^{r+1}.$$

Theorem 5.4.3. *The following is true.*

$$\sup_{\rho \in [t, t+\epsilon]} \chi\left(\mathcal{T}\left(\Xi_k, 0, s\right), H_\rho\right) \leq \eta_k^r\left(s, t, \epsilon\right).$$

Proof. Let us denote $\Psi = \mathcal{T}\left(\Xi_k, 0, s\right)$. Using Lemma 5.3.8, for any $\rho \in [t, t+\epsilon]$, we derive the following.

$$\begin{aligned}
&\chi\left(\Psi, H_\rho\right) \leq \sup_{i=1}^{r} \chi\left(\Psi, P_r(\epsilon) H_t\right) + \chi\left(\Psi, \frac{A_c^{r+1}}{(r+1)!} H_t\right) \epsilon^{r+1} \\
&\%\% \text{ by Lemma 5.4.2} \\
&\leq \sup_{i=1}^{k} \beta_k\left(s, P_i\left(\epsilon\right) H_t\right) + \beta_k\left(\frac{A_c^{r+1}}{(r+1)!} H_t\right) \epsilon^{r+1}. \qquad \square
\end{aligned}$$

Verification algorithm. We begin with $k = 3$ reference operators that correspond to the two end points of the sampling interval and the middle point. The algorithm first finds suitable scaling factors s such that the template complex zonotope with Ξ_k as the template operators contracts with respect to $\omega_i^k \forall i \in \{1, \ldots, k\}$. Then we check whether the contraction of the template complex zonotope by all the reachability operators is less than one. For checking contraction,

Algorithm 2 Exponential stability verification of $\mathbb{H}$

Initialize $k = 3$.
Choose an $M \in \mathbb{Z}_{>3}$ as the bound of k.
Choose $tol > 0$ as the discretization parameter.
while $k \leq M$ and $t < \overline{\boldsymbol{\tau}}$ **do**
    Find a vector of scaling factors s solving Equations 5.4 and 5.5.
    Initialize $t = \underline{\boldsymbol{\tau}}$ and $h = tol$.
    Set $r :=$ order of Taylor expansion (typically ≤ 2).
    while $h \geq tol$ **do**
        if $\eta_k^r(s, t, h) < 1$ **then**
            $t \leftarrow t + h; h \leftarrow h + tol$
        else
            $h \leftarrow h - tol$
        end if
        if $h < tol$ **then**
            $k \leftarrow k + 1$.
        end if
    end while
end while
if $t \geq \overline{\boldsymbol{\tau}}$ **then**
    System is exponentially stable
else
    Inconclusive
end if

we first discretize the sampling interval by a grid of size $tol > 0$ and then compute the bound on contraction in the forward tol neighborhood of each gird point using Theorem 5.4.3. We choose an order of Taylor expansion, typically not greater than two. Starting with $t = \underline{\tau}$ and $h = tol$, for any t and h, we check that $\eta_k^r(s,t,h) < 1$. If successfully, we increment the value of t to $t+h$ and h to $h + tol$. If not successful, we reduce the value of h to $h - tol$. If we have verified contraction until a point $t > \overline{\tau}$, then we have successfully verified global exponential stability of the system. Otherwise, if h becomes less than zero at some point, we start another loop by increasing k to $k+1$ and repeat the procedure. We hope to verify contraction within a reasonable value of k. Otherwise, we terminate without any conclusion. The steps of the procedure are systematically described in Algorithm 2. We shall discuss the experimental results based on this algorithm in the next section.

5.5 Experiments

We evaluated our algorithm on two benchmark examples of linear impulsive systems below and compared it with other state-of-the-art approaches. For convex optimization, we use CVX version 2.1 with Matlab 8.5.0.197613 (R2015a). The reported experimental results were obtained on Intel(R) Core(TM) i5-3470 CPU @ 3.20GHz.

Example 1. We consider a networked control system with uncertain but bounded transmission period. A networked control system is composed of a plant and a controller that interact with each other by transmission of feedback input from controller to the plant. If the system dynamics is linear with linear feedback, then for uncertain but bounded transmission period, we can equivalently represent it as a linear impulsive system where

$$A_c = \begin{pmatrix} A_p & 0 & B_p \\ 0 & 0 & 0 \\ 0 & 0 & 0 \end{pmatrix}, \; A_r = \begin{pmatrix} \mathbb{I} & 0 & 0 \\ B_o C_p & A_o & 0 \\ D_o C_p & C_o & 0 \end{pmatrix}$$

for some parameter matrices A_p, B_p, B_o, C_p, A_o, C_o, and D_o. The sampling interval Δ of the linear impulsive system specifies bounds on the transmission interval. Our example of a networked control system is taken from Björn et al. [WAA02]. The system is originally described by discrete time transfer functions, which has

Reference	t_{min}	t_{max}
Value recommended in [WAA02]	0.08	0.22
NCS toolbox [BvLD+12]	0.08	0.4
Template complex zonotope	0.08	0.58

Table 5.1: Experimental results: Example 1

Reference	t_{min}	t_{max}
Lyapunov, parametric LMI [HDTP13]	0.1	0.3
Polytopic set contractiveness [FM14]	0.1	0.475
Khatib et al. [KGD15]	0.1	0.514
Template complex zonotope	0.1	0.496

Table 5.2: Experimental results: Example 2

an equivalent state space representation with parameter matrices

$$A_p = \begin{pmatrix} -1 & 0 \\ 1 & 0 \end{pmatrix}, \; B_p = \begin{pmatrix} 1 \\ 0 \end{pmatrix}, \; C_p = \begin{pmatrix} 0 & 1 \end{pmatrix},$$
$$A_o = 0.4286, \; B_o = -0.8163, \; C_o = -1D_o = -3.4286.$$

Given the lower bound on the transmission period as $t_{min} = 0.8$, we want to find as high a value of t_{max} as possible for which the system is GES.

Example 2. We consider the following linear impulsive system from Hetel et. al. [HDTP13], that describes an LMI based approach to verify stability. The specification is given by

$$A_c = \begin{pmatrix} 0 & -3 & 1 \\ 1.4 & -2.6 & 0.6 \\ 8.4 & -18.6 & 4.6 \end{pmatrix}, \; A_r = \begin{pmatrix} 1 & 0 & 0 \\ 0 & 1 & 0 \\ 0 & 0 & 0 \end{pmatrix}.$$

Setting and Results. While implementing the algorithm for stability verification, we used first order Taylor expansion, a tolerance of $tol = 0.01$ for Example 1 and $tol = 0.006$ for Example 2. We required $k = 3$ number of reachability operators for both examples, for synthesizing a suitable template complex zonotope used in checking contraction. We could verify exponential stability in a sampling interval $[0.08, 0.58]$ for Example 1 and $[0.1, 0.496]$ for Example 2. For the first example, our method outperforms other approaches as given in Table 5.1. For the second example, our method larger bounds than the Lyapunov function approach [HDTP13] and polytopic set contractiveness based approach [FM14], as

reported in Table 5.2. Although our bound is smaller than the one found by the approach of [KGD15], still the difference is only 0.018.

CHAPTER 6

Conclusion

6.1 Contributions

The complex zonotope set representation provides a computationally efficient framework for utilizing the complex valued eigenstructure of affine hybrid systems for their verification, while retaining the essential computational advantages of real zonotopes. We have developed practical algorithms using complex zonotopes for verification of linear invariance properties of discrete time systems and exponential stability of linear impulsive systems. We summarize the main contributions of this dissertation below.

- *Complex zonotope:* Our most important contribution is the extension of real zonotopes to the complex valued domain by complex zonotopes, which can capture contraction along complex vectors, but still are computationally as efficient as a real zonotope. Just like real zonotopes, a complex zonotope is closed under Minkowski sum, linear transformation and their computation is also efficient. The support function of a complex zonotope can also be computed by a simple algebraic expression. But additionally, a complex zonotope can efficiently encode positive invariants for linear transformations by incorporating complex eigenvectors as generators. On the other hand, eigenvectors having non-zero real and imaginary parts can not be used as generators in real zonotopes. Moreover, complex zonotopes are geometrically more expressive since their real projections can represent non-polytopic sets in addition to polytopic zonotopes.
- *Template based representation:* We introduced a template based represen-

tation of a complex zonotope, by which we can add generators to a complex zonotope to find better approximations. In a real zonotope, adding a generator can increase the size of the denoted set. This problem is addressed by the template based representation of a complex zonotope, which has a set of scaling factors that determine the amount of contribution of each generator to the size of the set. Henceforth, to find a better approximations, we can add more generators to a complex zonotope and adjust the scaling factors.

- *Set operations:* Apart from the simpler computations like linear transformation, Minkowski sum and support function, we developed a convex program to efficiently check-inclusion between template complex zonotopes. Then, we developed the augmented complex zonotope representation to efficiently over-approximate the intersection with sub-parallelotopes. The error in over-approximation can be regulated by adjusting the scaling factors. The main advantage of augmented complex zonotope is that we can still compute the support function efficiently. It provided an alternative to the previous known variations of real zonotopes for computing the intersection, because their extension to complex zonotope makes computation of the support function intractable.
- *Verification of discrete time affine hybrid systems:* We developed a convex program based on computing positively invariant augmented complex zonotopes to verify linear invariance properties of discrete time affine hybrid systems. We performed experiments on three benchmark examples that demonstrate the efficiency of our approach.
- *Stability verification of linear impulsive systems:* We developed an algorithm to find contractive complex zonotopes that verify global exponential stability of linear impulsive systems with sampling uncertainty. The novelty of our algorithm lies in using the eigenstructure of reachability operators for stability verification, i.e., to find contractive complex zonotopes. Our experiments on two benchmark examples demonstrate either better or competitive performance compared to state of the art approaches.

6.2 Future work

Some of the directions for extending this research on complex zonotopes are discussed below.

1. *Non-linear systems:* Hybrid systems with non-linear differential and difference equations are inherently more difficult to verify than affine hybrid systems having linear differential or difference equations. For reachability

analysis of affine hybrid systems, complex zonotopes have the advantage that they are closed and have low computational complexity under affine transformations. However, complex zonotopes are not closed under non-affine transformations due to which extending their usage to non-affine hybrid systems is computationally challenging. To address this problem, we can develop convex relaxations to approximate the non-affine images of complex zonotopes. Alternatively, just like polynomial real zonotopes, we can extend complex zonotopes to polynomial complex zonotopes. But then the degree of a polynomial complex zonotope grows exponentially with the iterative application of non-affine functions. So, we have to compute over-approximations a polynomial complex zonotope of higher degree with a polynomial complex zonotope of lower degree.

2. *Continuous time dynamics:* The set operations we have developed are mainly useful for computing positive invariants of discrete time dynamics or simpler cases of continuous dynamics that can be easily discretized in time. But for computing positively invariant complex zonotopes for more general continuous time dynamics, we have to compute bounds on the vector field at the boundary of a complex zonotope.

3. *Program verification:* Complex zonotopes can be used as an abstract domain for program verification. Indeed, our template based representation of complex zonotope is closer in spirit to the template based approaches in abstract interpretation. We have to experimentally find out the performance of complex zonotopes when applied to numerical program verification.

More experimentation has to be done to understand the practical issues with using complex zonotopes. Nevertheless, complex zonotopes provide an exemplary approach for future set representations to efficiently encode the eigenstructure of a system for increasing the accuracy of reachability analysis techniques.

Bibliography

[AaNSGP16] Xavier Allamigeon, Stéphane Gaubert and“ Nikolas Stott, Eric Goubault, and Sylvie Putot. A scalable algebraic method to infer quadratic invariants of switched systems. *ACM Trans. Embedded Comput. Syst.*, 15(4):69:1–69:20, 2016. (*Cited on page 9.*)

[ACH+95] Rajeev Alur, Costas Courcoubetis, Nicolas Halbwachs, Thomas A Henzinger, P-H Ho, Xavier Nicollin, Alfredo Olivero, Joseph Sifakis, and Sergio Yovine. The algorithmic analysis of hybrid systems. *Theoretical computer science*, 138(1):3–34, 1995. (*Cited on page 1.*)

[ADM02] Eugene Asarin, Thao Dang, and Oded Maler. The d/dt tool for verification of hybrid systems. In *International Conference on Computer Aided Verification*, pages 365–370. Springer, 2002. (*Cited on page 4.*)

[AGG10] Assalé Adjé, Stéphane Gaubert, and Eric Goubault. Coupling policy iteration with semi-definite relaxation to compute accurate numerical invariants in static analysis. In *Programming Languages and Systems, 19th European Symposium on Programming, ESOP 2010, Held as Part of the Joint European Conferences on Theory and Practice of Software, ETAPS 2010, Paphos, Cyprus, March 20-28, 2010. Proceedings*, pages 23–42, 2010. (*Cited on page 10.*)

[AGG+17] Xavier Allamigeon, Stéphane Gaubert, Eric Goubault, Sylvie Putot, and Nikolas Stott. A fast method to compute disjunctive quadratic invariants of numerical programs. *ACM Transactions on Embedded Computing Systems (TECS)*, 16(5s):166, 2017. (*Cited on pages 2 and 9.*)

[AGW15] Assalé Adjé, Pierre-Loïc Garoche, and Alexis Werey. Quadratic zonotopes - an extension of zonotopes to quadratic arithmetics. In *Programming Languages and Systems - 13th Asian Symposium,*

APLAS 2015, Proceedings, pages 127–145, 2015. (*Cited on pages 3 and 7.*)

[AK11a] M. Althoff and B.H. Krogh. Zonotope bundles for the efficient computation of reachable sets. In *Decision and Control and European Control Conference (CDC-ECC), 2011 50th IEEE Conference on*, pages 6814–6821, Dec 2011. (*Cited on page 78.*)

[AK11b] Matthias Althoff and Bruce H Krogh. Zonotope bundles for the efficient computation of reachable sets. In *Decision and Control and European Control Conference (CDC-ECC), 2011 50th IEEE Conference on*, pages 6814–6821. IEEE, 2011. (*Cited on page 8.*)

[AL14] Nikolaos Athanasopoulos and Mircea Lazar. Alternative stability conditions for switched discrete time linear systems. In *IFAC World Congress*, pages 6007–6012, 2014. (*Cited on pages 77, 78, and 80.*)

[Alt13] Matthias Althoff. Reachability analysis of nonlinear systems using conservative polynomialization and non-convex sets. In *Proceedings of the 16th international conference on Hybrid systems: computation and control, HSCC 2013*, pages 173–182, 2013. (*Cited on pages 7 and 8.*)

[AS12] Gianluca Amato and Francesca Scozzari. The abstract domain of parallelotopes. *Electronic Notes in Theoretical Computer Science*, 287:17–28, 2012. (*Cited on page 5.*)

[BGP+09] Olivier Bouissou, Eric Goubault, Sylvie Putot, Karim Tekkal, and Franck Vedrine. Hybridfluctuat: A static analyzer of numerical programs within a continuous environment. In *International Conference on Computer Aided Verification*, pages 620–626. Springer, 2009. (*Cited on page 7.*)

[BHZ08] Roberto Bagnara, Patricia M Hill, and Enea Zaffanella. The parma polyhedra library: Toward a complete set of numerical abstractions for the analysis and verification of hardware and software systems. *Science of Computer Programming*, 72(1-2):3–21, 2008. (*Cited on page 4.*)

[BM08] Franco Blanchini and Stefano Miani. *Set-theoretic methods in control*. Springer, 2008. (*Cited on pages 5 and 9.*)

[Bri13] Corentin Briat. Convex conditions for robust stability analysis and stabilization of linear aperiodic impulsive and sampled-data systems under dwell-time constraints. *Automatica*, 49(11):3449–3457, 2013. (*Cited on page 78.*)

[BvLD+12] N.W. Bauer, S.J.L.M. van Loon, M.C.F. Donkers, N van de Wouw, and W.P.M.H. Heemels. Networked control systems toolbox: Robust stability analysis made easy. In *IFAC Workshop on Distributed Estimation and Control in Networked Systems (NECSYS)*, pages 55–60, 2012. (*Cited on pages 78 and 88.*)

[CC76] Patrick Cousot and Radhia Cousot. Static determination of dynamic properties of programs. In *Proceedings of the 2nd International Symposium on Programming, Paris, France*. Dunod, 1976. (*Cited on page 5.*)

[CGT08] Chaohong Cai, R. Goebel, and A.R. Teel. Smooth lyapunov functions for hybrid systems part ii: (pre)asymptotically stable compact sets. *Automatic Control, IEEE Transactions on*, 53(3):734–748, 2008. (*Cited on page 78.*)

[DG11] Thao Dang and Thomas Martin Gawlitza. Template-based unbounded time verification of affine hybrid automata. In *Asian Symposium on Programming Languages and Systems*, pages 34–49. Springer, 2011. (*Cited on page 5.*)

[DM98] Thao Dang and Oded Maler. Reachability analysis via face lifting. In *International Workshop on Hybrid Systems: Computation and Control*, pages 96–109. Springer, 1998. (*Cited on page 5.*)

[DT13] Parasara Sridhar Duggirala and Ashish Tiwari. Safety verification for linear systems. In *Embedded Software (EMSOFT), 2013 Proceedings of the International Conference on*, pages 1–10. IEEE, 2013. (*Cited on page 9.*)

[FLGD+11] Goran Frehse, Colas Le Guernic, Alexandre Donzé, Scott Cotton, Rajarshi Ray, Olivier Lebeltel, Rodolfo Ripado, Antoine Girard, Thao Dang, and Oded Maler. Spaceex: Scalable verification of hybrid systems. In *Proc. 23rd International Conference on Computer Aided Verification (CAV)*, LNCS. Springer, 2011. (*Cited on pages 4, 5, and 67.*)

[FM14] Mirko Fiacchini and Irinel-Constantin Morarescu. Set theory conditions for stability of linear impulsive systems. In *Proceedings CDC 2014*, 2014. (*Cited on pages 77, 78, 80, and 88.*)

[Fre08] Goran Frehse. Phaver: algorithmic verification of hybrid systems past hytech. *International Journal on Software Tools for Technology Transfer*, 10(3):263–279, 2008. (*Cited on page 4.*)

[Fri10] Emilia Fridman. A refined input delay approach to sampled-data control. *Automatica*, 46(2):421–427, 2010. (*Cited on page 78.*)

[Fuj] Hisaya Fujioka. Stability analysis of systems with aperiodic sample-and-hold devices. *Automatica*, 45(3):771–775. (*Cited on page 78.*)

[Fuj09] Hisaya Fujioka. A discrete-time approach to stability analysis of systems with aperiodic sample-and-hold devices. *Automatic Control, IEEE Transactions on*, 54(10):2440–2445, 2009. (*Cited on page 78.*)

[GBY08] Michael Grant, Stephen Boyd, and Yinyu Ye. Cvx: Matlab software for disciplined convex programming, 2008. (*Cited on page 28.*)

[GGP10] Khalil Ghorbal, Eric Goubault, and Sylvie Putot. A logical product approach to zonotope intersection. In Tayssir Touili, Byron Cook, and Paul Jackson, editors, *Computer Aided Verification: 22nd International Conference, CAV 2010, Edinburgh, UK, July 15-19, 2010. Proceedings*, 2010. (*Cited on pages 8 and 35.*)

[Gir05a] Antoine Girard. Reachability of uncertain linear systems using zonotopes. In *Hybrid Systems: Computation and Control, 8th International Workshop, HSCC 2005, Zurich, Switzerland, March 9-11, 2005, Proceedings*, pages 291–305, 2005. (*Cited on page 2.*)

[Gir05b] Antoine Girard. Reachability of uncertain linear systems using zonotopes. In *In Hybrid Systems : Computation and Control, LNCS 3414*, pages 291–305. Springer, 2005. (*Cited on pages 7 and 78.*)

[GLG08] Antoine Girard and Colas Le Guernic. Zonotope/hyperplane intersection for hybrid systems reachability analysis. In *International Workshop on Hybrid Systems: Computation and Control*, pages 215–228. Springer, 2008. (*Cited on pages 2, 7, and 8.*)

[GPV12] Eric Goubault, Sylvie Putot, and Franck Védrine. Modular static analysis with zonotopes. In *Static Analysis - 19th International Symposium, SAS 2012*, volume 7460, pages 24–40. Springer, 2012. (*Cited on page 78.*)

[GST09] R. Goebel, R.G. Sanfelice, and A. Teel. Hybrid dynamical systems. *Control Systems, IEEE*, 29(2):28–93, 2009. (*Cited on page 78.*)

[HDI06] L. Hetel, J. Daafouz, and C. Iung. Stabilization of arbitrary switched linear systems with unknown time-varying delays. *Automatic Control, IEEE Transactions on*, 51(10):1668–1674, 2006. (*Cited on page 78.*)

[HDTP13] Laurentiu Hetel, Jamal Daafouz, Sophie Tarbouriech, and Christophe Prieur. Stabilization of linear impulsive systems through a nearly-periodic reset. *Nonlinear Analysis: Hybrid Systems*, 7(1):4–15, 2013. (*Cited on pages 78, 82, and 88.*)

[HKPR11] L. Hetel, A. Kruszewski, W. Perruquetti, and J.-P. Richard. Discrete and intersample analysis of systems with aperiodic sampling. *Automatic Control, IEEE Transactions on*, 56(7):1696–1701, 2011. (*Cited on page 78.*)

[HLCS03] L. Hu, J. Lam, Y. Cao, and H. Shao. A lmi approach to robust h2 sampled- data control for linear uncertain systems. *IEEE Trans. Syst. Man Cybern.*, 33(1):149155, 2003. (*Cited on page 78.*)

[HOW14] Thomas Heinz, Jens Oehlerking, and Matthias Woehrle. Benchmark: Reachability on a model with holes. In *ARCH@ CPSWeek*, pages 31–36, 2014. (*Cited on pages 67, 69, and 70.*)

[JM09] Bertrand Jeannet and Antoine Miné. Apron: A library of numerical abstract domains for static analysis. In *Computer Aided Verification*, pages 661–667. Springer, 2009. (*Cited on page 78.*)

[KGBM04] Michal Kvasnica, Pascal Grieder, Mato Baotic, and Manfred Morari. Multi-parametric toolbox (mpt). In *HSCC*, pages 448–462. Springer, 2004. (*Cited on page 4.*)

[KGD15] Mohammad Al Khatib, Antoine Girard, and Thao Dang. Stability verification of nearly periodic impulsive linear systems using reachability analysis. In *5th IFAC Conference on Analysis and Design of Hybrid Systems ADHS 2015*. ACM, October 2015. (*Cited on pages 77, 78, 80, 88, and 89.*)

[KV06] Alex A Kurzhanskiy and Pravin Varaiya. Ellipsoidal toolbox (et). In *Decision and Control, 2006 45th IEEE Conference on*, pages 1498–1503. IEEE, 2006. (*Cited on pages 2 and 9.*)

[Kva05] Michal Kvasnica. Minkowski addition of convex polytopes, 2005. (*Cited on page 4.*)

[KW14] Chung-Yao Kao and Dian-Rong Wu. On robust stability of aperiodic sampled-data systems - an integral quadratic constraint approach. In *American Control Conference, ACC 2014, Portland, OR, USA, June 4-6, 2014*, pages 4871–4876, 2014. (*Cited on page 78.*)

[LDA13] M. Lazar, A.I. Doban, and N. Athanasopoulos. On stability analysis of discrete-time homogeneous dynamics. In *System Theory, Control and Computing (ICSTCC), 2013 17th International Conference*, pages 297–305, 2013. (*Cited on pages 77 and 78.*)

[LPY98] Gerardo Lafferriere, George J Pappas, and Sergio Yovine. *Decidable hybrid systems*. Citeseer, 1998. (*Cited on page 1.*)

[LSF10] Kun Liu, Vladimir Suplin, and Emilia Fridman. Stability of linear systems with general sawtooth delay. *IMA Journal of Mathematical Control and Information*, 27(4):419–436, 2010. (*Cited on page 78.*)

[Min06] Antoine Miné. The octagon abstract domain. *Higher-Order and Symbolic Computation*, 19(1):31–100, 2006. (*Cited on pages 5 and 19.*)

[Mir07] L. Mirkin. On the use of time-varying delay to represent sample-and-hold circuits. In *Decision and Control, 2007 46th IEEE Conference on*, pages 420–425, 2007. (*Cited on page 78.*)

[MK14] Ibtissem Ben Makhlouf and Stefan Kowalewski. Networked cooperative platoon of vehicles for testing methods and verification tools. In *ARCH@ CPSWeek*, pages 37–42, 2014. (*Cited on pages 2, 7, 71, 73, and 74.*)

[MMD13] FréDéRic Mazenc, Michael Malisoff, and Thach N. Dinh. Robustness of nonlinear systems with respect to delay and sampling of the controls. *Automatica*, 49(6):1925–1931, June 2013. (*Cited on page 78.*)

[NHT08] Payam Naghshtabrizi, Joao P Hespanha, and Andrew R Teel. Exponential stability of impulsive systems with application to uncertain sampled-data systems. *Systems & Control Letters*, 57(5):378–385, 2008. (*Cited on pages 77 and 78.*)

[NT04] D Nešić and Andrew R Teel. A framework for stabilization of nonlinear sampled-data systems based on their approximate discrete-time models. *IEEE Transactions on Automatic Control*, 49(7):1103–1122, 2004. (*Cited on page 78.*)

[NUoC07] P. Naghshtabrizi and Santa Barbara. Electrical & Computer Engineering University of California. *Delay Impulsive Systems: A Framework for Modeling Networked Control Systems*. University of California, Santa Barbara, 2007. (*Cited on page 77.*)

[OHRLL13] H. Omran, L. Hetel, J.-P. Richard, and F. Lamnabhi-Lagarrigue. On the stability of input-affine nonlinear systems with sampled-data control. In *Control Conference (ECC), 2013 European*, pages 2585–2590, 2013. (*Cited on page 78.*)

[OHRLL14] Hassan Omrana, Laurentiu Hetela, Jean-Pierre Richarda, and Franoise Lamnabhi-Lagarriguec. Stability analysis of bilinear systems under aperiodic sampled-data control. *Automatica*, 50(4):1288 – 1295, 2014. (*Cited on page 78.*)

[PJ04] Stephen Prajna and Ali Jadbabaie. Safety verification of hybrid systems using barrier certificates. In *International Workshop on Hybrid Systems: Computation and Control*, pages 477–492. Springer, 2004. (*Cited on page 10.*)

[PR05] Stephen Prajna and Anders Rantzer. On the necessity of barrier certificates. *IFAC Proceedings Volumes*, 38(1):526–531, 2005. (*Cited on page 10.*)

[RCT05] Enric Rodríguez-Carbonell and Ashish Tiwari. Generating polynomial invariants for hybrid systems. In *International Workshop on Hybrid Systems: Computation and Control*, pages 590–605. Springer, 2005. (*Cited on page 10.*)

[RGK+04] SV Rakovic, P Grieder, Michal Kvasnica, DQ Mayne, and Manfred Morari. Computation of invariant sets for piecewise affine discrete time systems subject to bounded disturbances. In *Decision and Control, 2004. CDC. 43rd IEEE Conference on*, volume 2, pages 1418–1423. IEEE, 2004. (*Cited on pages 5, 67, 75, and 76.*)

[RJGF12] Pierre Roux, Romain Jobredeaux, Pierre-Loïc Garoche, and Eric Feron. A generic ellipsoid abstract domain for linear time invariant systems. In *Hybrid Systems: Computation and Control (part of CPS Week 2012), HSCC'12, Beijing, China, April 17-19, 2012*, pages 105–114, 2012. (*Cited on page 9.*)

[SDI08a] Sriram Sankaranarayanan, Thao Dang, and Franjo Ivancic. Symbolic model checking of hybrid systems using template polyhedra. In *TACAS*, volume 4963 of *Lecture Notes in Computer Science*, pages 188–202. Springer-Verlag, 2008. (*Cited on pages 5 and 19.*)

[SDI08b] Sriram Sankaranarayanan, Thao Dang, and Franjo Ivani. Symbolic model checking of hybrid systems using template polyhedra. In C.R. Ramakrishnan and Jakob Rehof, editors, *Tools and Algorithms for the Construction and Analysis of Systems*, volume 4963 of *LNCS*, pages 188–202. Springer Berlin Heidelberg, 2008. (*Cited on page 78.*)

[Seu12] Alexandre Seuret. A novel stability analysis of linear systems under asynchronous samplings. *Automatica*, 48(1):177–182, 2012. (*Cited on page 78.*)

[SNM03] Robert Shorten, Kumpati S Narendra, and Oliver Mason. A result on common quadratic lyapunov functions. *IEEE Transactions on automatic control*, 48(1):110–113, 2003. (*Cited on page 9.*)

[SP13] Alexandre Seuret and M Peet. Stability analysis of sampled-data systems using sum of squares. *Automatic Control, IEEE Transactions on*, 58(6):1620–1625, 2013. (*Cited on page 78.*)

[SRKC00] B Izaias Silva, Keith Richeson, Bruce Krogh, and Alongkrit Chutinan. Modeling and verifying hybrid dynamic systems using checkmate. In *Proceedings of 4th International Conference on Automation of Mixed Processes*, volume 4, pages 1–7, 2000. (*Cited on page 4.*)

[SRMB16] Joseph K Scott, Davide M Raimondo, Giuseppe Roberto Marseglia, and Richard D Braatz. Constrained zonotopes: A new tool for set-based estimation and fault detection. *Automatica*, 69:126–136, 2016. (*Cited on pages 8 and 35.*)

[SSM04] Sriram Sankaranarayanan, Henny B Sipma, and Zohar Manna. Constructing invariants for hybrid systems. In *International Work-*

shop on Hybrid Systems: Computation and Control, pages 539–554. Springer, 2004. (*Cited on pages 9 and 10.*)

[Tiw08] Ashish Tiwari. Generating box invariants. In *International Workshop on Hybrid Systems: Computation and Control*, pages 658–661. Springer, 2008. (*Cited on page 5.*)

[TNK98] A. Teel, D. Nesic, and P.V. Kokotovic. A note on input-to-state stability of sampled-data nonlinear systems. In *Proceedings of the IEEE Conference on Decision and Control*, pages 2473–2478, 1998. (*Cited on page 78.*)

[WAA02] Bjorn Wittenmark, Karl Johan Astrom, and Karl-Erik Arzen. Computer control: An overview. *IFAC Professional Brief*, 1 2002. (*Cited on pages 87 and 88.*)

[YVE88] Mikheev Yu.V., Sobolev V.A., and Fridman E.M. Asymptotic analysis of digital control systems. *Automation and Remote Control*, 49(9):11751180, 1988. (*Cited on page 78.*)

[Zas75] Thomas Zaslavsky. *Facing up to Arrangements: Face-Count Formulas for Partitions of Space by Hyperplanes: Face-count Formulas for Partitions of Space by Hyperplanes*, volume 154. American Mathematical Soc., 1975. (*Cited on page 8.*)